UNIVERSIDADE DA BEIRA INTERIOR
Engenharia

Optimization of Small Cells Deployment and Frequency Assignment using Spectrum Sharing

(versão final após defesa)

Bruno Cruz da Silva

Dissertação para obtenção do Grau de Mestre em
Engenharia Eletrotécnica e de Computadores
(2º ciclo de estudos)

Orientador: Prof. Doutor Fernando J. S. Velez

Covilhã, Dezembro de 2018

I would like to dedicate this dissertation to my parents, especially Carlos Silva, who always helped me, and Margarida Cruz for all the support she gave me and for always helping me to take the best decision. To My Grandparents, especially my grandfather, who sadly is not here to see this work, i will never forget him. I want to dedicate it to a special person, which is my grandmother Lucia because she always supported me throughout my University Degree on Electrical and Computer Engineering, helping with everything since the beginning.

Acknowledgements

To my adviser, Prof. Dr. Fernando Velez, for all his dedication and patience throughout this journey. I want also to thank a lot to friends that I met along the way while doing this dissertation, first of all, my Brazilian brother, Rooderson Andrade that always supported, helped and guided me. Emanuel Mahina, a good friend that always supported me and read this dissertation a lot of times. Emanuel Teixeira that helped with some ideas and content to this dissertation. Anderson Rocha, other Brazilian brother, who helped me. To engineer Rui Paulo for his help on performing the simulations with LTE-Sim, and for his support, hard work and patience. And some other great friends from UBI who helped me their own way and I will remember them forever, Ricardo Alves, João Curto, Matheus Belúcio, Alfredo Taunay, Rafael Masson, Alessio Mugnaini, Haphisa Souza, Amanda Brinhosa, Renan Cunha, César Lima, Arlindo Isaac, Analcisio Rodino, Ntunitangua Pindi, Ananias Muxiri, Fortunato Fiau, Dinis Mianga. Finally, I would like to thank all the teachers that participated and helped me with my formation as a Master in Eletrical and Computer Engineering. The author would like to thank to Qualcomm and Ericsson for their permission to use the images. I would especially like to thank the Instituto de Telecomunicações for the opportunity to carry out my research and for the scholarship supported by National Funding from the FCT - Fundação para a Ciência e a Tecnologia, through UID/EEA/50008/2013 and the equipment that was made available for the laboratory by ORCIP. The support from COST CA 15104 IRACON and CONQUEST (CMU/ECE/0030/2017) have also been of fundamental important.

Abstract

5G New Radio is an air-interface technology with the objective of improving performance, flexibility [1], [2],[3] scalability and efficiency of current mobile networks. 5G NR is envisioned to support multiple services and devices where the heterogeneous networks will be of such importance with the densification of small cells, and different techniques will be used such as carrier aggregation, spectrum sharing or dual connectivity. This dissertation aims to explore the optimization of small cell networks using the spectrum sharing in the UHF, SHF and millimeter wave bands for urban environments. In the study, different scenarios and topologies have been considered, while frequencies of 2.6 GHz and 3.5 GHz have been considered for the UHF/SHF bands, and 28, 38, 60 and 73 GHz for the millimeter wave bands. A linear topology has been considered for the millimeter waves that contains a scenario with sharing and another without shared spectrum, while in the UHF and SHF bands a hexagonal topology has been considered, containing both a scenario without spectrum sharing and six spectrum sharing topologies, divided by its region in the cell, as Northeast, East, Southeast and Soutwest. Propagation models are the Urban Micro LoS for UHF/SHF, a two-slope model, and the modified Friis equation for the millimeter waves. Different reuse patterns have also been considered, i.e., k = 3 and k = 4. However, for the millimeter wave scenario only k = 3 has been considered. With the established scenario and the considered models, the performance parameters such as the CNIR, PHY throughput, supported throughput, average CNIR/SINR have been obtained and discussed. In the UHF/SHF bands, by comparing the curves for the supported throughput and the average CNIR, we can observe that the trend of the values, i.e., the line shapes, are very similar. The 28 GHz frequency band has the highest supported throughput, reaching 45 Mbps. The supported throughput at the 38, 60 and 73 GHz is higher than the one for the UHF/SHF bands for the shortest Rs. For longer coverage distances, the supported throughput is clearly higher for the UHF/SHF frequency bands (compared to the 38, 60 and 73 GHz frequency bands). LTE-Sim, a open source framework developed in the University of Bari [4], commonly known as an event-driven simulator written in $C++$ has been used for packet-level simulations. Results for the goodput, packet loss ratio and delay have been obtained. One scenario with only a small cell cluster, with one picocell and six co-channel pico cells, has been considered in the simulations. The goodput and packet loss ratio achieved by simulation are complementary to each other (where achieved goodput is slightly higher at 2.6 GHz, compared to the 3.5 GHz frequency band). By comparing the analytical and simulation results for the supported throughout/goodput (without sharing) there are differences, as analytical results do not consider packet errors, and for a number of users higher than $16-18$, the PLR is too high even for distances longer than $100-150$ m, while for 16 or less users the PLR is only high for coverage distances up to circa 100 m. These differences between analytical and simulation results can be mainly explained by the fact that the number of users are not considered in the analytical formulation (saturation conditions are assumed instead), and also because of the high value for the PLR. The maximum delay is 55 ms. Hence, e.g., for gaming applications, latency will be adequate.

Keywords

Small Cell, 5G, New Radio, Spectrum Sharing, LTE-Advanced, ITU-R propagation model, System capacity, HetNet, mmWaves

Resumo

O 5G New Radio irá melhorar o desempenho, flexibilidade [1], [2], [3] escalabilidade e eficiência das redes móveis atuais. O 5G NR suportará serviços e dispositivos múltiplos onde as redes heterogéneas serão de grande importância, especialmente devido à densificação de pequenas células, e às diferentes técnicas que serão usadas, tal como a agregação de espectro, a partilha de espectro e conectividade dupla. Esta dissertação tem como objetivo explorar a otimização de redes de pequenas células utilizando a partilha de espectro nas bandas de UHF, SHF e na banda das ondas milimétricas para ambientes urbanos. Neste estudo foram considerados diferentes cenários e topologias, as frequências de 2.6 GHz e 3.5 GHz, e 28, 38, 60 e 73 GHz (bandas das ondas milimétricas). Considerou-se uma topologia linear para as ondas milimétricas, com e sem partilha de espectro , enquanto nas bandas UHF e SHF considerou-se uma topologia hexagonal, contendo tanto um cenário sem partilha de espectro como um cenário onde os interferentes na partilha de espectro organizam-se em diferentes posições relativamente à célula, ou seja, Nordeste, Este, Sudeste e Sudoeste. Os modelos de propagação são o $UrbanMicroLoS$ para UHF/SHF, um modelo com expoente de propagação duplo, e a fórmula de Friis modificada para a banda das ondas milimétricas. Consideraram-se diferentes padrões de reutilização, ou seja, k = 3 e k = 4. No entanto, para o cenário de ondas milimétricas, apenas k = 3 foi considerado. Obtiveram-se as métricas de desempenho como o CNIR, o débito binário, o débito binário suportado e o CNIR/SINR médio. Nas bandas UHF/SHF, comparando as curvas do débito binário suportado e do CNIR médio, observa-se que a tendência, ou seja, a forma das curvas, é similar. A banda de 28 GHz tem o débito binário suportado superior, atingindo os 45 Mbps. O débito binário suportado nos 38, 60 e 73 GHz é superior ao débito suportado nas bandas UHF/SHF para valores mais reduzidos de R. Para distâncias de cobertura mais longas, o débito binário suportado é claramente superior para as bandas de UHF/SHF (em comparação com as bandas de frequência de 38, 60 e 73 GHz). Utilizou-se o LTE-Sim, um simulador de código aberto desenvolvido na Universidade de Bari [4], um simulador orientado a eventos em $C++$, para simulações a nível de pacotes. Foram obtidos resultados para o goodput, a taxa de perda de pacotes (PLR) e o atraso. Considerou-se uma topologia contendo uma picocélula e seis picocélulas ao seu redor, partilhando o mesmo canal. Existem diferenças nos resultados analíticos e de simulação para o débito binário suportado/goodput (sem partilha de espectro), dado que os resultados analíticos não consideram erros nos pacotes, e para um número de utilizadores, superior a $16-18$, o PLR é muito superior mesmo para distâncias mais longas do que $100-150$ m, enquanto para 16 ou menos utilizadores o PLR é apenas elevado para distâncias de cobertura até cerca de 100 m. Estas diferenças entre resultados analíticos e de simulação podem ser facilmente explicadas pelo facto de o número de utilizadores não ser considerado na formulação analítica (assumindo-se condições de saturação), e também devido aos valores elevados do PLR. O goodput e a taxa de perda de pacotes obtidas por simulação são complementares entre si (sendo ligeiramente superior a 2.6 GHz, em comparação com os 3.5 GHz). Pode-se concluir que quanto maior é o raio da célula, maior é o goodput. No entanto, para um número reduzido de utilizadores, o goodput também é reduzido. O atraso máximo é de 55 ms. Consequentemente, por exemplo para aplicação de jogos, a latência é adequada.

Palavras-chave

Pequenas Células, 5G, New Radio, Partilha de Espectro, LTE-Advanced, Modelos de propagação do ITU-R , Capacidade de sistema, Redes Heterogéneas, Ondas milimétricas

Table of Contents

List of Figures

List of Tables

Acronyms

3D	Three Dimensional
3GPP	Third Generation Partnership Project
AC	Average CNIR
ARIB	Association of Radio Industries and Businesses
ATIS	Alliance for Telecommunications Industry Solutions
BBU	BaseBand Unit
BS	Base Station
CA	Carrier Aggregation
CAPEX	Capital Expenditures
CBRS	Citizen Broadband Radio Service
CC	Carrier Component
CCSA	China Communications Standards Association
CIR	Carrier to Interference Ratio
CMU	Carnegie Mellon University
CNIR	Carrier to Noise plus Interference Ratio
COST	European Cooperation n Science and Technology
CQI	Channel Quality Indicator
C-RAN	Cloud-Radio Access Network
DC	Direct Current
DCo	Dual Connectivity
DL	Downlink
eMBB	Enhanced Mobile BroadBand
eNB	Evolved Node B
eLAA	enhanced LAA
eLWA	enhanced LWA
ETSI	European Telecommunications Standards Institute
FDD	Frequency Division Duplex
FSS	Fixed Satellite Services
gNB	Next Generation Node B
HetNets	Heterogeneous Networks
HSPA	High Speed Packet Access
IMT	International Mobile Telecommunications
IoT	Internet of Things
IRACON	Inclusive Radio Communications
ITU-R	International Telecommunication Union-Radiocommunication Sector
LAA	Licensed Assisted Access
LE	Large Enterprise
LoS	Line of Sight
LSA	Licensed Shared Access
LTE	Long-Term Evolution
LTE-A	Long Term Evolution-Advanced
LTE-A	LTE Advanced

LTE-U	LTE-Unlicensed
LWA	LTE-WLAN Aggregation
MCC	Mission Critical Communication
MCS	Modulation and Coding Scheme
mIoT	massive IoT
MLE	Medium to Large-sized Enterprise
M-LWDF	Maximum Largest Weighted Delay First
mMTC	massive Machine Type Communications
mmWaves	Millimeter Waves
MO	Mobile Operator
NR	New Radio
OFDM	Orthogonal Frequency Division Multiplexing
OPEX	Operational Expenditures
OPs	Organizational Partners
PC	Primary Cell
PDSCH	Physical Downlink Shared Channel
PLR	Packet Loss Ratio
RAN	Radio Access Network
RF	Radio Frequency
RRH	Remote Radio Head
RRM	Radio Resource Management
SAS	Spectrum Allocation Server
SC	Small Cell
SCe	Secondary Cell
SHF	Super High Frequency
SINR	Signal to Interference and Noise Ratio
SMB	Small to Medium-sized Business
SME	Small to Medium-sized Enterprises
SOHO	Small Office/Home Office
SON	Self Organizing Networks
TDD	Time Division Duplex
TSDSI	Telecommunications Standards Development Society of India
TTA	Telecommunications Technology Association
TTC	Telecommunication Technology Committee
TTI	Transmission Time Interval
UBI	Universidade da Beira Interior
UE	User Equipment
UHF	Ultra High Frequency
UL	Uplink
UMi LoS	Urban Micro Line of Sight
URLLC	Ultra Reliable and Low Latency Communications
UTRAN/EUTRAN	UMTS Terrestrial Radio Access Network
VoIP	Voice over IP
VTC	Vehicular Technology Conference

Chapter 1

Introdution

So far in the mobile communications sector, most of the base stations have been high power macro base stations. The need to improve network quality, achieve higher data rates and more capacity leads to new innovative techniques. One of those innovations is to use small cell deployments in opposition to the reality. These small cells have recently been deployed in Long Term Evolution Advanced (LTE-A) networks, which include Self Organizing Networks (SON) for automatic configuration and better optimization. Small cell deployments are different from traditional macro cells and their optimization requires new competences and tools. For example, the location is important for the maximal benefit of the small cell, if a small cell is deployed close to the hotspot users, it can offload lot of the macro cell traffic. However, if is not an optimal deployment then it hardly collects any traffic and increases interference.
For radio resource optimization, different deployments are studied, in which different techniques are considered, such as spectrum sharing.
For LTE spectrum sharing usage, in Europe, there are three important frequency bands [11]:

- From 700 until 3500 MHz, aggregated together;
- 5 GHz unlicensed bands for small cells;
- 3.5 GHz for small cells and micro cells.

Another main problem is interference management. Existing interference is critical between macro and small cells in the co-channel deployments, as it can affect every receiver. Nowadays in the 5G New Radio (NR) spectrum usage has been enhanced with one of the biggest and most important novelties, which are the use of millimetre Waves (mmWaves) and the existence of a wider range of spectrum. mmWaves refers to the part of the electromagnetic spectrum between microwave and infra-red waves, i.e. between 30 and 300 GHz.This spectrum is highly used in our daily life, such as in alarms or in sensors for car parking.

1.1 Motivation

Low availability of land base station installations, inter-cell interference, and costly infrastructure are obstacles to increasing network coverage and capacity. Today, both mobile services and applications usage and pace are accelerating. The statistics show beyond any doubt that wireless and cellular network technologies need to be enhanced to support such demands. To provide a solution towards meeting new and ever more stringent end-user requirements, mobile stakeholders are preparing the 5G technology of mobile broadband networking. So 5G will be characterized by ultra-high traffic volume density, ultra-high connection density or ultra-high mobility, moving from cell centric to user-centric technology. The spectrum scarcity nowadays, and the policy of spectrum licensing potentially leads to highly inefficient use of spectrum. Large quantities of the assigned spectrum are used sporadically, while other bands have an increase in spectrum demand, unlicensed and licensed spectrum have possible advantages [12], [13],

which could lead to a greater spectral efficiency. Optimization of the access through the use of shared bands between license holders and secondary users allows the assignment of underutilized spectrum resources, different technologies have been enhanced with the idea of dynamic spectrum sharing through dynamic spectrum allocation. Small Cells (SCs) are adequate candidates to accomplish the regulation in terms of limitation on the maximum transmitter power, therefore sharing between primary and secondary users is useful when the primary system has been give exclusive rights through licensing, as there are generally times and/or locations where other devices could transmit in this spectrum without causing harmful interference.

1.2 State of the Art

1.2.1 Introduction

The cellular wireless communications industry witnessed tremendous growth in the past decade with over four billion subscribers worldwide. It is expected that by 2020 there will be 30 billions connected devices across the world. A lot of operators are evaluating their options, and SC deployments figures high in their priorities with 60% of operator considering them to be an important part of their 4G service [14]. Also low availability of land for base stations installations, inter-cell interference, and costly infrastructure are obstacles to increasing network coverage and capacity. In these Heterogeneous Networks (HetNets) scenarios towards 5G, SC based Cloud Radio Access Networks (C-RAN) [15] are an excellent alternative that offers improved interference control, access control, and manageability. In the next generation, the HetNets will be of such importance with the densification of small cells, and different techniques will be used such as carrier aggregation, spectrum sharing or dual connectivity. This technologies were used by previous generations, such as LTE, and are now being developed/enhanced for 5G NR, in 3rd Generation Partnership Project (3GPP) release 15 and release 16. These topics will be introduced and discussed in this section.

1.2.2 3GPP

The 3GPP [16] joins different telecommunications standard development organizations, such as The Association of Radio Industries and Businesses (ARIB), The Alliance for Telecommunications Industry Solutions(ATIS), China Communications Standards Association (CCSA), The European Telecommunications Standards Institute (ETSI), Telecommunications Standards Development Society (TSDSI), Telecommunications Technology Association (TTA), and Telecommunication Technology Committee (TTC), mostly common known as Organizational Partners (OPs) and provides their members with a stable environment to produce the reports and specifications that define 3GPP technologies, and are organized by stages, as shown in figure 1.1.
3GPP 5G standards were managed by the Radio Access Network (RAN) group's consultative workshop, held in Phoenix, USA, in September 2015. 3GPP is concluded in the conclusion of Release 15 in June/July 2018 and is in the stage 1 of Release 16 as shown in figure 1.1 [3]. While release 15 is focused on deliver the first set of 5G standards, release 16 will fully meet the IMT 2020 requirements for the 5G system. The same way, 4G was called LTE, 5G is called NR. Besides while the 4G and the previous generations of mobile networks interconnected people, by delivering better voice and faster data services [5], 5G NR will connect much more, as presented in figure 1.2.

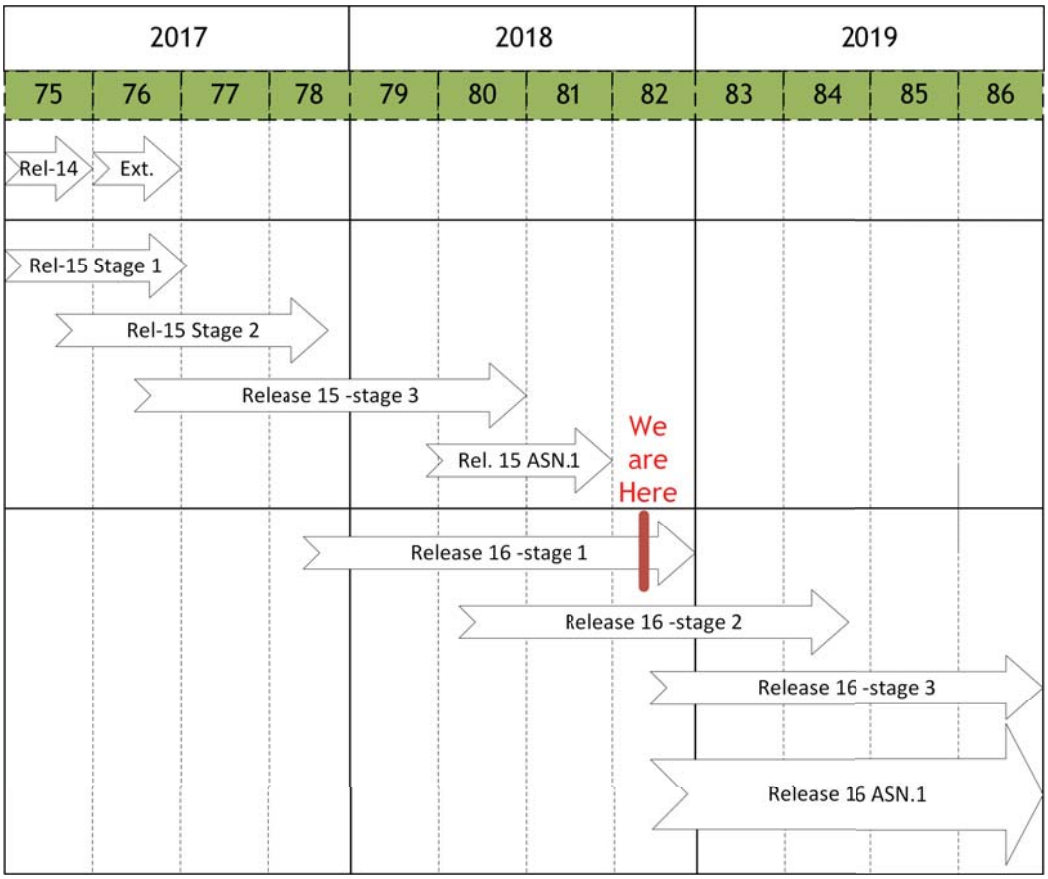

Figure 1.1: 3GPP Timeline

1.2.3 5G New Radio

5G New Radio is an air-interface technology with the objective of improving performance, flexibility [1], [2],[3], scalability and efficiency of current mobile networks. According to 3GPP, 5G New Radio features will be phased, as it is not possible to be standardize all in time for the Rel-15 to complete. To meet the commercial requirements for early 5G deployments in 2018, the first NR specification have been available by the end of 2017, that is, even before the closure of 3GPP release 15.
NR specifications will be divided into two phases:

Phase 1 **- Release** 15 - It addresses a more urgent subset of the commercial needs and is being completed by June/July 2018. The first specification is limited to non-standalone NR operation, implying that NR deployments relies on LTE for initial access and mobility. 5G NR phase 1 will feature both cases, standalone and non-standalone operation mode. In the non-standalone operation mode, the mobile devices use 4G and 5G at the same time [17] , that maintains a connection between LTE evolved Node B (eNB) and 5G next Generation Node B (gNB).
Phase 2 **- Release** 16 - It will addresses all identified user cases and requirements. In 5G NR phase 2 will feature only the standalone case. In standalone operation mode, the mobile devices will only use 5G with gNB.
It was concluded that the standards will address three major use cases each driving a very diverse set of requirements, as follows:

- **Enhanced Mobile BroadBand (eMBB)**

Data-intensive applications, i.e., video streaming or gaming. Different objectives and characteristics for eMBB are represented in the table **??** and figure **??**

- **massive Machine Type Communications (mMTC) or massive Internet of Things (mIoT)**
  mMTC is based on such requirements such as low cost, low energy devices, with small data volumes on a mass scale contrary to enhanced mobile broadband, represented in figure **??**, where peak rates are prioritized. Here the objectives is on scalable connectivity for an increasing number of devices, wide area coverage and deep indoor penetration [18], [2].

- **Ultra-Reliable and Low Latency Communications (URLLC) or Mission Critical Control (MCC)**
  Mobile Networks meets new demands as a lot of communications. Hence, a changes from the wait/background traffic to the interactive real-time communications, so a introduction to significantly reduce end-to-end latency and achieve higher reliability is presented in [19], [20]. Both quality service metrics are needed for safety, as low latency is crucial to ensure some applications such as Autonomous Vehicles, Industry Control/Automation, Virtual Reality or even Remote Robotics for a surgery, as shown in figure **??**. Therefore URLLC will ensure a crucial low latency whether is human-to-human, human-to-machine or machine-machine communication. Also minimizing latency and increasing reliability can open up a lot of profitable new business opportunities for the industry, as well as allow the creation of new applications that will require to have short or almost no delay.

Figure 1.2: 5G NR use cases, extracted from [5], with permission

As shown in figure 1.4, 5G NR is envisioned to support multiple services and devices. There are three main services in 5G NR, as follows:

- Diverse Spectrum;
- Diverse Services and Devices;
- Diverse Deployments.

The most important aspects will be discussed below.

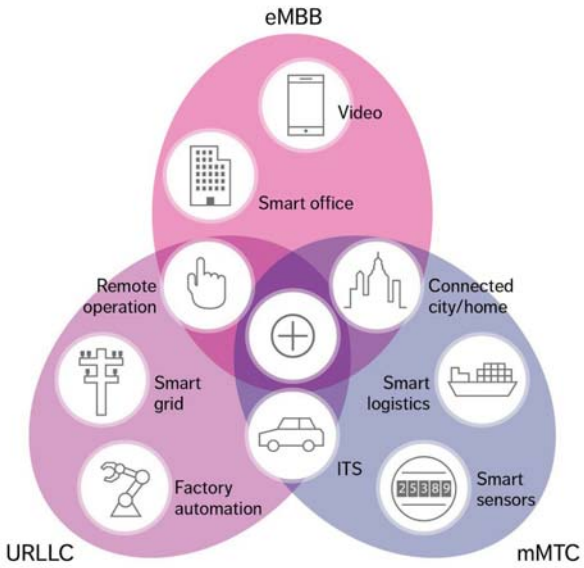

Figure 1.3: 5G use cases and examples of associated applications, extracted from [6], with permission

Figure 1.4: 5G New Radio features extracted from [5], with permission

1.2.3.1 Diverse Spectrum

One of the main features is the diverse spectrum, which can be improved by the use of spectrum sharing, achieving a higher spectrum efficiency. Spectrum sharing becomes increasingly important to the needs for faster data rates and increased network capacity using unlicensed spectrum aggregation techniques in an opportunistic manner. 5G will bring the next level of convergence, with support for licensed, shared and unlicensed spectrum. In 3GPP release 15 New Radio (5G NR) there are four technologies:

- **LTE-Unlicensed/ Licensed Assisted Access (LTE-U/LAA)** - Licensed Assisted Access (LAA) is introduced in 3GPP release 13 as a part of the LTE-A Pro and for deployment in unlicensed spectrum. Unlicensed spectrum is attractive because of the large amount of available spectrum. The main concept is to use carrier aggregation framework and aggregate carriers in licensed and unlicensed bands. However the use of licensed band is subject to

regulatory requirements that could be other systems (e.g., WiFi) sharing the spectrum, so coexistence could be a problem.

- **LTE-WLAN Aggregation (LWA)** - Release 14 enhanced LWA (eLWA) adds support for 60 GHz band (802.11ad and 802.11ay commonly known as WiGig) with 2.16 GHz of bandwidth and UL aggregation.
  Differently then LTE-U/LAA, LWA can be deployed without hardware changes to the network infrastructure equipment and Mobile Devices
- **MulteFire** - Based on release 13 (LAA for DL) and release 14 (eLAA for UL), multefire, uses Voice over LTE (VoLTE), this technology operates with a 20 MHz bandwith and is capable to achieve data rates up to 400 Mbps (using 4x4 MIMO with 256-QAM).
- **Citizen Broadband Radio Service (CBRS)/Licensed Shared Access (LSA)** - LTE at 3.5 GHz, uses the channels 42 [$3550 - 3660$ MHz] and 43 [$3660 - 3700$ MHz] which were used for military radars, as the US Navy and Fixed Satellite Services (FSS). CBRS works differently from other technologies because to use CBRS spectrum, one must individually request and be assigned a band by a Spectrum Allocation Server (SAS) programmatically. The SAS calculates the Radio Frequency (RF) density and channel availability using terrain and radio propagation data before authorizing the request. Finally, when the use of spectrum is no longer required, the channel is freed up for use by other requests [21].

These spectrum sharing techniques are shown in figure 1.5.

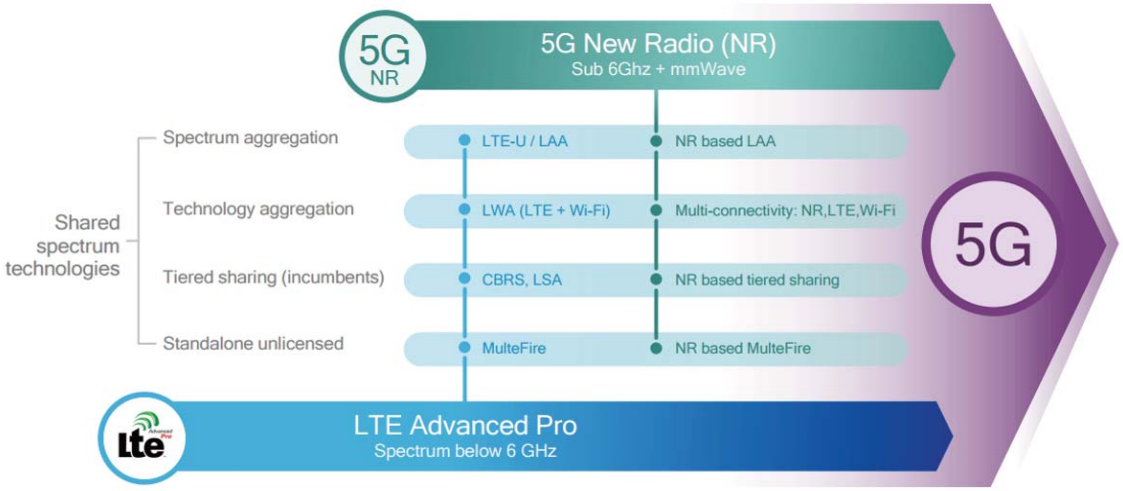

Figure 1.5: Spectrum sharing techniques from 5G NR, extracted from [5], with permission

The other bigger difference from 4G and the previous generations is the **wide array of the spectrum**. Getting the most out of array of spectrum bands, 5G NR will make use of diverse spectrum going from the low bands to mmWaves, as shown in the table 1.1 and in figure 1.6.

Table 1.1: Subcarrier spacing for different frequency ranges

Frequency band	Subcarrier spacing	Maximum bandwidth
0.45 GHz - 6 GHz	15/30/60 KHz	50/100/200 MHz
24 GHz - 52.6 GHz	60/120 KHz	200/400 MHz

Another enhancement proposed for 5G are the **Duplexing Techniques**, i.e., Frequency Division Duplex (FDD), Time Division Duplex (TDD) and Half Duplex, which are enhanced for the new generation.

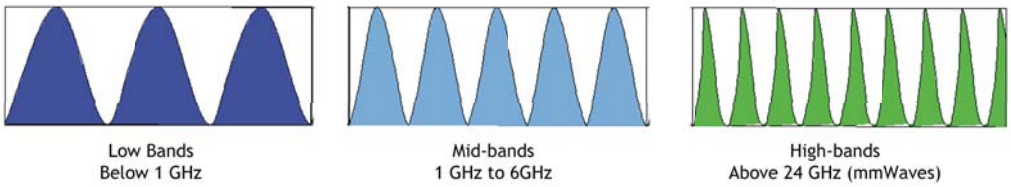

Figure 1.6: Array of spectrum for 5G NR

1.2.3.2 Dual Connectivity

Dual Connectivity (DCo) permits a User Equipment (UE) to communicate simultaneously to a macro and a SC at the same time. With the introduction of this technology there was three enhancements:

- Mobility - DCo via control-plane/user-plane splits between the macro cell and SC layers;
- Throughput - As UE can receive Physical Downlink Shared Channel (PDSCH) transmission of macro and SC at the same time, the throughput will increase;
- Uplink/Downlink (UL/DL) power imbalance - When a UE is becoming closer to a SC it will have a stronger UL connection with the SC, but on other side will have a stronger DL connection with the macro cell due to the higher transmitter power.

The advantage of DCo is the following: as the UE moves between coverage areas of the SCs, it can receive data from the nearest SC at any instant. However since it receives control-plane data from the macro, there is no handover when it switches SCs.

1.2.3.3 Carrier Aggregation

Carrier Aggregation (CA) was first introduced in release 10. CA [7] consists of the aggregation of two or more component carriers (CC) that can have a bandwidth of 1.4, 3, 5, 10, 15, 20 MHz and a maximum of five CC can be aggregated.
There are three types of carrier aggregation, which are the following ones:

- Inter-Band, non-contiguous, as shown in figure 1.7;

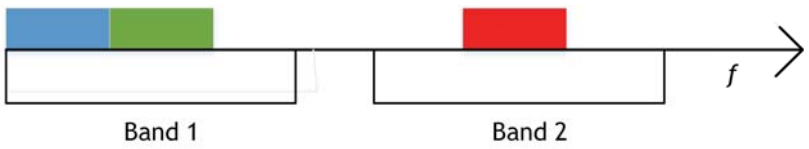

Figure 1.7: Example of Inter-Band, non-contiguous, adapted from [7]

- Intra-Band, non-contiguous, as shown in figure 1.8;
- Intra-Band, contiguous, as shown in figure 1.9.

When the UE received two carriers that are from different frequency bands represented in figure 1.7, it is called inter band non-contiguous.

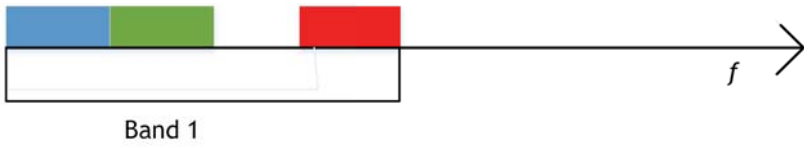

Figure 1.8: Example of Intra-Band, non-contiguous, adapted from [7]

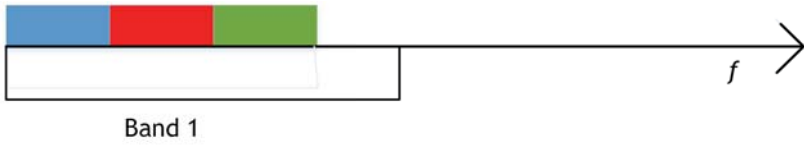

Figure 1.9: Example of Intra-Band, contiguous, adapted from [7]

It is usable when one operator has more than 20 MHz bandwidth available from the same frequency band, where the space between the center frequencies of two contiguous CCs is N*300 KHz, Where N is an integer as seen in 1.9.
This is needed in some countries where there is another operator or other system in between, in this case the CCs are separated by one, or more, frequency gaps as shown in figure 1.8.
In release 10, both bands have to be FDD bands or TDD bands but in release 12 it was introduced an enhancement called FDD-TDD carrier aggregation, allowing to extent the carrier aggregation framework in such a way that the Primary Cell (PC) could be on FDD band and Secondary Cell (SCe) could be on a TDD band or vice versa.

1.2.3.4 Heterogeneous Networks and Small Cells

Nowadays, wireless technologies have enabled new services, such as video games or videos, that have amused human beings and transformed social interactions. The services we use today consume more bandwidth than before and we want them fast, reliable, and affordable.
High capacity can be achieved by improving spectral efficiency, employment of more spectrum and the increase of network density. One of the ways to get more network density is through deploying an overlay network of SCs over the macro coverage area, in which a SC can be an indoor femtocell or an outdoor picocell. For the deployment we can have a compact BS or a distributed antenna system controlled by a central controller. The different types of SCs have low transmitter power/coverage. Together with macro cells, they are referred to as Hetnets, as shown in figure 1.10.
Deploying an overlay of SCs in regions is which there is a heavy data demand is an adequate solution and solve the problem, because SCs can offload data from the macro coverage area, improve frequency reuse, as they can adapt to spatio-temporal variations in the traffic using dynamic interference management techniques and are more energy efficient. A macrocell needs a power amplifier with a fixed Direct Current (DC) power supply, even if there is no data being transmitted. This part translates to a higher energy consumption, so if we use a SCs, the low transmitter power of the SC may reduce the impact of both. The deployment of pico cells reduces the consumption by 25%-30% compared to macrocell-only baseline.
SCs are low-powered cellular radio access nodes that operate in licensed and unlicensed spectrum that have a range of 10 meters to a few kilometers with different applications and achievable range. SCs can be femtocells, picocells or microcells, as shown in figure 1.11.

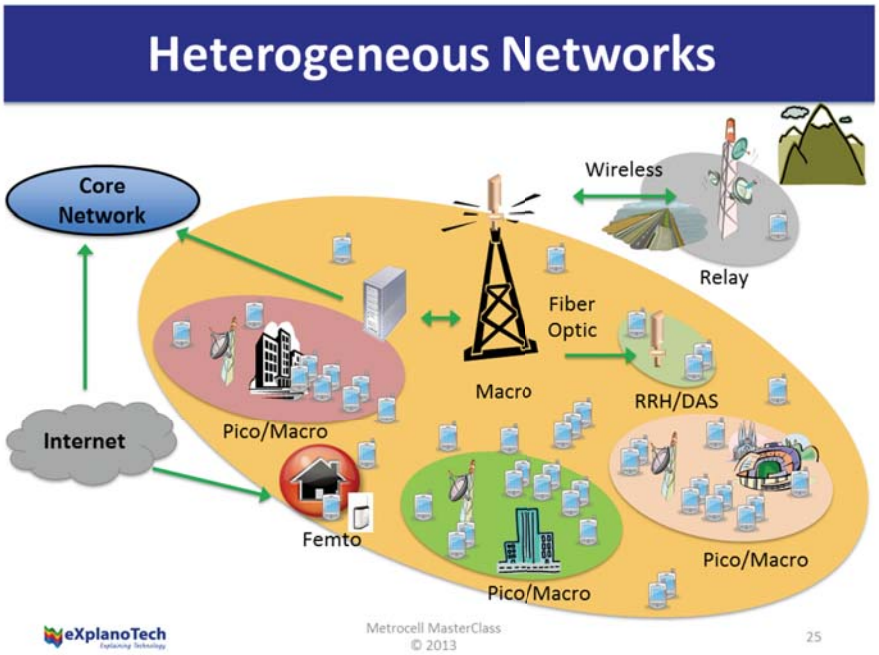

Figure 1.10: Heterogeneous Networks, extracted from [8]

Picocells

Supporting up to 100 users over a range of less than 229 m, picocells are frequently deployed indoors to improve poor wireless and cellular coverage within a building, such as an office floor or retail space.

These SCs offer enhanced capacities, better coverage areas and are deployed by operators to target a specific public, such as railway stations, aircraft, or music shows but can also been used indoors to improve poor wireless and cellular coverage within a building, although they are open to public, there could be a preferential grade of service for police or public safety personnel. To increase coverage over a large area, the operator needs to install multiple picocells. Picocells are specific to a particular wireless technology, such as LTE or High Speed Packet Access (HSPA).

Femtocells

Femtocells are small stand-alone low power nodes that are typically installed indoors, can be user installed to improve coverage area within a small vicinity, such as home office or a dead zone within a building. Unlike picocells and microcells are available only to paid subscribers, with coverage and number of users depending on the nature of their installation and are only design to support only a handful of users and is only capable of handling a few simultaneous call sessions. Residential femtocells can be categorized as Small Office/Home Office (SOHO), and enterprise femtocells can be categorized as Small to Medium-sized business (SMB), Small to Medium-sized Enterprises (SME), Medium to Large-sized Enterprise (MLE) and Large Enterprise (LE).

Microcells

Microcells are difficult to precisely distinguish from picocells, but their coverage area is the prime delineator. Microcells can cover areas less than a mile in diameter and uses power control to limit this radius. Microcells can be deployed temporarily in anticipation of high-traffic within a limited area, such as a sporting event, however, they are also installed as a permanent feature

of mobile cellular networks.

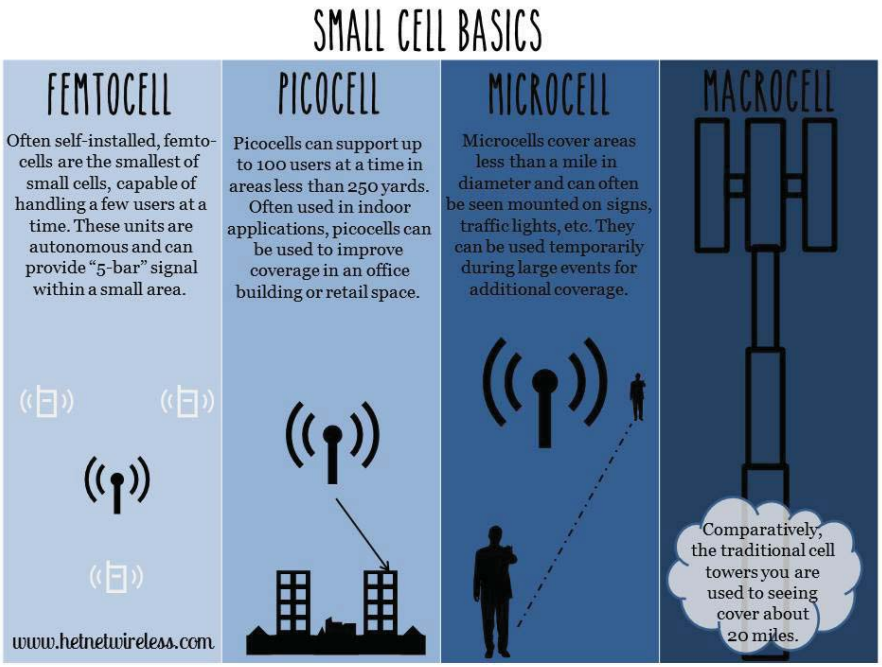

Figure 1.11: Small Cells Basics, extracted from [9]

1.2.3.5 Small Cell Deployment

The keys aspects and challenges for small cell deployment are the following ones:

- Co-channel and separate frequency deployment of SCs;
- Macro coverage;
- SC density;
- Outdoor and indoor;
- Backhaul connectivity;
- Traffic characteristics.

Several solutions have been standardized in LTE releases 10 and 11. Along release 12, the following three scenarios have been studied:

- **Scenario 1** - SCs deployed in the same carrier as the macrocell;
- **Scenario 2** - SCs deployed with one carrier and the macrocell deployed with another carrier;
- **Scenario 3** - Stand-Alone SCs.

1.2.3.6 Future Perspectives

The mobile traffic is increasing year after year, strategy analytics estimated that mobile traffic grow by 100% in 2012, and in 2017 we already have an increase of 400% of data traffic. Because of such increasing the profit margin of most operators have also been decreasing globally, and there are two main reasons:

- Flat rate pricing policies that prevent the mobile data revenues of an operator to scale proportionally with the increasing usage of mobile broadband data;
- The cost, such as Capital Expenditures (CAPEX) and Operational Expenditures (OPEX), in the Operation and maintenance expenditures for the deployment of more base stations with the objective to provide more capacity and enhanced coverage.

Because of the cost reduction, energy efficiency and a better capacity, SC Hetnets are therefore being increasingly adopted by wireless operators globally, as shown in figure 1.12, a forecast from market research future.

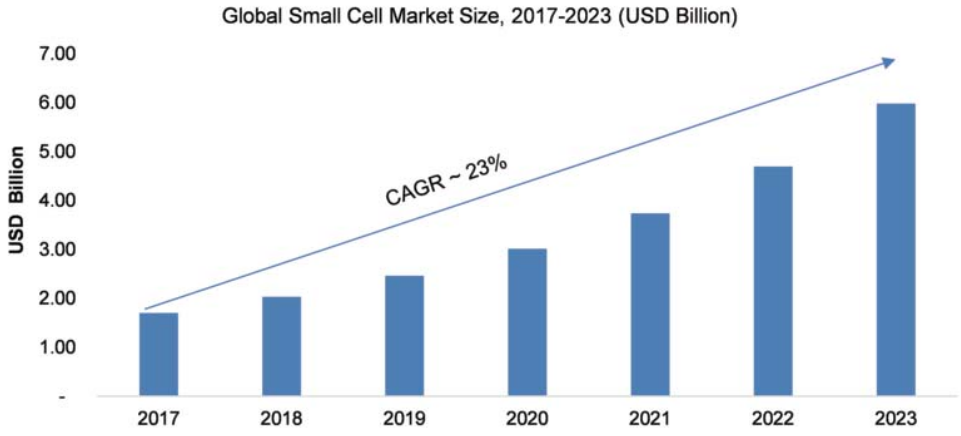

Figure 1.12: View Chart for revenues from the small cells market, extracted from [10]

1.3 Objectives and Approach

This MSc dissertation proposes the study of small cell deployments, considering different scenarios, with and without spectrum sharing. As such, it is possible to study the behaviour of these small cell network and analyze the lessons learned from the research. The main objective is using spectrum sharing to obtain high spectral efficiency, through the massification of small cells, as well as the optimization of the small cell deployments. The proposal is to address frequency assignment locally, only considering interference from co-channel SCs in a given neighbourhood while evaluating performance. As adaptive Modulation and Coding Schemes (MCSs) are present one will propose a dynamic procedure to define Signal to Interference plus Noise Ratio/carrier-to-noise-plus-interference-ratio (SINR/CNIR) threshold for the MCS that define the cell range. A given frequency will be assigned in each of the cells. If the SINR/CNIR overcomes the established threshold then a new frequency will be assigned. Using the database from wigle.net, it is possible to determine the position of the existing infrastructure and consideration of the choice of the placement/deployment of the SC Layer eNBs. Frequency assignment algorithms with and without spectrum sharing will then be proposed and applied to the new cellular topology, from

a range of existing or new proposed algorithms with implications of Remote Radio Head (RRH) and SCs with Spectrum Sharing. For this aim we will need an analytical formulation of the CNIR equations and underlying PHY and supported throughput in a macro and micro-urban environment using the Wi-Fi Hotspots from wigle.net as SCs. The average CNIR in the SC layer of the HetNets aims at determining the values of the transmitted power that correspond to a target threshold for the CNIR_min. With this analytical formulation we will have the variation of the Downlink (DL) CNIR from/at a user equipment and with the obtained values for the normalized transmitter power, the analysis of the cell capacity will be based on [22]. Scenarios with exclusive spectrum access and spectrum sharing will be explored. Spectrum sharing assumes that two or more mobile operators/carriers have dedicated spectrum for macro cellular layer while SCs will use exclusive shared spectrum (by paying a fee) or share the access to non-licensed spectrum in an opportunistic manner as in appendix A.

1.4 Contributions

The main contributions of this MSc dissertation is the elaboration of the analytical formulation for the Average CNIR/SINR while considering the two-slope propagation model at the Ultra High Frequencies/Super High Frequencies (UHF/SHF) bands which is shown in section 2.5, and the performance evaluation of SC deployments through simulation with LTE-Sim. This dissertation is based on research on the performance evaluation of SCs deployments from Instituto de Telecomunicações - Covilhã, and is contributing to the CONQUEST Carnegie Mellon University (CMU) Portugal exploratory project (CMU/ECE/0030/2017). Other contributions were the formulations of different performance parameters, such as:

- CNIR/SINR and Physical throughput;
- 3D view of the PHY throughput mapped into MCSs and 3D view of the Intermittent scenario performance evaluation parameters.

The underlying programs and functions that implement the proposed algorithms are explained and presented in the appendix B. There has also been an elaboration of a proposal called ”Mapping Tool” which was an initial idea for planning and frequency assignment, has not really been used yet to obtain results. The outcome from this research has already been presented in the following venues:

- A poster presentation on ”Insights on Spectrum Sharing in Heterogeneous Networks with Small Cells” in the seminar from the Portuguese Thematic Network on Mobile Communications of 2/2/2018;
- A recent results paper [**?**] in 2018 IEEE 87th Vehicular Technology Conference (VTC) Spring Porto of 3–6/6/2018;
- A temporary document TD(18)07020 in the Cartagena meeting of the COST CA 15104 the Inclusive Radio Communications (IRACON) European Cooperation in Science and Technology (COST) CA15104 of 30/5-1/6/2018.

1.5 Outline of the Dissertation

To reach the objectives, in this chapter first a brief state of art was presented, where topics such as 5G NR or 3GPP vision are discussed. Then, in chapter 2 a scenario is purposed with a central cell, 6 co-channel cells from the same mobile operator, one cell for a second mobile operator, and a central cell with a user walking from the cell center to the cell edge, considering the reuse patterns $k = 3$ and $k = 4$. Different performance metrics will be considered such as SINR/CNIR, Physical throughput and Supported throughput. These performance metrics will be compared between the different cells from the other operator and the results will be discussed, a scenario of the mmWaves will be added, with the objective of comparing the performance between mmWaves and UHF/SHF. In chapter 3 these same scenario will be simulated in a open source framework called LTE-Sim, where a real simulation can be simulated with different number of users, using different services such as Voice over IP (VoIP) or data extensive, for example video streaming, these users will walk randomly in the cell, and the results of these simulation will be discussed and compared with the results that were obtained with the propagation model on Matlab. Finally the simulation will be considered and a comparison between Matlab and LTE-Sim is performed. In the packet level simulations not only goodput is obtained but also Packet Loss Ratio (PLR) and delay, while considering the 3GPP threshold of 150 ms for the maximum delay [23]. Conclusions are drawn in 4, where the lessons learned are briefly discussed and suggestions for future research are presented.

Chapter 2

Cellular Radio and Network Optimization

2.1 Propagation Model

In the past few years we have witnessed a phenomenal growth in the wireless industry, in terms of both mobile technology and subscribers. With all this terms growing up, several propagation models have been developed and proposed for cellular systems operating in different environments (outdoor, urban, suburban, rural and indoor). The aim of cellular wireless network design is to optimize system capacity. The path loss model represents the reduction of the signal when it is propagating from the transmitter to the receiver, in this case from the User Equipment (UE) to the Base Station (BS), as shown in figure 2.1. There are three different pathways to model the path loss, as follows:

- Deterministic;
- Stochastic;
- Empirical.

In this work, the chosen propagation model is ITU-R-2135 model [24] applied to Urban Micro (UMi) Scenarios Line of Sight (LoS) with a minimum distance of 10 m. The UMi LoS propagation model is a two slope model that contains a dual slope pathloss and where the equations are as follows:

$$\begin{aligned} PL1 &= 22\log_{10}(d) + 28 + 20\log_{10}(f), when\ d \leq d'_{BP} \\ PL2 &= 40\log_{10}(d) + 7.8 - 18\log_{10}(h'_{BS}) - 18\log_{10}(h'_{UE}) + 2\log_{10}(f), when\ d > d'_{BP} \end{aligned} \quad (2.1)$$

where d is the distance in m, f is the frequency in GHz, h_{BS} is the height of the base station in m, h_{UE} is the height of the user equipment in m, (h_{BS} and h_{UE} are based on the following variables $h_{BS} = 10m$ and $h_{UE} = 1.5m$ that become $h'_{UE} = h_{UE} - 1$ and $h'_{BS} = h_{BS} - 1$), and d'_{BP}, the breakpoint distance, is given by:

$$d'_{BP} = \frac{4h'_{UE}h'_{BS}f}{c} \quad (2.2)$$

where f is the centre frequency in Hz, $c = 3.0 * 10^8$ in m/s which is the propagation velocity in free space, h'_{UE} and h'_{BS} are the effective antenna heights at the BS and the UE in m. For 2.6 GHz the breakpoint distance is 156 m and for 3.5 GHz is 210 m. The received power is computed using the Friis equation shown in equation 2.3.

$$P_R = P_E + G_E + G_R - PL \quad (2.3)$$

where P_R is the received power given in dBW, P_E is the transmitter power given in dBW, G_E and G_R are the transmitter and receiver gains of the antennas in dBi respectively and PL is the pathloss values given in dB.

2.2 Cellular Topology

This section presents a description of a cellular layer to make coverage and frequency planning. In a fully symmetrical hexagonal plan with a given frequency reuse distance, D, with $D = \sqrt{3k}R$, and R is the radius of the hexagonal cell. Inside of the central cell, will be a user going from the cell center to the cell edge, $10 <= d <= R$. One consider two values for the reuse pattern, which are $k = 3$ and $k = 4$. The $\frac{C}{I}$ formulation is given by the following equation:

$$\frac{C}{I} = \frac{1}{2(rcc+1)^{-\gamma} + 2(rcc)^{-\gamma} + 2(rcc-1)^{-\gamma}} \quad (2.4)$$

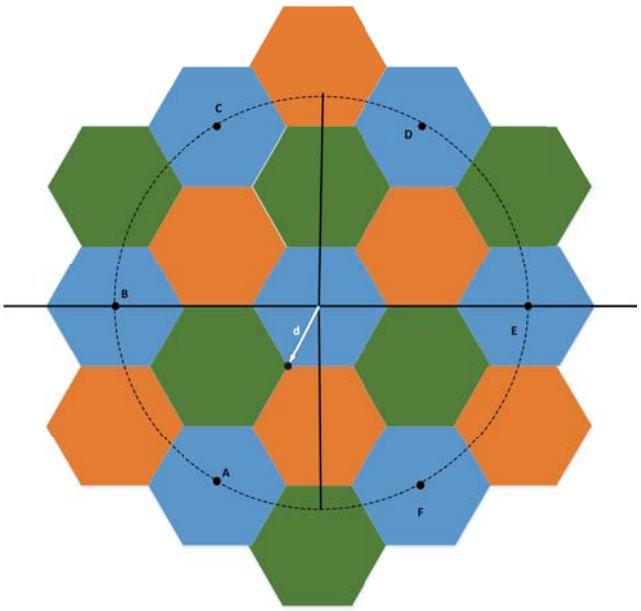

Figure 2.1: Scenario with $k = 3$, where first interference ring with six interferers are represented

2.2.1 Cellular Planning Scenario with first ring of interference without shared spectrum scenario

The coordinates of UE for the worst case scenario are $(\frac{-R}{2}; \frac{-\sqrt{3}R}{2})$, while for a general scenario are $(\frac{-d}{2}; \frac{-\sqrt{3}d}{2})$. To compute the distance between the interferents and the UE, a equation is given by $d = \sqrt{(x-x_0)^2 + (y-y_0)^2}$.

In the first part it was considered a reuse pattern $k = 3$, and only one interference ring, so we have six interferers (SC eNBA, SC eNBB, SC eNBC, SC eNBD, SC eNBE, SC eNBF).

Figure 2.1 represents the six interferers and above we have the distance for the worst case scenario:

- For the interferent SC eNBA the coordinates are $(\frac{-3R}{2}; \frac{-3\sqrt{3}R}{2})$;
- For the interferent SC eNBB the coordinates are $(-3R; 0)$;
- For the interferent SC eNBC the coordinates are $(\frac{-3R}{2}; \frac{3\sqrt{3}R}{2})$;
- For the interferent SC eNBD the coordinates are $(\frac{3R}{2}; \frac{3\sqrt{3}R}{2})$;
- For the interferent SC eNBE the coordinates are $(3R; 0)$;
- For the interferent SC eNBF the coordinates are $(\frac{3R}{2}; \frac{-3\sqrt{3}R}{2})$.

The computation of the distance between UE and SC eNBA is as follows:

$d = \sqrt{(\frac{-R}{2} + \frac{3R}{2})^2 + (\frac{-\sqrt{3}R}{2} + \frac{3\sqrt{3}R}{2})^2}$
$d = \sqrt{R^2 + (\sqrt{3}R)^2}$
$d = 2R$
As we need to define distance as $D + xR$ we have:
$3R + xR = 2R$
$x = -1$
So, one obtains $d = D - R$

The computation of the distance between UE and SC eNBB is as follows:

$d = \sqrt{(\frac{-R}{2} + 3R)^2 + (\frac{-\sqrt{3}R}{2} - 0)^2}$
$d = \sqrt{7}R$
As we need to define distance as $D + xR$ we have:
$3R + xR = \sqrt{7}R$
$x = -0.35$
So, one obtains $d = D - 0.35R$

The computation of the distance between UE and SC eNBC is as follows:

$d = \sqrt{(\frac{-R}{2} + \frac{3R}{2})^2 + (\frac{-\sqrt{3}R}{2} - \frac{3\sqrt{3}R}{2})^2}$
$d = \sqrt{13}R$
As we need to define distance as $D + xR$ we have:
$3R + xR = \sqrt{13}R$
$x = 0.61$
So, one obtains $d = D + 0.61R$

The computation of the distance between UE and SC eNBD is as follows:

$d = \sqrt{(\frac{-R}{2} + \frac{-3R}{2})^2 + (\frac{-\sqrt{3}R}{2} - \frac{3\sqrt{3}R}{2})^2}$
$d = 4R$
As we need to define distance as $D + xR$ we have:
$3R + xR = 4R$
$x = 1$;
So, one obtains $d = D + R$

The distance between interferers SC eNBE, SC eNBF and the UE are equal to the distance between interferers SC eNBC and SC eNBB. Hence the result of the calculated distances is shown in figure 2.2.

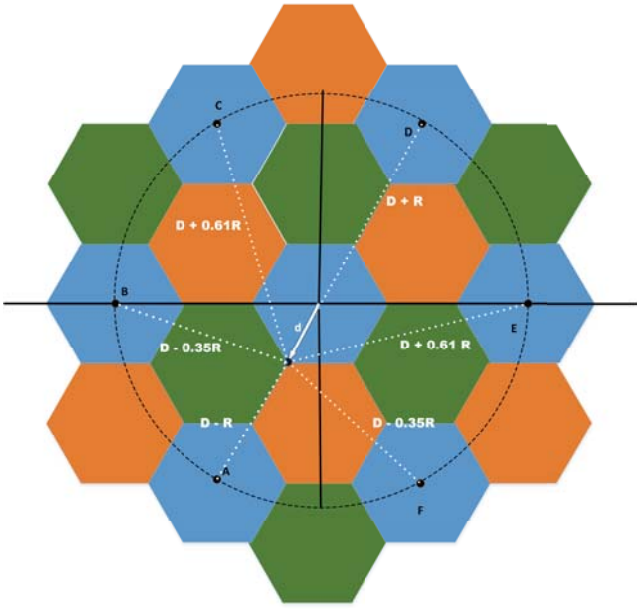

Figure 2.2: Cell planning for $k = 3$ with distance calculated for the worst case scenario

So the CIR formula for the worst case scenario, user at the cell edge, is as follows:

$$\frac{C}{I} = \frac{1}{2(D-0.35R)^{-\gamma} + (D+R)^{-\gamma} + (D-R)^{-\gamma} + 2(D+0.61R)^{-\gamma}} \quad (2.5)$$

The general CIR formula without sharing is as follows:

$$\frac{C}{I} = \frac{1}{2(d_{UB})^{-\gamma} + (D+d)^{-\gamma} + (D-d)^{-\gamma} + 2(d_{UE})^{-\gamma}} \quad (2.6)$$

where d_{UB} is the distance between the user and the co-channel SC eNBB and d_{UE} is the distance between the user and the co-channel SC eNBE. These distances are given by:

$$d_{UB} = \sqrt{(\frac{-d}{2} - 3R)^2 + (\frac{-\sqrt{3}d}{2})^2} \quad (2.7)$$

$$d_{UE} = \sqrt{(\frac{-d}{2} + 3R)^2 + (\frac{-\sqrt{3}d}{2})^2} \quad (2.8)$$

For a reuse pattern $k = 4$, represented in the figure 2.3, we have the six interferers. The UE coordinates are the same as for $k = 3$, and we also obtain the distance for the worst case scenario:

- For the interferent SC eNBA the coordinates are $(-3R; R\sqrt{3})$;
- For the interferent SC eNBB the coordinates are $(-3R; -R\sqrt{3})$;
- For the interferent SC eNBC the coordinates are $(0; -2R\sqrt{3})$;

- For the interferent SC eNBD the coordinates are $(3R; -R\sqrt{3})$;
- For the interferent SC eNBE the coordinates are $(3R; R\sqrt{3})$;
- For the interferent SC eNBF the coordinates are $(0; 2R\sqrt{3})$.

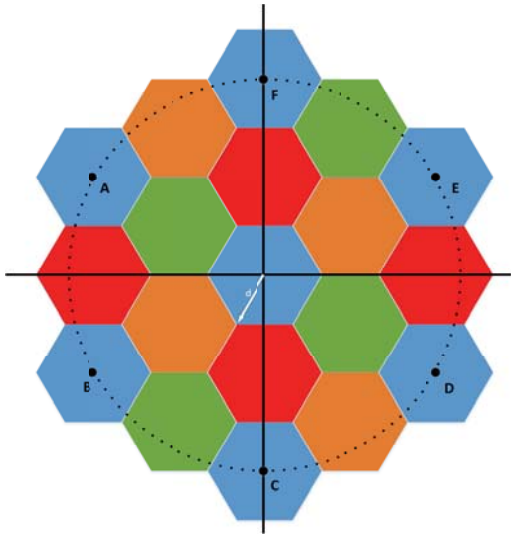

Figure 2.3: Scenario with $k = 4$, first interference ring and six interferers

The computation of the distance between UE and SC eNBA is as follows:

$d = \sqrt{(\frac{-R}{2} + 3R)^2 + (\frac{-\sqrt{3}R}{2} - R\sqrt{3})^2}$
$d = \sqrt{\frac{25R^2}{4} + (\frac{27R^2}{4})^2}$
$d = \sqrt{13}R$
As we need to define distance as $D + xR$ we have:
$\sqrt{12}R + xR = \sqrt{13}R$
$x = 0.14$
So, one obtains $d = D + 0.14R$

The computation of the distance between UE and SC eNBB is as follows:

$d = \sqrt{(\frac{-R}{2} + 3R)^2 + (\frac{-\sqrt{3}R}{2} + R\sqrt{3})^2}$
$d = \sqrt{\frac{25R^2}{4} + (\frac{3R^2}{4})^2}$
$d = \sqrt{7}R$
As we need to define distance as $D + xR$ we have:
$\sqrt{12}R + xR = \sqrt{7}R$
$x = -0.81$
So, one obtains $d = D - 0.81R$

The computation of the distance between UE and SC eNBE is as follows:

$d = \sqrt{(\frac{-R}{2} - 3R)^2 + (\frac{-\sqrt{3}R}{2} - \sqrt{3}R)^2}$
$d = \sqrt{\frac{49R^2}{4} + (\frac{27R^2}{4})^2}$
$d = \sqrt{19}R$

As we need to define distance as $D + xR$ we have:
$\sqrt{12}R + xR = \sqrt{19}R$
$x = 0.89$
So, one obtains $d = D + 0.89R$

Interferers SC eNBC, SC eNBD and SC eNBF are equal to interferers SC eNBB, SC eNBA and SC eNBE so the result of the computed distances is shown in figure 2.4.

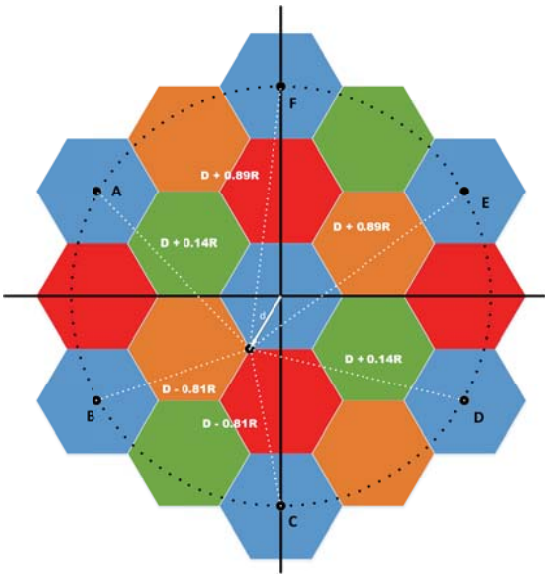

Figure 2.4: Cell planning for $k = 4$ with distance calculated for the worst case scenario

So the CIR formula for the worst case scenario, with the user at the cell edge, is as follows:

$$\frac{C}{I} = \frac{1}{2(D + 0.14R)^{-\gamma} + 2(D - 0.81R)^{-\gamma} + 2(D + 0.89R)^{-\gamma}} \quad (2.9)$$

While the general CIR formula without sharing, is as follows:

$$\frac{C}{I} = \frac{1}{2(d_{UC})^{-\gamma} + 2(d_{UD})^{-\gamma} + 2(d_{UF})^{-\gamma}} \quad (2.10)$$

where d_{UC} is the distance between the user and the co-channel SC eNBC, d_{UD} is the distance between the user and the co-channel SC eNBD and d_{UF} is the distance between the user and the co-channel SC eNBF.

These distances are given as follows:

$$d_{UC} = \sqrt{(\frac{-d}{2})^2 + (\frac{-\sqrt{3}d}{2} + 2R\sqrt{3})^2} \quad (2.11)$$

$$d_{UD} = \sqrt{(\frac{-d}{2} - 3R)^2 + (\frac{-\sqrt{3}d}{2} + R\sqrt{3})^2} \quad (2.12)$$

$$d_{UF} = \sqrt{(\frac{-d}{2})^2 + (\frac{-\sqrt{3}d}{2} - 2R\sqrt{3})^2} \quad (2.13)$$

2.2.2 Cellular Optimization and Planning with Spectrum Sharing

In scenarios with spectrum sharing, it is expected to have small cells from different Mobile Operators (MO) placed close to each other. So in addition to the six co-channel interferers has been added one small cell from a different operator. Figure 2.5 illustrates the position of the six interferers considered. The interference that outcomes from an interferer placed at the East corner is equal to the Northwest corner (represented in blue and pink, respectively). Also in terms of distance, the interference that outcomes from an interferer placed at the West corner is equal to Southeast corner (represented in yellow and purple, respectively). For this reason, only four of the six cases were analysed. The four cases are:

1 - In the first case, the interferer (SC eNB from MO #2) is in the Southeast of the central cell, causing interference in the central cell, on top of the other six co-channel cells at the first ring of interference (from MO #1), represented in purple;

2 - In the second case, the interferer from MO #2 is in the left hand side of the central cell, in the Southwest of the central cell, causing interference in the central cell, on top of the other six co-channel cells at the first ring of interference (from MO #1), represented in black (this is the worst-case);

3 - In the third one, the SC from MO #2 is in the East of the central cell, causing interference in the central cell, on top of the other six co-channel cells at the first ring of interference (from MO #1), represented in blue;

4 - In the fourth case, the SC from MO #2 is in the Northeast of the central cell, causing interference in the central cell, on top of the other six co-channel cells at the first ring of interference (from MO #1), represented in red.

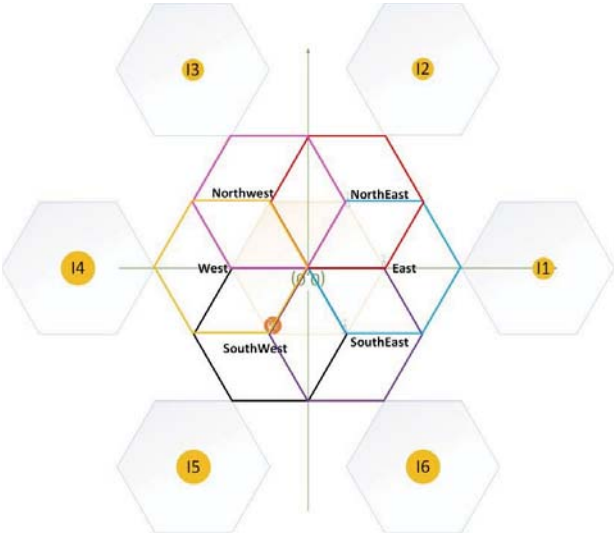

Figure 2.5: Definition of the six interferers for the sharing scenario, where different cases are superimposed

Considering sharing corresponds to add $d_{sharing}$ in the denominator of the CIR formula, where $d_{I-sharing}$ is the same for $k = 3$ and $k = 4$ and is computed as follows:

- East Interferer:

$$\sqrt{(R+\frac{d}{2})^2+(\frac{\sqrt{3}}{2})^2} \quad (2.14)$$

- Northeast Interferer:

$$\sqrt{(\frac{R}{2}+\frac{d}{2})^2+(\frac{\sqrt{3}d}{2}+\frac{\sqrt{3}R}{2})^2} \quad (2.15)$$

- Southwest Interferer:

$$R-d \quad (2.16)$$

- Southeast Interferer:

$$\sqrt{(\frac{R}{2}+\frac{d}{2})^2+(\frac{\sqrt{3}d}{2}-\frac{\sqrt{3}R}{2})^2} \quad (2.17)$$

For $k=3$ we use the general CIR formula with sharing,which is given by:

$$\frac{C}{I}=\frac{1}{2(d_{UB})^{-\gamma}+(D+d)^{-\gamma}+(D-d)^{-\gamma}+2(d_{UE})^{-\gamma}+d_{sharing}^{-\gamma}} \quad (2.18)$$

While for $k=4$ is given by:

$$\frac{C}{I}=\frac{1}{2(d_{UC})^{-\gamma}+2(d_{UD})^{-\gamma}+2(d_{UF})^{-\gamma}+d_{sharing}^{-\gamma}} \quad (2.19)$$

2.3 Comparison Between Performance Parameters for Different Transmitter Powers

In the performance evaluation, different transmitter powers have been considered for the 3.5 GHz and 2.6 GHz frequency bands to compensate coverage issues. The consideration of low power at 2.6 GHz is due to the fact that one frequency is higher than the other. Hence to choose a more adequate power for each band, different values for transmitter power are shown in table 2.1.
To test different behaviours the transmitter powers from the table 2.1 were used to compute performance parameters, such as:

- CNIR;
- Physical throughput;
- Average CNIR/SINR;
- Pathloss;
- Received power.

Table 2.1: Different transmitter powers considered for both frequencies

Transmitter power [dBW] (2.6 GHz)	Transmitter power [dBW] (3.5 GHz)
-16	-10
-13	-7
-10	-4
-7	-1
-4	2
-1	5
2	8

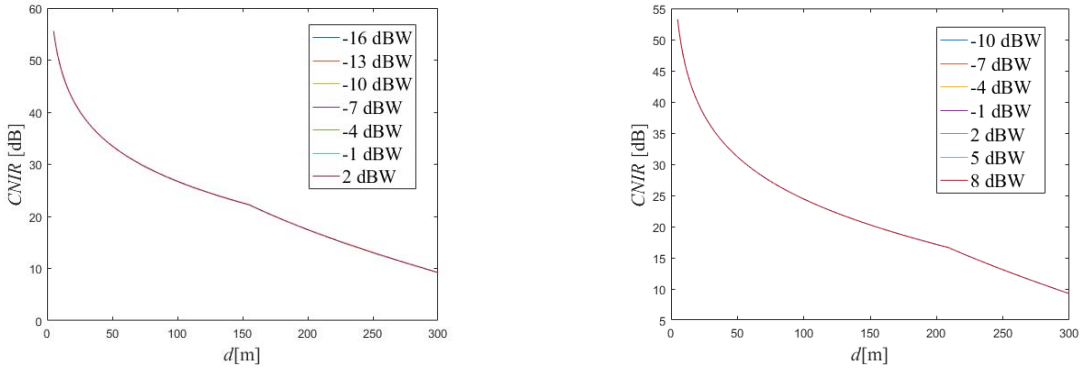

(a) 2.6 GHz (b) 3.5 GHz

Figure 2.6: Different CNIR values for different transmitter powers

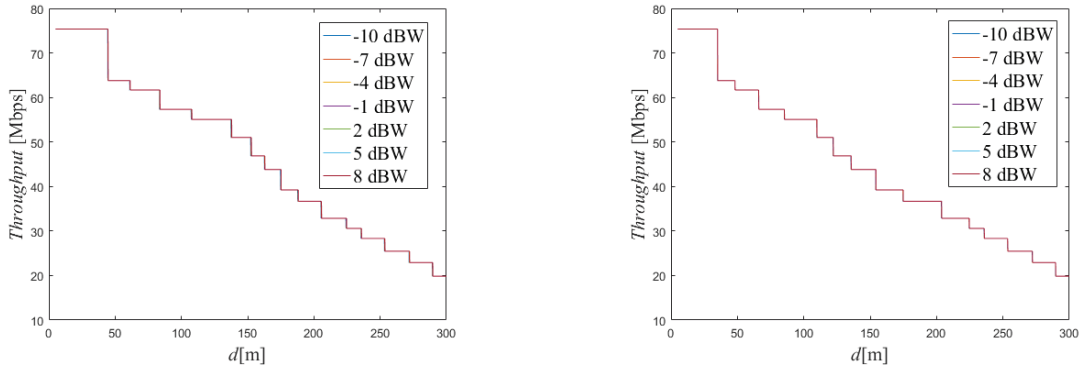

(a) 2.6 GHz (b) 3.5 GHz

Figure 2.7: Different Physical throughput values for different transmitter powers

The first parameters analyzed were the CNIR and Physical throughput. However, it is shown that both are not dependent of the transmitter power, being the CNIR only limited by noise, as it is shown in figure 2.6a and figure 2.6b. As the Physical throughput is dependent on the CNIR, will be the same for different transmitter powers, as shown in figure 2.7a and figure 2.7b.

If the CNIR values are the same for every value of the transmitter power, the average CNIR will be the same too as it will be shown in section 2.8.

A comparison between the two bands for the pathloss and the received power, is shown in figure 2.8a and figure 2.8b. The higher the pathloss, the less the received power for they are complementary. In this case, the pathloss for the 3.5 GHz band is higher than for the 2.6 GHz band. However a higher transmitter power is needed to generate similar coverage. The values

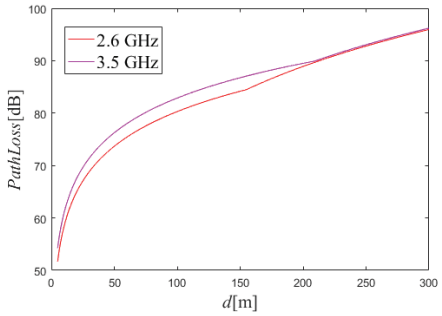

(a) Pathloss per distance comparison

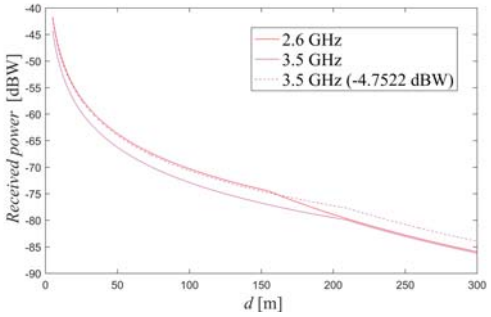

(b) Comparison of received power between 2.6 GHz and 3.5 GHz

Figure 2.8: Pathloss and received power

were found as follows:
First it was considered for this purpose the receiver power in the own/central cell. The average received power was computed for both bands using the same transmitter power, -7 dBW, and the 3.5 GHz breakpoint distance, both for computing purposes, as follows:

$$AveragePR_{2.6\text{GHz}} = -69.0385\,\text{dBW} \quad (2.20)$$

$$AveragePR_{3.5\text{GHz}} = -71.2863\,\text{dBW} \quad (2.21)$$

$$AveragePR_{2.6\text{GHz}} - AveragePR_{3.5\text{GHz}} = 2.2478\,\text{dBW} \quad (2.22)$$

$$PT_{2.6\text{GHz}} = -7\,\text{dBW} \quad (2.23)$$

$$PT_{3.5\text{GHz}} = -4.7522\,\text{dBW} \quad (2.24)$$

In order to obtain values of average received power that are to be almost the same in the two bands, their transmitter power can not be exactly the same as shown in figure 2.8b because of the two slope model, if we apply the difference of -2.2478 dBW, we obtain a transmitter power of -4.7522 dBW, which is higher than the transmitter power at 2.6 GHz band.
After all the comparisons and computing the results, the received powers for both bands have been decided. The parameters considered in the computations for 2.6 GHz and 3.5 GHz are shown in table 2.2.

2.4 CNIR and Physical Throughput

The values for the MCS, used to map CNIR into PHY throughput are represented in the table 2.3. To study the interference between the co-channel cells, a Matlab program called oBStoSS was created. The dependence of CNIR and the Physical throughput for $k = 4$ between co-channel cells have been obtained on the distance $10 \leq d \leq R$, as well as with the MOs (sharing) were

Table 2.2: Parameters considered

Parameters	2.6 GHz	3.5 GHz
Transmitter power [dBW]	-7	-4.7522
Transmitter gain [dBi]	17	17
Receiver gain [dBi]	0	0
Bandwidth [MHz]	20	20
Noise figure [dB]	5	5
Height(Base Station) [m]	9	9
Height(User Equipment) [m]	0.5	0.5
Propagation exponent 1[γ]	$d < d_{BP}$, γ = 2.2	$d_{BP} < d$, γ = 2.2
Propagation exponent 2[γ]	$d \geq d_{BP}$, γ = 4.0	$d_{BP} \geq d$, γ = 4.0

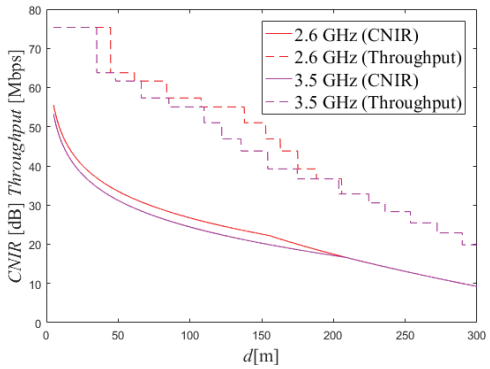

(a) No Interferer for both bands with $k = 3$

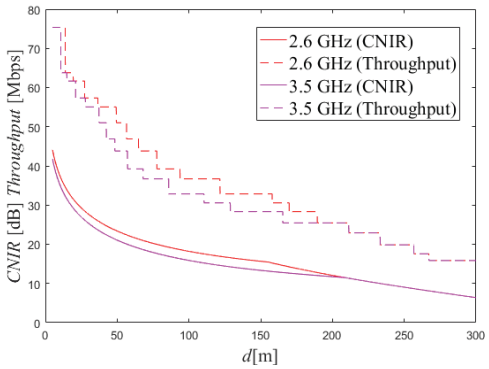

(b) East Interferer for both bands with $k = 3$

Figure 2.9: CNIR as a function of d for the No and East interferer scenario for $k = 3$

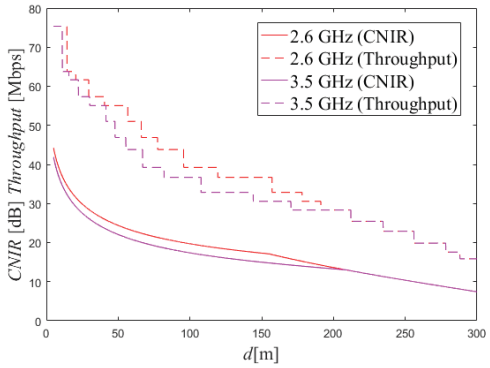

(a) Northeast Interferer for both bands with $k = 3$

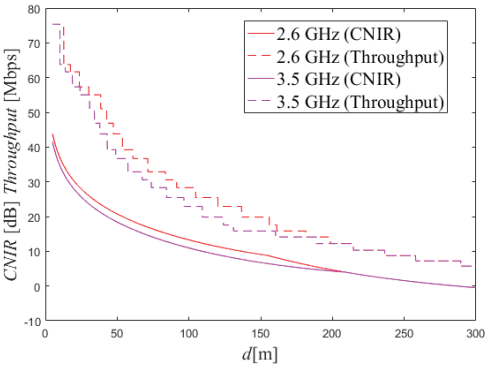

(b) Southeast Interferer for both bands with $k = 3$

Figure 2.10: CNIR as a function of d for the Northeast and Southeast scenario for $k = 3$

also considered in the computation of co-channel interference. In this subsection the graphics are divided by reuse pattern and include results at 2.6 and 3.5 GHz, the figures 2.9a, 2.9b, 2.10a and 2.10b are for $k = 3$, figures 2.11a, 2.11b, 2.12a and 2.12b are for $k = 4$.

For the shortest distances the Physical throughput is clearly higher, and the behaviour of the curve of the CNIR changes at the breakpoint distance because the CNIR decreases to lower values faster after d_{BP}.

Both bands have a slightly difference in Physical throughput and CNIR, becoming the same values when the 3.5 GHz breakpoint distance is reached, i.e., 210 m. The Southwest interferer sharing

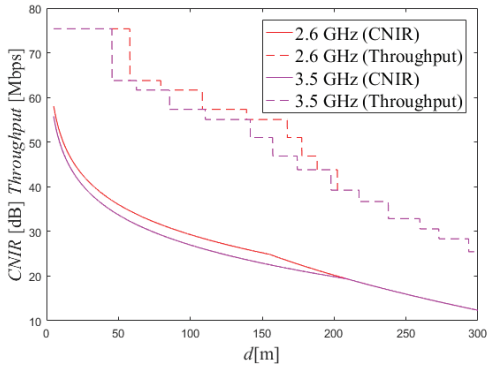

(a) No Interferer for both bands with $k = 4$

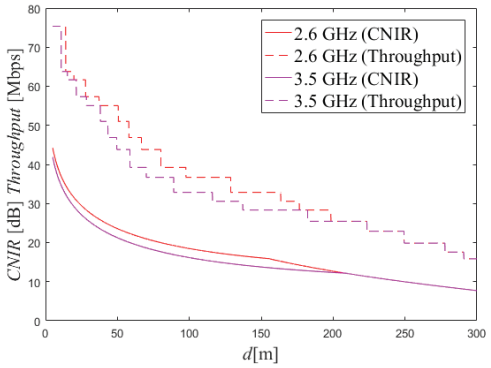

(b) East Interferer for both bands with $k = 4$

Figure 2.11: CNIR as a function of d for the No and East interferer scenario for $k = 4$

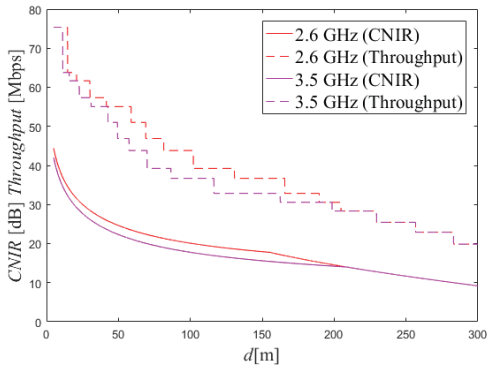

(a) Northeast Interferer for both bands with $k = 4$

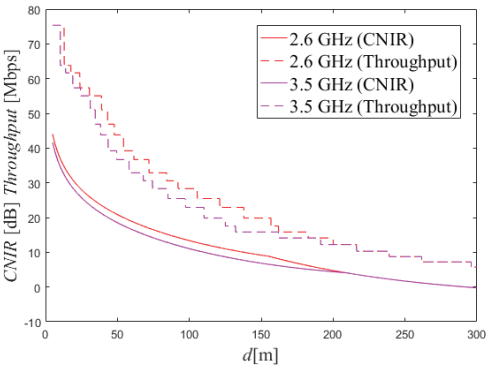

(b) Southeast Interferer for both bands with $k = 4$

Figure 2.12: CNIR as a function of d for the Northeast and Southeast scenario for $k = 4$

Table 2.3: Mapping CNIR into Physical throughput for 20 MHz bandwidth.

CNIR [dB]	MCS Index	Throughput [Mbps]
-4.63	1	2.797
-3.615	2	3.624
-2.6	3	4.584
-1.36	4	5.736
-0.12	5	7.224
1.17	6	8.76
2.26	7	10.296
3.595	8	12.216
4.73	9	14.112
6.13	10	15.84
7.53	11	15.84
8.1	12	17.568
8.67	13	19.848
9.995	14	22.92
11.32	15	25.456
12.78	16	28.336
14.24	17	30.576
14.725	18	30.576
15.21	19	32.856
16.92	20	36.696
18.63	21	39.232
19.975	22	43.816
21.32	23	46.888
22.395	24	51.024
23.47	25	55.056
25.98	26	57.336
28.49	27	61.664
31.545	28	63.776
34.6	29	75.376

scenario was not represented for both reuse patterns, due to the fact that the CNIR reaches zero, which means that both received powers, from central cell and interferers will be the same, and then negative values, which means that the UE will receive more interference power than the central, therefore there will be no communication, so Southwest sharing scenario is not considered. First of all, the scenario without interferer represented in figure 2.9a and in figure 2.11a, is the best of all the scenarios with both reuse patterns, on the other side the worst case of all is the Southeast interferer represented in figures 2.10b and 2.12b, that could be proved to the fact that when the user reaches 210 m, the Physical throughput is around 12 Mbps. The Northeast and East scenarios represented in the figures 2.9b, 2.10a, 2.11b and 2.12a are very similar, only with a difference of more or less 5 Mbps when the user reaches 210 m, being the Northeast scenario the best of all sharing scenarios.

2.4.1 3D view of the PHY throughput mapped into MCSs

After the CNIR and Physical throughput results were obtained, it was represented the Three Dimensional (3D) graphics for the best case scenarios with and without sharing, these 3D graphs were obtained with normalized distance, coverage radius and Physical throughput, mapped in MCSs. That way it is possible to understand the relation between the coverage radius and the distance walked by the UE, for the MCSs. The results obtained were for the best cases, without

sharing and the Northeast sharing scenario, so for the reuse pattern $k = 3$, it was obtained the figures 2.13, 2.14 and for the reuse pattern $k = 4$, it was obtained 2.15, 2.16, the 3D view charts for the 3.5 GHz band are in appendix C.

For the Northeast scenario in both bands, we can conclude that if a user is close to the cell center with a radius higher than the breakpoint distance, then higher Physical throughput values are achieved. Therefore it is seen that between 2.6 GHz and 3.5 GHz does not exist a big difference of the values of MCSs.

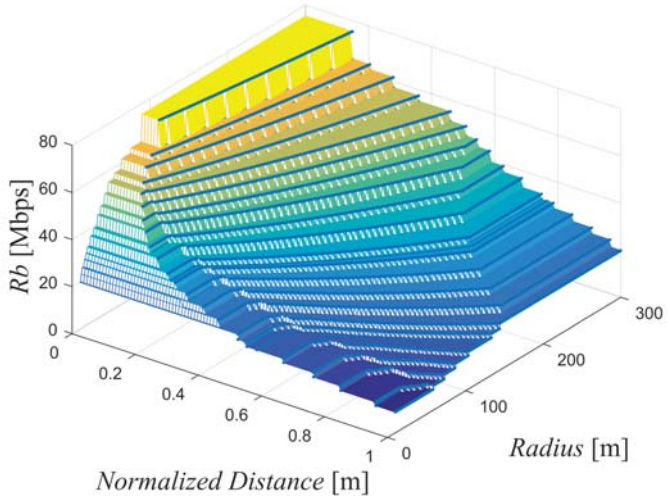

Figure 2.13: 3D View of the PHY throughput mapped into MCSs with No Interferer for 2.6 GHz with $k = 3$

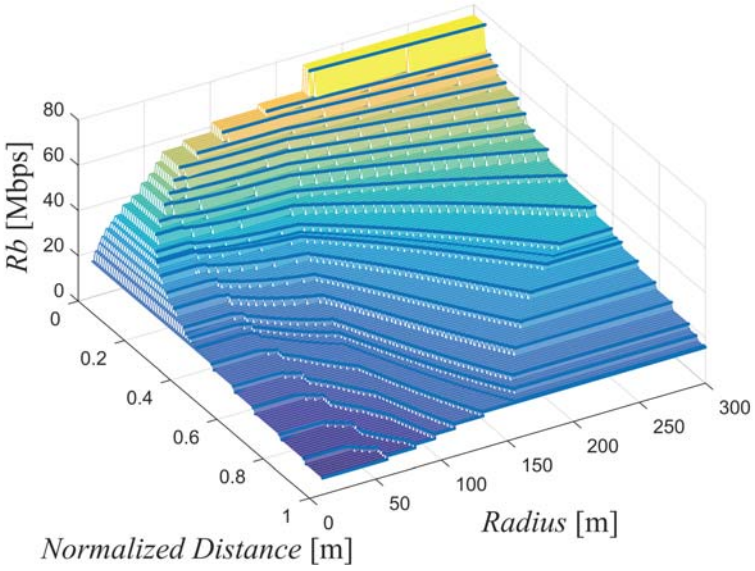

Figure 2.14: 3D View of the PHY throughput mapped into MCSs with Northeast Interferer for 2.6 GHz with $k = 3$

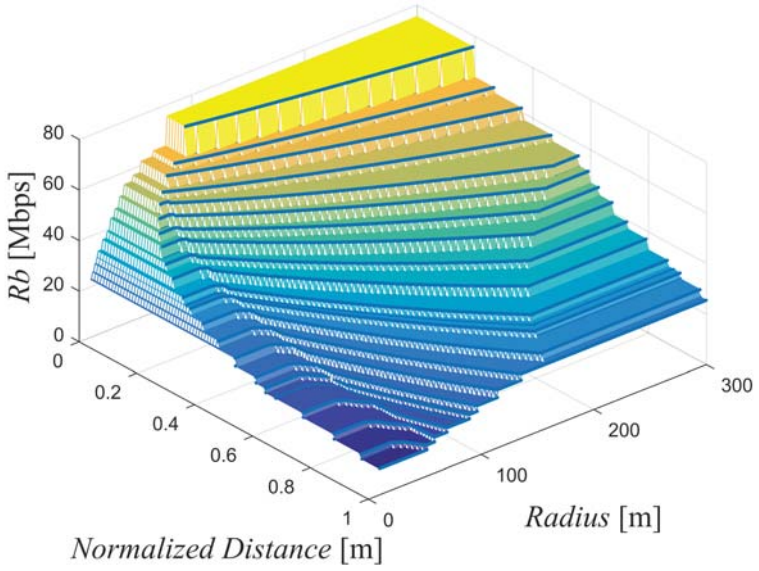

Figure 2.15: 3D View of the PHY throughput mapped into MCSs with No Interferer for 2.6 GHz with $k = 4$

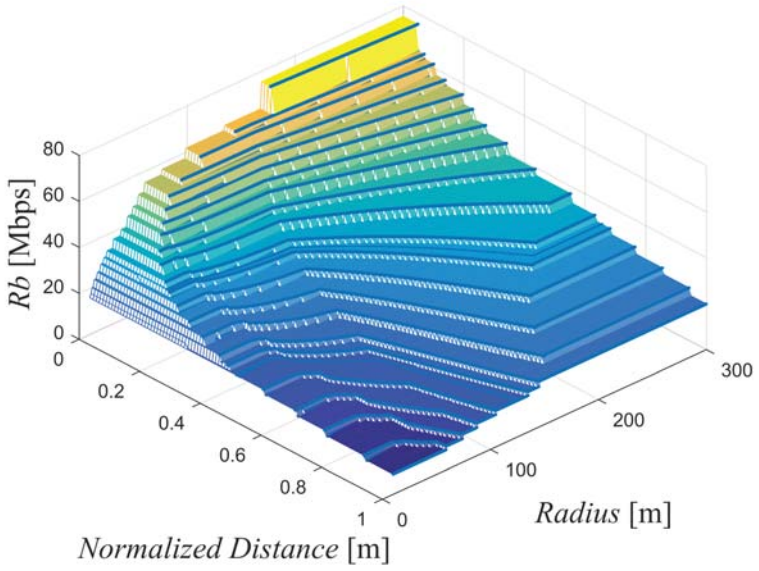

Figure 2.16: 3D View of the PHY throughput mapped into MCSs with Northeast Interferer for 2.6 GHz with $k = 4$

2.5 Analytical Formulation for the Average CNIR

SCs are being widely used in 4G communications and will be essential in future 5G HetNets. As 5G will also consider OFDM, we expect that the principles and lessons learned from analysing the optimization trade-off of 4G networks will remain. As far as the 5G channelisation and adaptive modulation and coding schemes are assumed, the results for system capacity and service quality obtained for 4G will certainly be generalized for broadband 5G New Radio, where more bandwidth, e.g., 100 MHz channels, will be available.

As it is fundamental to understand the impact of considering the two-slope propagation model,

as discussed in [25], in the optimization process, this section gives contributions to the fundamental aspects of the mapping between the average CNIR and the Supported throughput in a context of LTE Advanced SC HetNets and their evolution to 5G NR. LTE provides seamless Internet Protocol connectivity between user equipment (UE) and the packet data network, and an air interface based on Orthogonal Frequency Division Multiplexing (OFDM) in the downlink (DL) and single-carrier frequency-division multiple access (SC-FDMA) in the uplink (UL), both providing high flexibility in the frequency-domain scheduling. LTE has the flexibility to support time-/frequency-division duplexing (TDD/FDD) and half-duplex FDD schemes. This work assumes FDD and the DL.
In a saturated network, the average CNIR can be mapped into the Supported throughput obtained with the implicit function formulation considered in [26]. The only difference in the shape of these curves for the average CNIR and Supported throughput is a transformation that depends on the weights of each value of the PHY throughput that maps the different MCSs presented in the different coverage rings of the SC.
The average CNIR has therefore been evaluated for several inter-cell distances with a frequency reuse pattern three. By tuning the Base Stations (BSs) transmitter power, the average CNIR (AC) was kept constant, as will be shown in the figures 2.30a and 2.30b. In this work, a Matlab R2018a program to obtain all the average powers (of the own cell and interferers) has been implemented while solving the integrals defined by the areas on the cell. This program is shown in appendix D.

2.5.1 Average CNIR at a given position

In general, given a BS transmitter power PT_x, the UE CNIR at a position (x,y) can be expressed as:

$$CNIR(P_{tx},x,y)=\frac{P_{OW}(P_{tx},x,y)}{(1-\alpha)P_{OW}(P_{tx},x,y)+P_{nh}(P_{tx})+P_{Noise}} \quad (2.25)$$

Where P_{noise} is the noise power, α is the orthogonality level of the codes from P_{OW} which is the power received from the own cell and is equal to one, and P_{nh} is the amount of interfering power received from the neighbour cells (in this case we have six cells because it is a hexagonal cell topology). The propagation model used is UMi LoS, which is a two slope model with the pathloss equations given in 2.1.
The propagation UMi LoS can be used with frequencies between 2 GHz and 6 GHz, so the power received from the own cell can be given by two equations depending on the distance between the UE, the BSs, and the breakpoint distance.

$$\begin{aligned}&P_{OW}(P_{Tx},x,y)=P_{Tx}G_{Tx}G_{Rx}10^{(\frac{-36.2995+22\log_{10}(\sqrt{x^2+y^2})}{10})},\\&WhenR\leq d_{BP}\\&P_{OW}(P_{Tx},x,y)=P_{Tx}G_{Tx}G_{Rx}10^{(\frac{-8.62995-18\log_{10}(h_{BS})-18\log_{10}(h_{UE})+22\log_{10}(\sqrt{x^2+y^2})}{10})},\\&WhenR>d_{BP}\end{aligned} \quad (2.26)$$

Where G_{Tx} is the transmitter antenna gain, G_{Rx} is the receiver antenna gain, R is the cell radius and P_{Tx} is the transmitter power. P_{nh} is the interfering power received from the first ring of the six co-channel cells. It is given by:

$$P_{nh}(P_{Tx}, x, y) = \sum_{i=1}^{6} I_i(P_{Tx}, x, y), with I_i equals for every interferer \quad (2.27)$$

As for the areas, we will have two areas, area with the extraction of the hexagonal unit with apothem to the Fraunhofer distance for the P_{OW} and the total area of the cell for the P_{nh}, in which the respective formulas are:

$$A_{own} = \frac{3\sqrt{3}R^2 - r^2}{2} \quad (2.28)$$

$$A_{nh} = \frac{3\sqrt{3}R^2}{2} \quad (2.29)$$

Where r is the Fraunhofer distance.
In figure 2.17 is represented the hexagonal cell divided in two parts, which were used in both cases, own power and interferers, and the equations of the lines $y = \sqrt{3}(x + R)$ and $y = \sqrt{3}(-x + R)$. The own power case will be divided in three scenarios , represented in figures 2.18 and 2.19, while the interferers case will be divided in five scenarios, each one with a representation of the areas and cells, represented in figures 2.20, 2.21, 2.22, 2.23, 2.24, 2.25, 2.26, 2.27, 2.28 and 2.29.

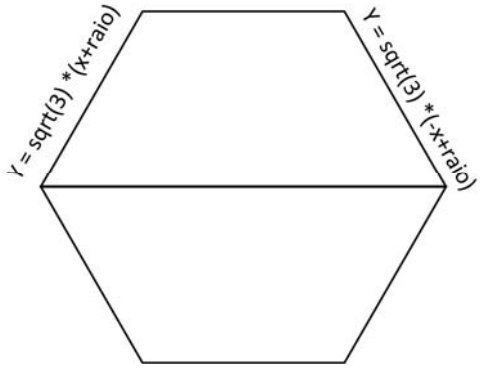

Figure 2.17: Hexagonal Cell

2.5.2 Average power of the Own Cell

As this only represents a small triangle, we will have 12 triangles to complete all the cell area, so the final equation will be as follows:
When we have PL1, then:

$$12\frac{pegegr10^{-2.8}(integrals)}{f^2 A_{own}} \quad (2.30)$$

if we have PL2, then:

$$12\frac{pegegr10^{-0.3957825248}(integrals)}{f^{0.2} A_{own}} \quad (2.31)$$

For all the Own Power scenarios, it was considered the equation as follows:

- For Pathloss1, we have:

$$Pathloss1 = \frac{1}{\sqrt{x^2 + y^2}^{2.2}} \quad (2.32)$$

- Else for the Pathloss2, then

$$Pathloss2 = \frac{1}{\sqrt{x^2 + y^2}^{4}} \quad (2.33)$$

And the integrals are represented for each scenario above.

1. First Scenario

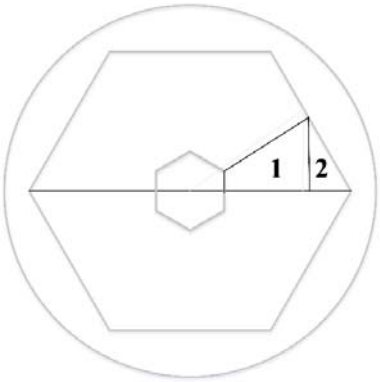

Figure 2.18: Division of the Own cell for the first scenario

When the radius of the cell is smaller than the breakpoint distance, we have:

$$\int_{r}^{\frac{3R}{4}} \int_{0}^{\frac{\sqrt{3}x}{3}} Pathloss1 dy dx \quad (2.34)$$

$$\int_{\frac{3R}{4}}^{R} \int_{0}^{\sqrt{3}(R-x)} Pathloss1 dy dx \quad (2.35)$$

2. Second Scenario

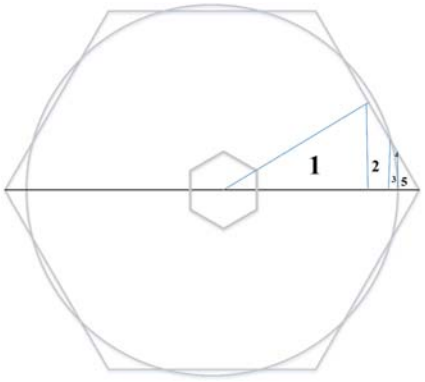

Figure 2.19: Division of the Own cell for the second scenario

When the radius of the cell is between the breakpoint distance and $\frac{\sqrt{3}}{2}$ of the breakpoint distance, we will have two pathlosses, such as:

$$\int_{r}^{\frac{3R}{4}} \int_{0}^{\frac{\sqrt{3}x}{3}} Pathloss1 dy dx \quad (2.36)$$

$$\int_{\frac{3R}{4}}^{6R+\frac{\sqrt{16d_{BP}^2-12R^2}}{8}} \int_{0}^{\sqrt{3}(R-x)} Pathloss1 dy dx \quad (2.37)$$

$$\int_{6R+\frac{\sqrt{16d_{BP}^2-12R^2}}{8}}^{d_{BP}} \int_{0}^{\sqrt{d_{BP}^2-x^2}} Pathloss1 dy dx \quad (2.38)$$

$$\int_{6R+\frac{\sqrt{16d_{BP}^2-12R^2}}{8}}^{d_{BP}} \int_{\sqrt{d_{BP}^2-x^2}}^{\sqrt{3}(R-x)} Pathloss2 dy dx \quad (2.39)$$

$$\int_{d_{BP}}^{R} \int_{0}^{\sqrt{3}(R-x)} Pathloss2 dy dx \quad (2.40)$$

3. Third Scenario

When the radius is higher than $\frac{\sqrt{3}}{2}$ of the breakpoint distance, we have:

$$\int_{r}^{\frac{\sqrt{3}d_{BP}}{2}} \int_{0}^{\frac{\sqrt{3}x}{3}} Pathloss1 dy dx \quad (2.41)$$

$$\int_{\frac{\sqrt{3}d_{BP}}{2}}^{d_{BP}} \int_{0}^{\sqrt{d_{BP}^2-x^2}} Pathloss1 dy dx \quad (2.42)$$

$$\int_{\frac{\sqrt{3}d_{BP}}{2}}^{d_{BP}} \int_{\sqrt{d_{BP}^2-x^2}}^{\frac{\sqrt{3}x}{3}} Pathloss2 dy dx \quad (2.43)$$

$$\int_{d_{BP}}^{\frac{3R}{4}} \int_{0}^{\frac{\sqrt{3}x}{3}} Pathloss2 dy dx \quad (2.44)$$

$$\int_{\frac{3R}{4}}^{R} \int_{0}^{\sqrt{3}(R-x)} Pathloss2 dy dx \quad (2.45)$$

2.5.3 Average Power of the Interferers

For all the average interferer power scenarios, it was considered the equation as follows:

- For Pathloss1, we have:

$$Pathloss1 = \frac{1}{\sqrt{(3R-x)^2+y^2}^{2.2}} \quad (2.46)$$

- Else for the Pathloss2, then

$$Pathloss2 = \frac{1}{\sqrt{(3R-x)^2+y^2}^{4}} \quad (2.47)$$

To compute the average power of the interferers, the problem was divided in five scenarios, such as:

1. First Scenario

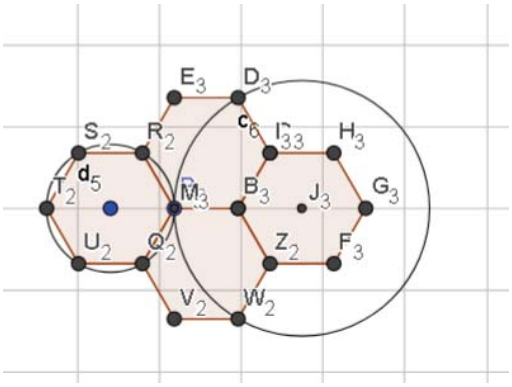

Figure 2.20: Scenario 1 for Interferer Power

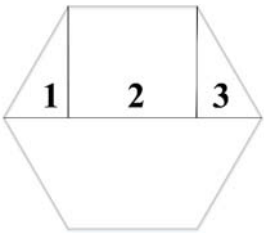

Figure 2.21: Division of the cell to calculate integrals

In the first scenario, we have radius higher than 78 meters. We only use a $Pathloss2$, because the cell will be always outside the circle.

$$\int_{-R}^{\frac{-R}{2}} \int_{0}^{\sqrt{3}(R+x)} Pathloss2 dy dx \quad (2.48)$$

$$\int_{\frac{-R}{2}}^{\frac{R}{2}} \int_{0}^{\frac{\sqrt{3}R}{2}} Pathloss2 dy dx \quad (2.49)$$

$$\int_{\frac{R}{2}}^{R}\int_{0}^{\sqrt{3}(R-x)} Pathloss2dydx \quad (2.50)$$

2. Second Scenario

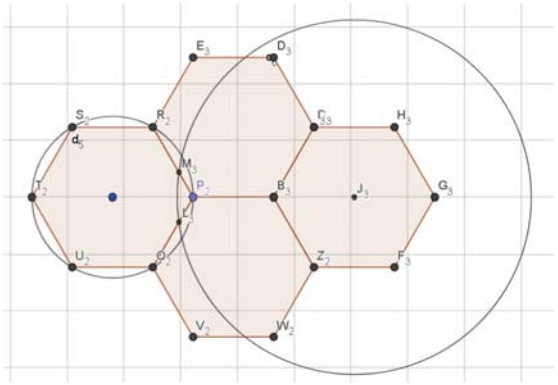

Figure 2.22: Scenario 2 for Interferer Power

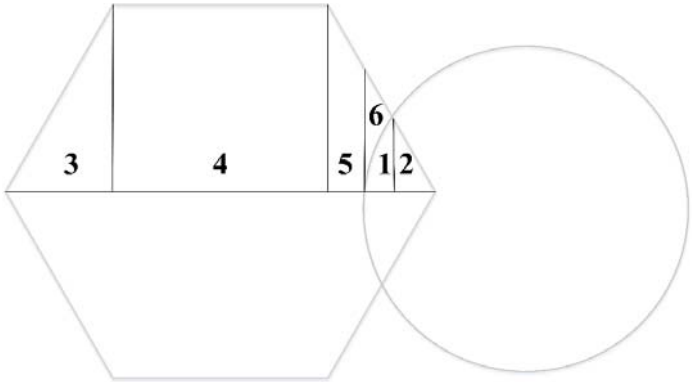

Figure 2.23: Division of the cell

In the second scenario, we have radius between $\frac{156d_{BP}}{59}$ and $\frac{d_{BP}}{2}$. We will use both pathlosses, because one part of the cell is outside the circle and there is another part that will be inside of the cell.

$$\int_{3R-d_{BP}}^{12R-\frac{\sqrt{16d_{BP}^2-48R^2}}{8}}\int_{0}^{\sqrt{d_{BP}^2-(3R-x)^2}} Pathloss1dydx \quad (2.51)$$

$$\int_{12R-\frac{\sqrt{16d_{BP}^2-48R^2}}{8}}^{R}\int_{0}^{\sqrt{3}(R-x)} Pathloss1dydx \quad (2.52)$$

$$\int_{-R}^{\frac{-R}{2}}\int_{0}^{\sqrt{3}(x+R)} Pathloss2dydx \quad (2.53)$$

$$\int_{\frac{-R}{2}}^{\frac{R}{2}} \int_{0}^{\frac{\sqrt{3}R}{2}} Pathloss2dydx \quad (2.54)$$

$$\int_{\frac{R}{2}}^{3R-d_{BP}} \int_{0}^{\sqrt{3}(R-x)} Pathloss2dydx \quad (2.55)$$

$$\int_{3R-d_{BP}}^{12R-\frac{\sqrt{16d_{BP}^2-48R^2}}{8}} \int_{\sqrt{d_{BP}^2-(3R-x)^2}}^{\sqrt{3}(R-x)} Pathloss2dydx \quad (2.56)$$

3. Third Scenario

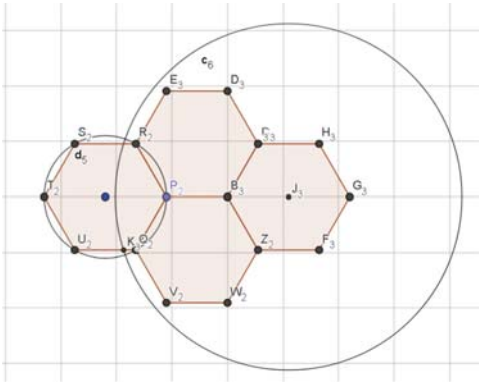

Figure 2.24: Scenario 3 for Interferer Power

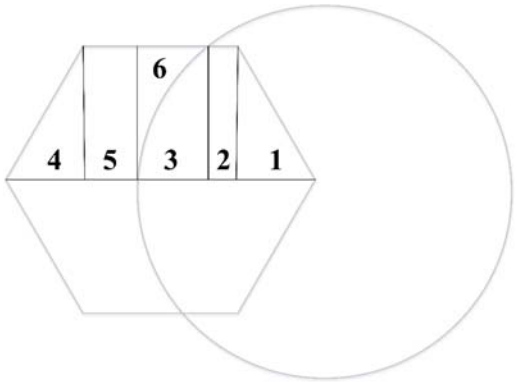

Figure 2.25: Division of the cell

In the third scenario we have a radius between $\frac{156d_{BP}}{43}$ and $\frac{156d_{BP}}{59}$

$$\int_{\frac{R}{2}}^{R} \int_{0}^{\sqrt{3}(R-x)} Pathloss1dydx \quad (2.57)$$

$$\int_{3R-\frac{\sqrt{4d_{BP}^2-3R^2}}{2}}^{\frac{R}{2}} \int_{0}^{\frac{\sqrt{3}R}{2}} Pathloss1dydx \quad (2.58)$$

$$\int_{3R-d_{BP}}^{3R-\frac{\sqrt{4d_{BP}^2-3R^2}}{2}} \int_{0}^{\sqrt{d_{BP}^2-(3R-x)^2}} Pathloss1 dydx \quad (2.59)$$

$$\int_{\frac{-R}{2}}^{-R} \int_{0}^{\sqrt{3}(x+R)} Pathloss2 dydx \quad (2.60)$$

$$\int_{\frac{-R}{2}}^{3R-d_{BP}} \int_{0}^{\frac{\sqrt{3}R}{2}} Pathloss2 dydx \quad (2.61)$$

$$\int_{3R-d_{BP}}^{3R-\frac{\sqrt{4d_{BP}^2-3R^2}}{2}} \int_{\sqrt{d_{BP}^2-(3R-x)^2}}^{\frac{\sqrt{3}R}{2}} Pathloss2 dydx \quad (2.62)$$

4. Forth Scenario

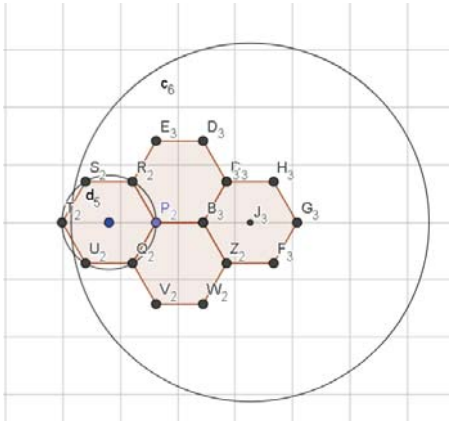

Figure 2.26: Scenario 4 for Interferer Power

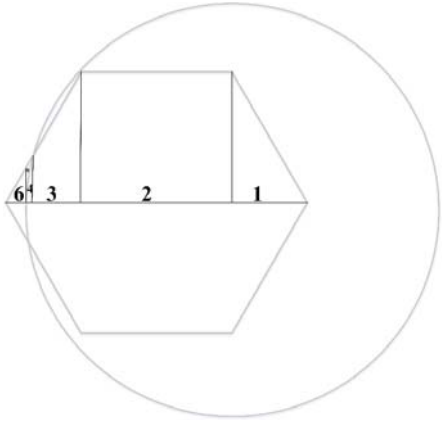

Figure 2.27: Division of the cell

In the fourth scenario we have a radius between $\frac{d_{BP}}{4}$ and $\frac{156d_{BP}}{43}$, we have:

$$\int_{\frac{R}{2}}^{R}\int_{0}^{\sqrt{3}(R-x)} Pathloss1dydx \quad (2.63)$$

$$\int_{\frac{-R}{2}}^{\frac{R}{2}}\int_{0}^{\frac{\sqrt{3}R}{2}} Pathloss1dydx \quad (2.64)$$

$$\int_{\frac{-\sqrt{d_{BP}^2-12R^2}}{2}}^{\frac{-R}{2}}\int_{0}^{\sqrt{3}(x+R)} Pathloss1dydx \quad (2.65)$$

$$\int_{3R-d_{BP}}^{\frac{-\sqrt{d_{BP}^2-12R^2}}{2}}\int_{0}^{\sqrt{d_{BP}^2-(3R-x)^2}} Pathloss1dydx \quad (2.66)$$

$$\int_{3R-d_{BP}}^{\frac{-\sqrt{d_{BP}^2-12R^2}}{2}}\int_{\sqrt{d_{BP}^2-(3R-x)^2}}^{\sqrt{3}(x+R)} Pathloss2dydx \quad (2.67)$$

$$\int_{-R}^{3R-d_{BP}}\int_{0}^{\sqrt{3}(x+R)} Pathloss2dydx \quad (2.68)$$

5. Fifth Scenario

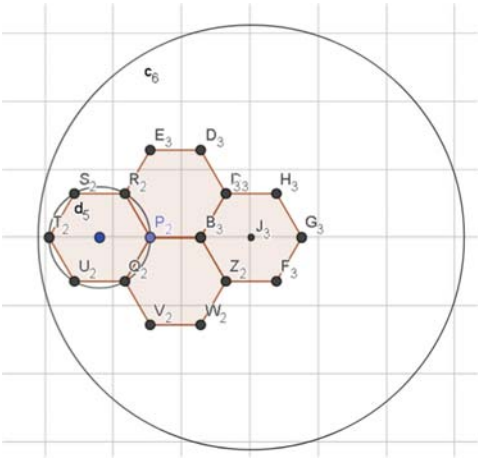

Figure 2.28: Scenario 5 for Interferer Power

In the fifth scenario we have a radius smaller than $\frac{d_{BP}}{4}$, we have:

$$\int_{\frac{R}{2}}^{R}\int_{0}^{\sqrt{3}(R-x)} Pathloss1dydx \quad (2.69)$$

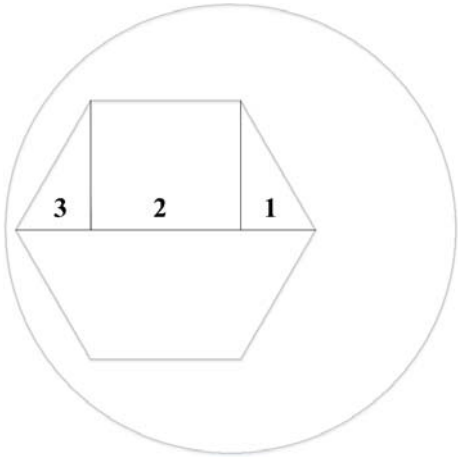

Figure 2.29: Division of the cell

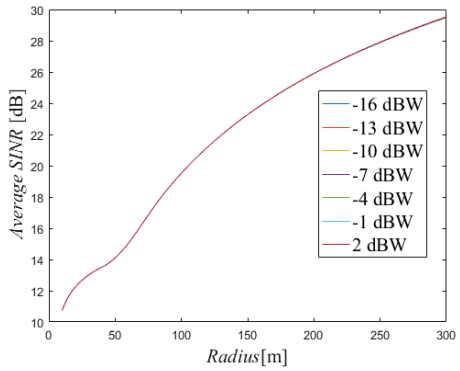

(a) 2.6 GHz

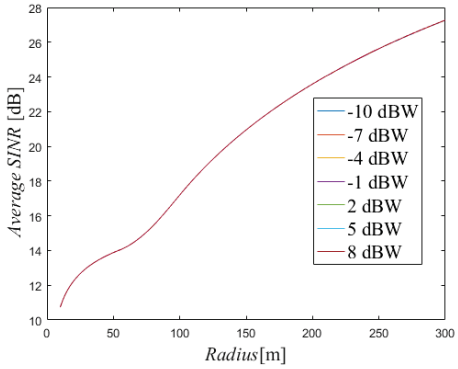

(b) 3.5 GHz

Figure 2.30: Average SINR different values for different transmitter powers

$$\int_{\frac{-R}{2}}^{\frac{R}{2}} \int_{0}^{\frac{\sqrt{3}R}{2}} Pathloss1 dy dx \quad (2.70)$$

$$\int_{-R}^{\frac{-R}{2}} \int_{0}^{\sqrt{3}(x+R)} Pathloss1 dy dx \quad (2.71)$$

As a result with the parameters listed on table 2.2, one obtains the average CNIR as a function of R.

The AC values as a function of R, for different transmitter powers, are shown in figure 2.30a and in figure 2.30b. Figure 2.31 shows the comparison of the values between the two bands. We can conclude that AC in this range of transmitter powers do not depend of the transmitter power. AC is only considered for scenarios without sharing, and with these values it is possible to get the Supported throughput values.

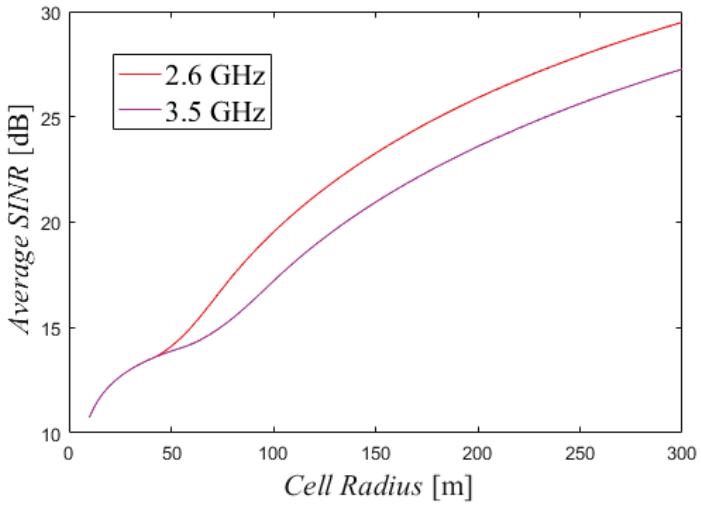

Figure 2.31: Comparison between Average SINR with different values for the transmitter power values for 2.6 GHz and 3.5 GHz

2.6 Supported Throughput

The Supported throughput is an weighted average value and is given by the following equation [26], [27]:

$$R_{b\_sup} = \sum_{i=1}^{n} \frac{R_{b_i}(d_i^2 - d_{i-1}^2)}{R^2} \quad (2.72)$$

where d is the distance in which there are MCSs transitions, R_b is the Physical throughput and R is the cell radius.
The transition distances will be the radius of the coverage rings presented in figure 2.32 as an example.

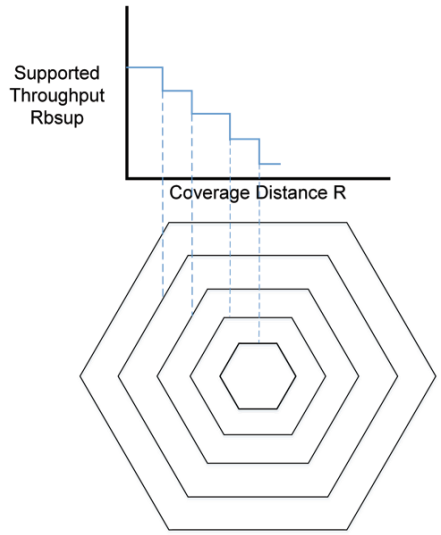

Figure 2.32: Areas of the coverage rings where a given value of PHY throughput for hexagonal has a transition

After the comparison of the CNIR and PHY throughput between bands and the different dis-

tances, have been obtained for $k = 3$ and $k = 4$, respectively of the Supported throughput for a coverage distance up to 300 m is in order. Different reuse patterns, the results shown in figure 2.33 for $k = 3$ and in figure 2.34 for $k = 4$.

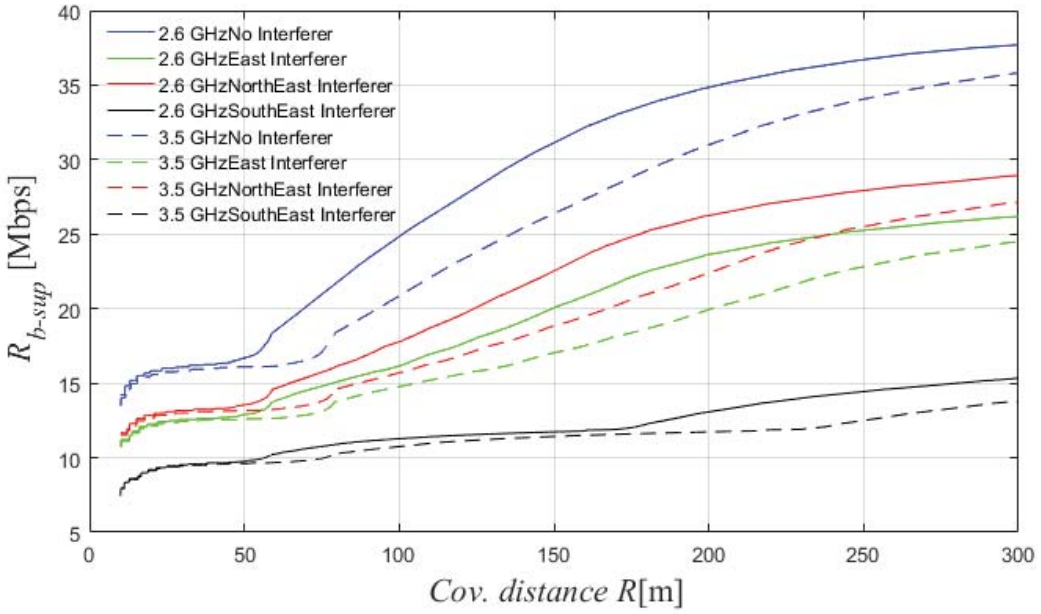

Figure 2.33: Comparison of the supported throughput for $k = 3$ in the pico cellular scenario, for different positions of the interferer from MO #2 and for the case without interference with 20 MHz bandwidth

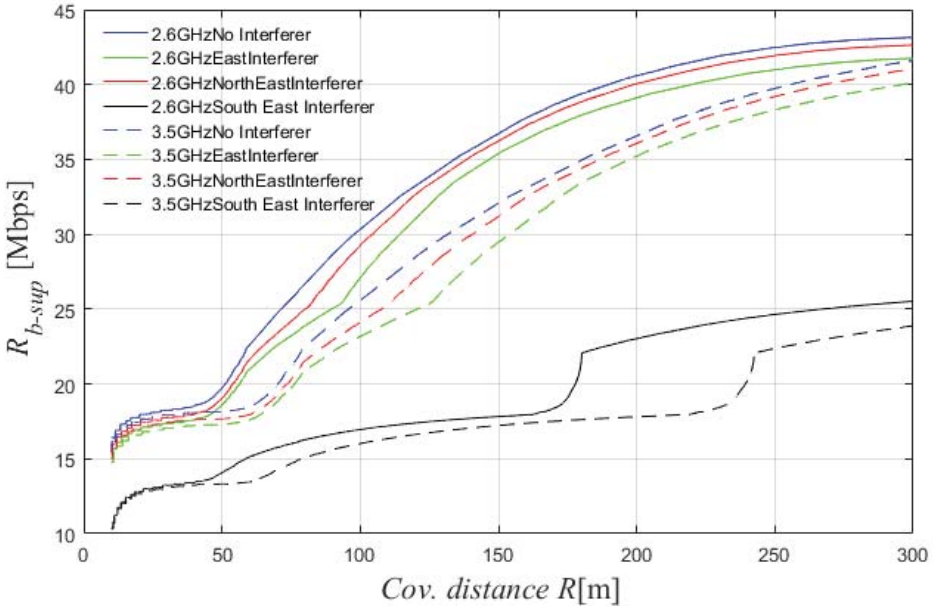

Figure 2.34: Comparison of the supported throughput for $k = 4$ in the pico cellular scenario, for different positions of the interferer from MO #2 and for the case without interference with 20 MHz bandwidth

By comparing all the curves in figures 2.33 and 2.34, it is observed that the Supported throughput

at 2.6 GHz is clearly higher than at 3.5 GHz, because of the breakpoint distance. For the case of Southeast scenario, the Supported throughput is similar for both reuse patterns up to $R = 52$ m for $k = 3$, and $R = 48$ m, for $k = 4$. The performance in the sharing scenario became better for distances longer than circa 125 m. For longer coverage distances the Supported throughput stabilizes after this value for the coverage distance i.e., 280 m (horizontal asymptote). It was concluded that the scenario without sharing is the best and the Southeast interferer scenario is the worst. We can conclude also that the interferers scenarios Supported throughput get higher values when it reaches the breakpoint distance and the scenario without sharing get higher when the user reaches 50 m for both $k = 3$ and $k = 4$.

2.7 Intermittent Scenario

While considering spectrum sharing one assumes that the cell from MO $\#2$ can cause interference in the remaining co-channel cells from MO $\#1$ either in a permanent (traffic from users supported in the cell 100% of the time) or intermittent way (traffic supported only part of the time). One can define the percentage of spectrum sharing use, α , meaning that with $\alpha = 0$ there is no traffic usage in the cell from MO $\#2$ (shared spectrum), while for $\alpha = 1$ resources are permanently occupied. By considering this very simple assumptions, figures 2.35 and 2.36 show the Supported throughput for $0 \leq \alpha \leq 1$. It is observable that the surface represents values of R_{b_sup} in between the scenarios without sharing $(\alpha = 0)$ and 100% sharing $(\alpha = 1)$. In order to study the influence of different frequency bands in the results of the Supported throughput as a function of radius, three dimensional (3D) graphs have been drawn, as in [25], where the radius (R) varies from 10 m to 300 m. The equation that was used to obtain the values for the intermittent scenario is above:

$$R_{b\_sup} = (\alpha)(R_{b\_supsharing}) + (1 - \alpha)(R_{b\_supwithoutsharing}) \quad (2.73)$$

where $R_{b\_supsharing}$ represents the supported throughput values for the sharing scenario, Northeast Interferer, in Mbps, α is the percentage of traffic in MO $\#2$ and $R_{b\_supwithoutsharing}$ represents the supported throughput values for the No sharing scenario. In the Intermittent scenario for UHF/SHF, we considered Northeast Interferer as the MO$\#2$ using $0 \leq \alpha < 1$ with a step of 0.01 and a radius of 300 m.

2.8 Comparison between UHF/SHF and Millimeter Wave Bands

In a simplistic approach, a scenario with “No sharing”, where MO has dedicated licensed spectrum for SCs, could be considered. In this framework, MOs are free to optimize throughput with respective frequency reuse. However, as there are limitations in the availability of dedicated spectrum for each operator, this work considers a second case of sharing without coordination, which means that each operator adopts the same frequency reuse strategy as in the first scenario. Spectrum sharing access assumes that two or more MOs have dedicated spectrum for macro cellular layer while SCs will share the access to spectrum in an opportunist manner. It is addressed a very simple sharing scenario, in the SC layer, where we simply start adding a/various co-channel cells, from a different operator, over the cellular topology from another (initial) operator. The aim of this section is to compare the system capacity, measured by the Supported

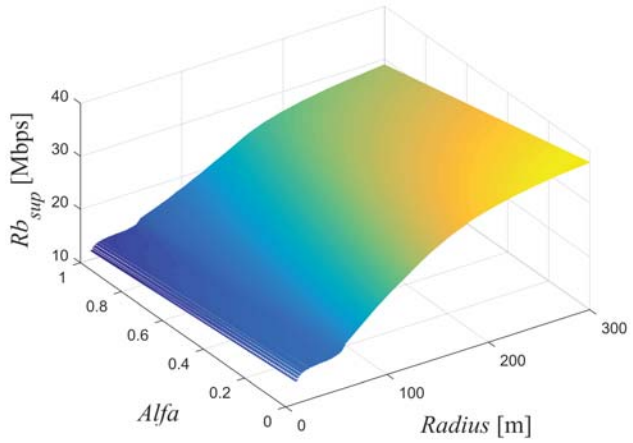

Figure 2.35: Variation of the Supported throughput for different percentages of spectrum sharing use, α ($0 \leq \alpha \leq 1$), for f = 2.6 GHz with $k = 3$

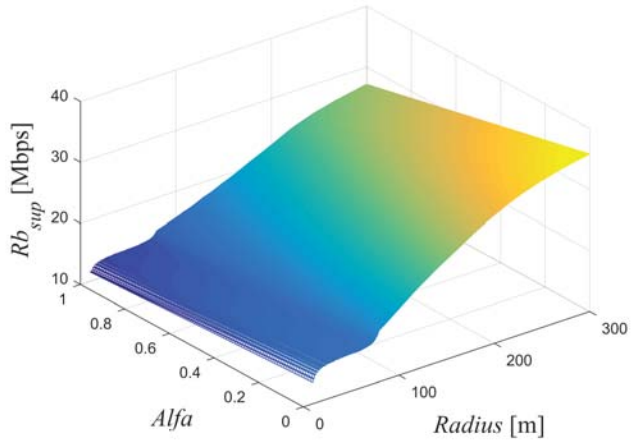

Figure 2.36: Variation of the Supported throughput for different percentages of spectrum sharing use, α ($0 \leq \alpha \leq 1$), for f = 3.5 GHz with $k = 3$

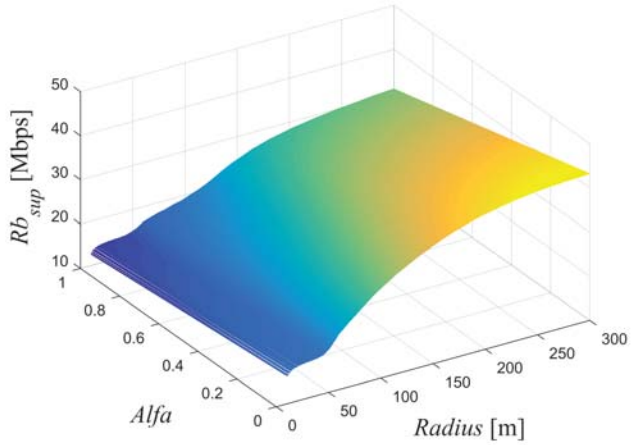

Figure 2.37: Variation of the Supported throughput for different percentages of spectrum sharing use, α ($0 \leq \alpha \leq 1$), for f = 2.6 GHz, $k = 4$

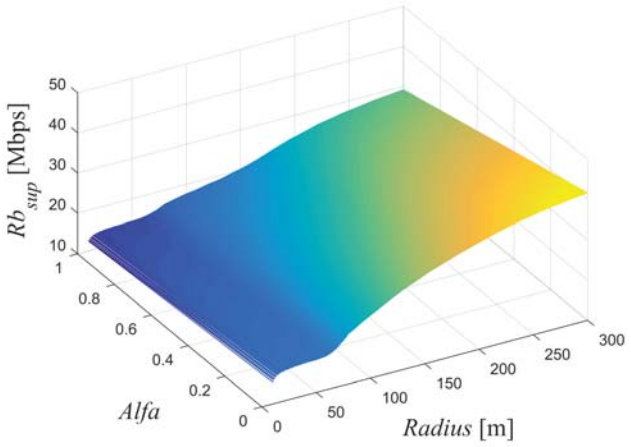

Figure 2.38: Variation of the Supported throughput for different percentages of spectrum sharing use, α ($0 \leq \alpha \leq 1$), for f = 3.5 GHz, $k = 4$

throughput, for cells of few hundred meters coverage in scenarios with simple frequency sharing configurations. The frequency bands in the SC layer are the UHF/SHF bands, 2.6 or 3.5 GHz respectively, and mmWaves (28, 38, 60 or 73 GHz).
From a detailed analysis of its variation of the Supported throughput with the coverage and reuse distances, for different values of the Channel Quality Indicator (CQI) and given International Telecommunication Union-Radiocommunication Sector (ITU-R) propagation models, an evaluation of the possible range for the reuse factor performed for the DL of LTE-A. By considering CQI and reference CNIR requirements recommended by 3GPP, DL peak bit rates along with the Transport Block Size assumed for single stream and bandwidths of 20 MHz, PHY and Supported throughputs are analysed [28]. In the UHF/SHF bands, six scenarios are considered East, Northeast, Southwest, Southeast, Northwest and West. The interference that outcomes from an interferer placed at the east corner is equal to the Northwest corner (represented in blue and pink, respectively) also the interference that outcomes from an interferer placed at the west corner is equal to Southeast corner (represented in yellow and purple, respectively). For this reason, four of the six cases are going to be analysed, i.e., Southwest, Southeast, East and Northeast. Figure 2.39 illustrates the position of the six interferers considered.
While in the UHF/SHF we consider a reuse pattern $k = 3$ with an hexagonal topology, in the mmWaves, it is considered $k = 3$ with a linear topology, all the throughput values were obtained from the table 2.3. In this section different parameters will be obtained and the results will be discussed, such as:

- CNIR and Physical throughput;
- Supported throughput;
- Intermittent scenario and 3D MCS View

The parameters used for the mmWaves are presented in table 2.4
For the mmWaves scenarios the propagation model considered is a modified Friis formula [29], [30], [31], [32] , in which the pathloss equations are as follows:

$$PL = 20\log_{10}(\frac{4\pi d_0}{\lambda}) + 10\bar{n}\log_{10}(\frac{d}{d_0}) + X_\sigma, LOS, when\ d \geq d_0 \quad \textbf{(2.74)}$$

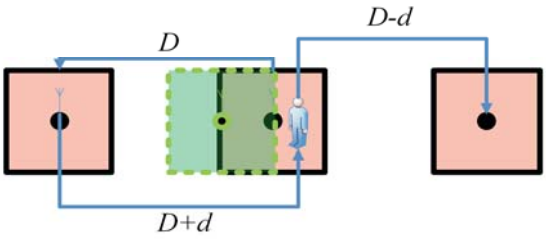

Worst-case bounds from a Manhattan grid in terms of CNIR are similar to the ones from a linear cellular topology

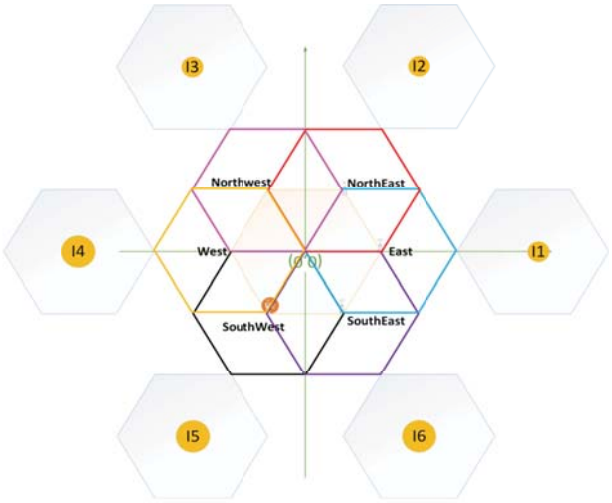

Definition of the six interferers for the sharing framework, where diferente cases are superimposed

Figure 2.39: Scenario Topologies

Table 2.4: Parameters considered for mmWaves

Transmitter Power [dBW]	0
Transmitter Gain [dBi]	3
Receiver Gain [dBi]	0
Bandwidth [MHz]	20
Noise Figure [dB]	7
Height(Base Station) [m]	7
Height(User Equipment) [m]	1.5
Propagation Exponent 1$[\gamma]$	28 GHz ($\gamma = 2.1$)
Propagation Exponent 2$[\gamma]$	38, 60 and 78 GHz ($\gamma = 2.3$)

$$PL_{LOS} = 20\log_{10}(\frac{4\pi}{\lambda}) + 10\bar{n}\log_{10}(d) + X_\sigma, LOS, when\ d \geq 1m \quad (2.75)$$

where $\bar{n}$ is the propagation exponent, λ is the wavelength, X_σ is the log-normal random variable with 0 dB mean with standard deviation σ, in dB, and d is the distance.

2.8.1 CNIR and Physical Throughput

In order to study the variation of the CNIR and PHY throughput with the coverage distance (for the downlink, DL), d, the PHY throughput is computed through the implicit function analytical formulation that was already applied in [25], [28], [26]. One example of the variation of the PHY throughput that corresponds to the curves of CNIR for the mmWaves frequencies without sharing is presented in figure 2.40, where sharing is considered with the interferer from mobile operator $\#2$ placed at a distance $R + d$ from the UE. These results can be compared to the ones for UHF/SHF bands from figures 2.9, 2.10, 2.11 and 2.12. Therefore for the no sharing scenario in the mmWave bands, the 28 GHz frequency band has the higher PHY throughput comparing with the other frequencies. Comparing the results between the UHF/SHF bands and mmWave bands, it is noticeable that the 28 GHz band has an higher PHY throughput than 2.6 GHz frequency

band, with the values of the first reaching 22 Mbps and the latter only reaching 20 Mbps for the No interferer scenario, in a distance of 300 m.

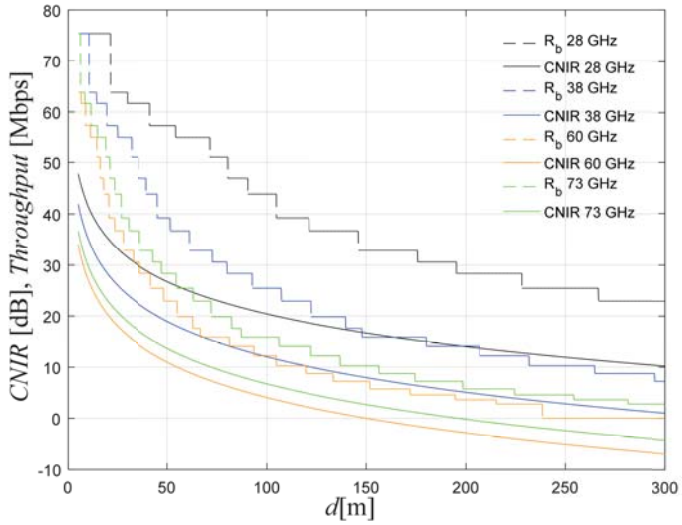

Figure 2.40: Variation of the CNIR/SINR and PHY throughput with d for 28 GHz, 38 GHz, 60 GHz, 73 GHz, for $R = 300$ m and $\sigma \neq 0$

2.8.2 Supported Throughput

In order to analyse the cases where R varies between 10 and 300 m, in this work we only consider $\sigma \neq 0$ for mmWaves [28]. By analysing the results from figure 2.41, generally, the Supported throughput for the sharing scenario is higher for the 28 GHz frequency band compared to the remaining mmWave frequencies (38, 60 and 73 GHz). One can also conclude that the system capacity decreases for increasing coverage distances. In the UHF/SHF scenario, 2.6 GHz Sharing (1) represents the East Interferer and 2.6 GHz Sharing (2) represents the Northeast Interferer, for these are the best cases for the sharing scenario. In the sharing scenario, the Supported throughput is highly reduced by the interference caused by the cell from a different MO. However, the ubiquitous coverage of the mobile communication system remains, as the PHY throughput does not reach zero inside the cell. To understand the practicability of considering spectrum sharing in UHF/SHF and mmWaves, figure 2.41 puts together all the curves from the analysis of these frequency bands with sharing and without sharing, respectively. It is noticeable that the Supported throughput performance for the 28 GHz frequency band, is the best compared to the other frequency bands considered, with values varying between the 45 Mbps and 39 Mbps for the scenario without sharing, and values varying between 30 Mbps and 33 Mbps for the scenario with shared spectrum. For all the other frequency bands, due to the behaviour arising from the two-slope model (Umi LoS) applied to 2.6 and 3.5 GHz, the Supported throughput at the mmWaves is higher than for the UHF/SHF bands for the shortest Rs. As an example, it is worthwhile to highlight that, with the Northeast Interferer, the Supported throughput at 38 and $60/73$ GHz is higher than:

- the supported throughput at 2.6 GHz, for coverage distances up to circa 155 and 160 m, respectively;
- the supported throughput at 3.5 GHz, for coverage distances up to circa 270, 180 and 190

m, respectively.

For longer coverage distances, the Supported throughput is clearly higher for the UHF/SHF frequency bands (compared to the 38, 60 and 73 GHz frequency bands).

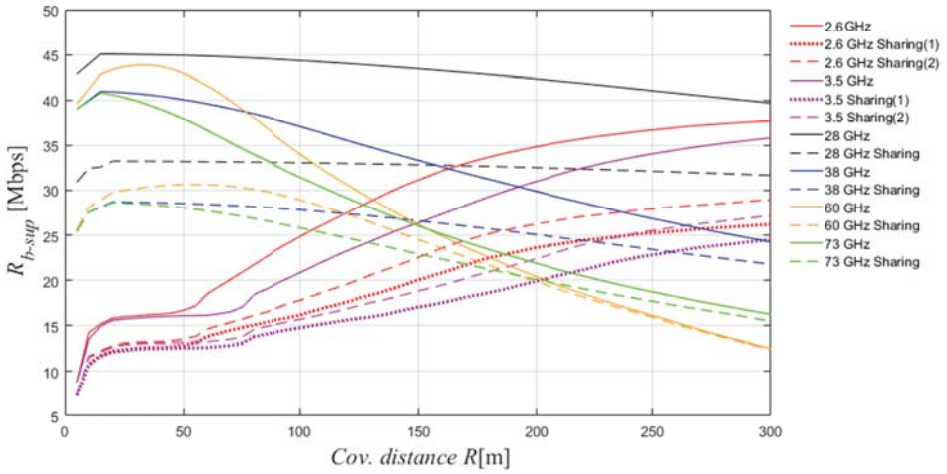

Figure 2.41: Supported throughput for a cell radius of 300 m and 20 MHz of bandwidth with both mmWaves and UHF/SHF

2.8.3 3D view of the PHY throughput mapped into MCSs and Intermittent scenario

In order to study the influence of different frequency bands in the results for system capacity as a function of cell size R varying from 10 m to 300 m, 3D view graphs have been drawn, as in [25], [28]. Through the analysis of 3D view of the PHY throughput mapped into MCSs, e.g., the Northeast interferer in figure 2.14 ($k = 3$), and figure 2.16, $k = 4$ (the best case for the considered sharing scenarios), the step-wise PHY throughput has an increasing behaviour with R and achieve the maximum value of 75.376 Mbps when the coverage reaches circa 140-150 m, i.e., around the breakpoint distance (d_{BP}). After this distance the highest MCSs are supported for a larger region of the cell, i.e., a broader range of the shortest normalized distances, as shown in figures 2.13 and 2.15, and then the PHY throughput keeps the maximum value (in the range of Rs presented here).
In the mmWaves, figure 2.42 presents an example for the PHY throughput at 28 GHz. As the corresponding breakpoint distance is a 1680 m, the behaviour for short coverage distances is the one for a single slope propagation model. As the coverage distances increases the upper MCSs are supported up to shorter distances inside the cells. These results allows for interpreting why at the mmWave bands the system capacity is clearly higher for the shortest coverage distances, ceasing to be better for longer distances (except for the 28 GHz band, whose supported throughput is always the highest one). This section also presents results for the PHY throughput for three scenarios as shown in figures 2.45, 2.46 and 2.47. In all these scenarios, the best performance occurs for the 28 GHz band.
For the Intermittent scenarios, we can conclude that the 28 GHz band has the best performance comparing to the remaining frequencies, in terms of Supported throughput with a variation from 45 Mbps, when $\alpha = 0$, to 34 Mbps, when $\alpha = 1$. In the intermittent scenario the values for the

60 GHz and 73 GHz bands are similar, with a difference of only 2 Mbps for the shortest Rs, due to the oxygen. We can conclude once again, that even when we consider sharing ($\alpha = 1$) and the mmWave bands enables to achieve higher throughputs are better for the shortest Rs, while the UHF/SHF bands are better for the highest Rs.

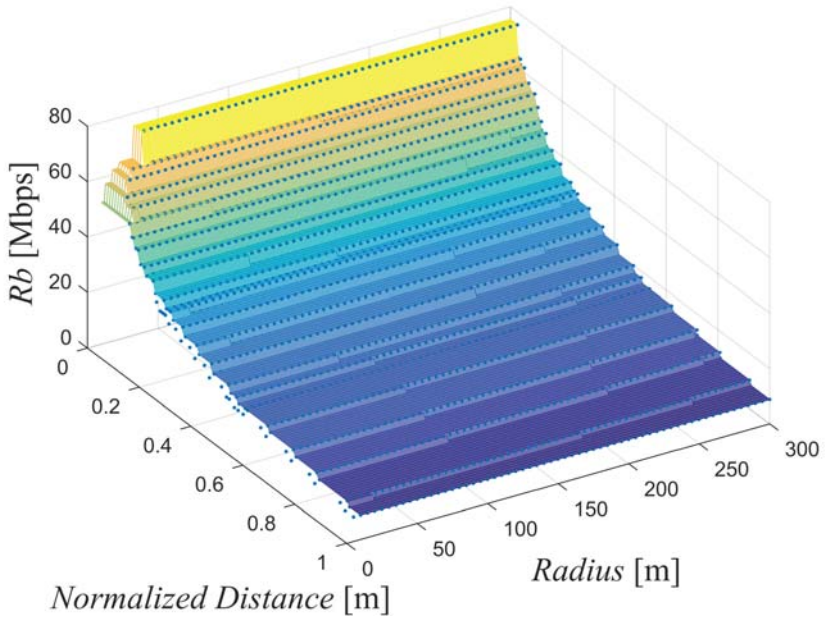

Figure 2.42: 3D view of the PHY throughput mapped into MCSs for the 28 GHz frequency band with interferer and $R = 300$ m

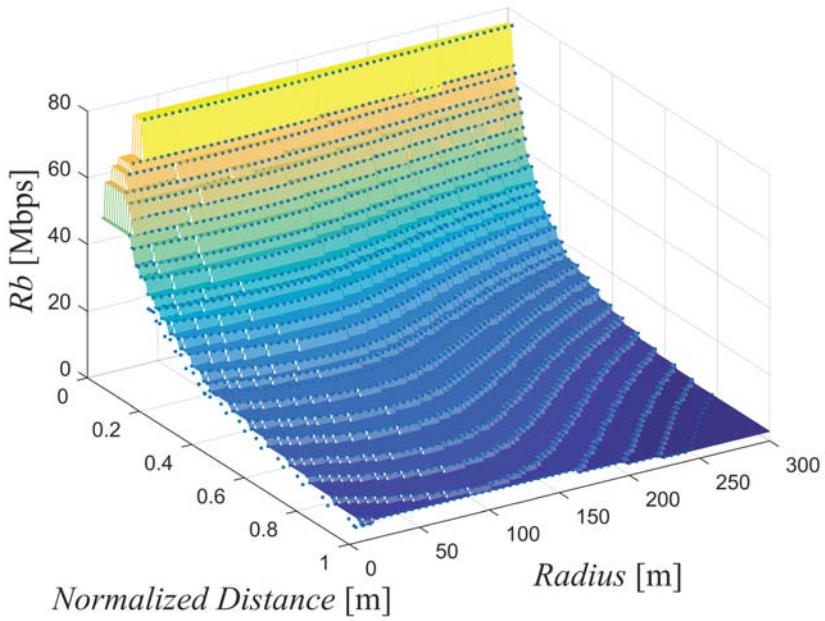

Figure 2.43: 3D view of the PHY throughput mapped into MCSs for the 60 GHz frequency band with interferer and $R = 300$ m

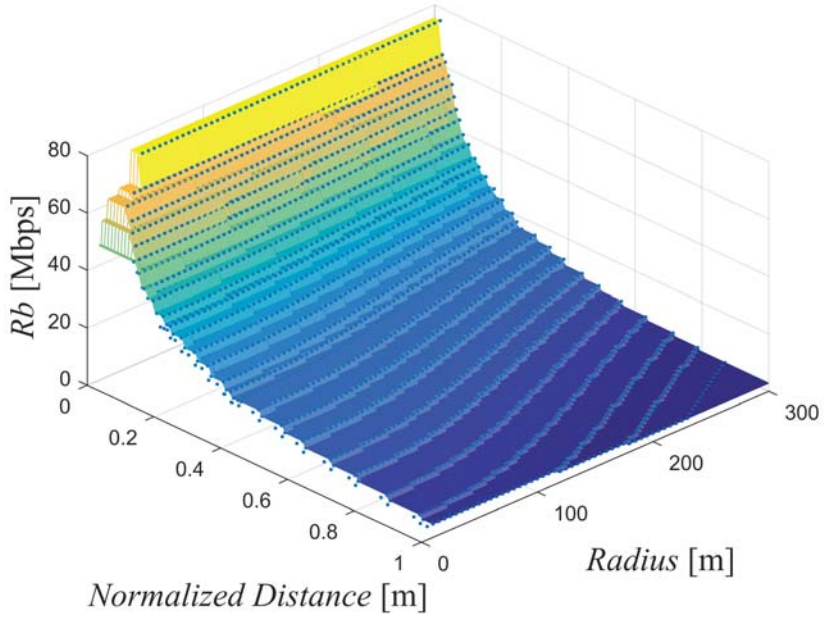

Figure 2.44: 3D view of the PHY throughput mapped into MCSs for the 73 GHz frequency band with interferer and $R = 300$ m

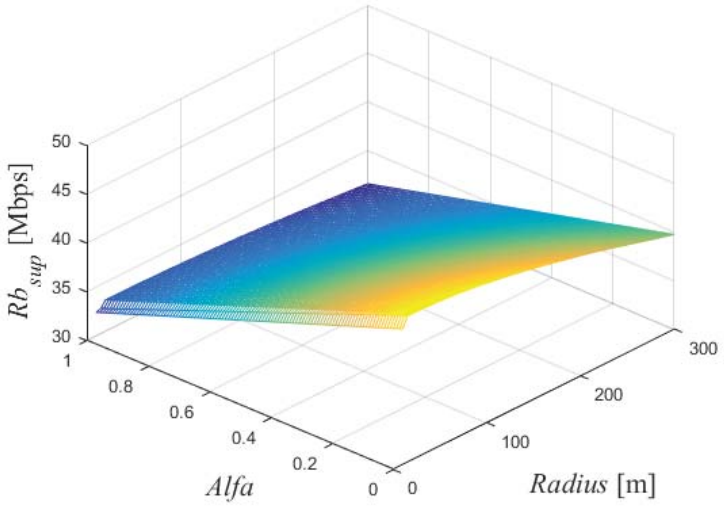

Figure 2.45: Intermittent scenario for 28 GHz frequency band and $R = 300$ m

2.9 Summary and Conclusions

This study analyses the viability of spectrum sharing for UHF/SHF, as well as for the mmWaves. The PHY and equivalent supported throughput within cells have been assessed while considering reuse pattern $k = 3$ and $k = 4$ for the UHF/SHF frequency bands and $k = 3$ (only) at the mmWaves, respectively.

We assume in this preliminary phase that LTE is also considered for the mmWaves. The computation of interference considers LoS propagation models. From this preliminary analysis, we have learned that the Supported throughput at the 38, 60 and 73 GHz is higher than the one for the UHF/SHF bands for the shortest Rs, however 28 GHz band has a different behaviour with

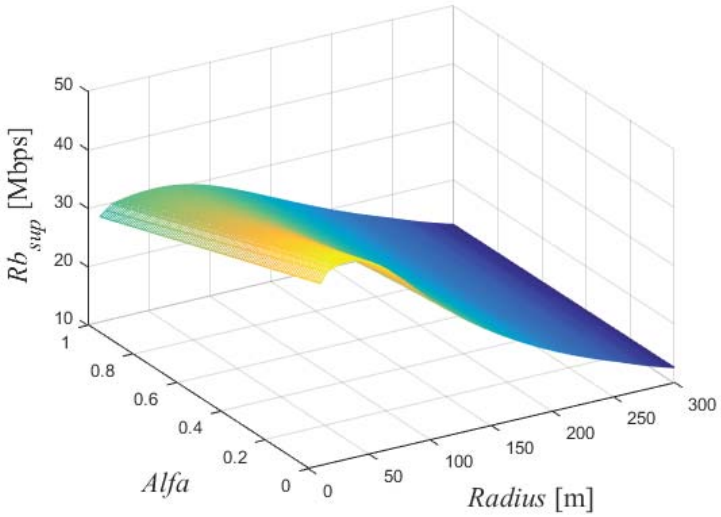

Figure 2.46: Intermittent scenario for 60 GHz frequency band and $R = 300$ m

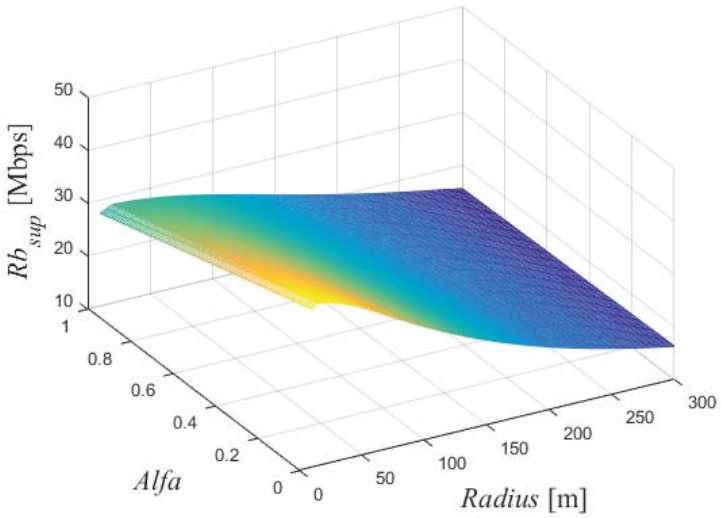

Figure 2.47: Intermittent scenario for 73 GHz and $R = 300$ m

the highest throughput with and without sharing.

For all the other frequencies considered, we have learned that the highest system capacity and the highest MCSs are achievable for the shortest coverage distances at mmWaves bands, which have a higher throughput up to 156 m, after this coverage radius, the 2.6 and 3.5 frequency bands have higher Supported throughput values, reaching a maximum of 38 Mbps. In fact, due to the behaviour arising from the two-slope propagation model (Umi LoS) applied to 2.6 and 3.5 GHz, for shorter Rs the mmWaves have the highest values.

The 28 GHz frequency band has the highest Supported throughput, reaching 45 Mbps.

The spectrum usage does influence on the results of throughput because for the both cases, the mmWaves band have a bigger supported throughput for shorter radius $(R \leq 156m)$ while the UHF/SHF have the same but for longer radius $(R > 156m)$, with exception of the 28 GHz frequency band, which has always a higher supported throughput for all the cell radius. The average SINR has been analytically studied for different values of the transmitter power. We

have been able to conclude that Average SINR does not depend of the transmitter power and that it has the same values at 2.6 GHz and 3.5 GHz frequency bands up to a cell radius of circa 50 m. Then, when the cell radius is longer than 50 m, the supported throughput at 2.6 GHz is higher than at 3.5 GHz. By comparing the curves for the supported throughput and the average SINR, we can observe that the values and the line shape are very similar.
As far as the 5G channelization and adaptive MCSs are assumed, the results for system capacity and service quality obtained for 4G will certainly be generalized for broadband 5G New Radio. As 5G will also consider OFDM, it is expected that the principles and lessons learned from analysing the optimization of the trade-off of 4G networks will remain.

Chapter 3

Packet-level Simulations with LTE-Sim

3.1 Simulation

The Simulation [33] is used in order to study a question of interest, the facility of a process of interest is called a system, and has to be made on a set of assumption of how it works. These assumptions will normally use a form of mathematical or logical relationships creating a model which is used to try to understand how a system works or behaves. The way to study this system will depend on the model it is inserted. So, for example, if the model is simple enough then probably mathematical models can be used, such as algebra or calculus in order to obtain information about the interest questions of the main problem. This kind of approaches are called analytic solutions. However, most of real-world systems are too complex to allow these models to be evaluated by an analytic solution. So these models will need to be studied by means of simulation. In a simulation, a computer is used to evaluate a model, numerically in which the data is gathered in order to estimate the desired true characteristics of the model. Simulations have great importance, especially in the industry, as a way to test if a product or a technology would justify some investment or construction, because it would not be cost-effective to build or create something and then remove it later, if it does not work out. An as example of simulation, we have the simulations in this dissertation, where we use a propagation model considering LoS and dual pathloss, we try to use an analytical solution gathering the values using the distance and the model proposed to get values such as the throughput which has a mathematical equation to be computed.
Nowadays the applications areas where simulation is numerous and diverse are for example:

- Designing and analysing manufacturing systems;
- Evaluating Military weapon systems;
- Determining hardware requirements or protocols for networks;
- And much more.

So following three main topics systems, models and simulations. A system is defined as a collection of entities that act together toward the accomplishment of some logical end. In practice the system depends on the objectives of the studies as the collection of entities that comprise that system might be only a subset of the overall for another, a system will depends on the objectives of a particular study, as an example, we have entities such as a person walking from the center eNB to the cell edge. So the system to this particular study is a person who is inserted in a cell that belongs to a cellular layer, walking from point A to point B. A system always has a state, this is defined to be the collection of variables necessary to describe a system at a particular time, always related to the objectives of the study. So in this specific case or study examples of state variables is the distance from the chosen cell to the user equipment depending on the case that is being studied, not all the parameters of the study/simulation can be considered study variables because they are constant for example the parameters of the cell

towers like the Gains of the antennas or the transmission power.
A system can be categorized in two types:

- Discrete;
- Continuous.

A discrete system is a system in which the state variables change instantaneously at separated points in time, while a continuous system is when the state variables change continuously with respect to time. Few systems in practice are only discrete or continuous. However since the most of time one type of the system is predominant for most system, it is usually possible to classify a system as either discrete or continuous. In the case of study in this research, the system is discrete because we get values from mathematical equations depending on the distance between the UE and the central eNB, which is changing with the step chosen.
There are different ways in which a system can be studied, such as:

- Experiment with actual system vs Experiment with a model of the system;
- Physical model vs Mathematical model;
- Analytical solution vs Simulation.

Once again in this specific case of study, analytic solution vs simulation, where diverse equations and a mathematical model is used which represents the Path loss LoS to obtain different values, for example received power, interference, and physical throughput. An analytical solution can be obtained with just paper and pencil. However the problem is that some analytical solutions can become complex, requiring a lot of computing resources. As such an analytical solution to a mathematical model is available and computationally efficient then is desirable to study the model analytically, instead of by simulation. Even though some mathematical models can be very complex and this can affect the possibility of an analytical solution, in this case, and only in this case, the model must be studied by means of simulation.
When we talk about simulation using mathematical models, we should classify the different simulation models by the following three different dimensions:

- Static vs Dynamic solution models;
- Deterministic vs Stochastic simulation models;
- Continuous vs Discrete simulation.

3.2 What is LTE-Sim?

LTE-Sim is a open source framework developed in the University of Bari [4] commonly known as an event-driven simulator written in $C++$, using the object-oriented paradigm. This powerful simulator can encompass several aspects of LTE networks, including models of both the Evolved UMTS Terrestrial Radio Access (E-UTRAN) and the evolved packet system, DL and UL transmissions, single and multi-cell environments, Quality of Service (QoS) management, multiusers environment, user mobility, handover procedures, and frequency reuse techniques.

3.3 Simulation Environment

In this work, the performance is evaluated for inter-cell distances, being these ones the central cell and the six co-channel cells, with a reuse pattern $k = 3$, as a continuation of the cellular planning made in chapter 2. The users, from 12 to 20, are uniformly distributed throughout the central cell, walking in a random direction with a constant speed of 3 km/h. Each scenario was simulated 50 times, then these results have been averaged and the confidence intervals represented. The video traffic is addressed in this research, as a trace-based application which send packets based on realistic video trace files, so to study the performance on this scenarios it was considered the H.264 3.1 Mbps video bit rate flow with a 20 MHz bandwidth. In the proposed scenario it is used a DL packet scheduler. The simulation method is based on [23]. A DL packet scheduler was chosen for these simulations, which is Modified Largest Weighted Delay First (M-LWDF) because in the case of addressed video applications, this scheduler outperform the others as cited in [34].
MLWDF is an algorithm designed to support multiple real-time data users and supports multiple data users with different QoS requirements. In every Transmission Time Interval (TTI), the scheduler computes a metric, $w_{i,j}$, for the ith flow in the jth sub-channel. If the ith flow is a real time flow then the metric is computed as follows:

$$w_{i,j} = a_i D_{HOL,i} * \frac{r_{i,j}}{\bar{R}_i} \quad (3.1)$$

Where $D_{HOL,i}$ is the ith flow head of line (HOL) packet delay, $r_{i,j}$ is the instantaneous available rate (of the ith flow in the jth sub-channel) and $\bar{R}_i$ is ith flow average transmission rate, computed as follows [4]:

$$\bar{R}_i = 0.8\bar{R}_i(k-1) + 0.2R_i(k) \quad (3.2)$$

Where $R_i(k)$ is the data rate achieved by the ith flow during the kth TTI and $\bar{R}_i(k-1)$ is the data rate estimation in the previous TTI. Given two flows with equal HOL, α_i weights the metric so that the user with the strongest requirements in terms of acceptable loss rate and deadline expiration will be preferred for allocation [35] and is given by [4]:

$$\alpha_i = -\frac{log(\delta_i)}{\tau_i} \quad (3.3)$$

Where τ_i is packet delay threshold and δ_i is maximum probability that $D_{HOL,i}$ exceeds the delay threshold of the ith flow, respectively. To study the performance of the proposed scenario, simulations have been performed. This simulations count on some units of study, such as Packet Loss Ratio (PLR) or goodput. The parameters considered for the simulations are presented in table 3.1. The video application at 3.1 Mbps is characterized in [34].

Table 3.1: Simulation Parameters

Scheduler	M-LWDF
Reuse pattern	3
Simulation duration	46 s
Flow duration	40 s
Frame structure	FDD
Bandwidth	20 MHz
Slot duration	0.5 ms
Scheduling Time (TTI)	1 ms
Number of RBs	100 RB
Max delay	0.1 s
Video bitrate	3.1 Mbps [34]
UE mobility	random direction, 3 kmph

3.4 Simulation Results

3.4.1 Small Cell Scenario

The SC scenario considers the central cell and the six co-channel cells, using a reuse pattern $k = 3$ and considering cell radius up to 300 m. This scenario is represented in the figure 3.1.

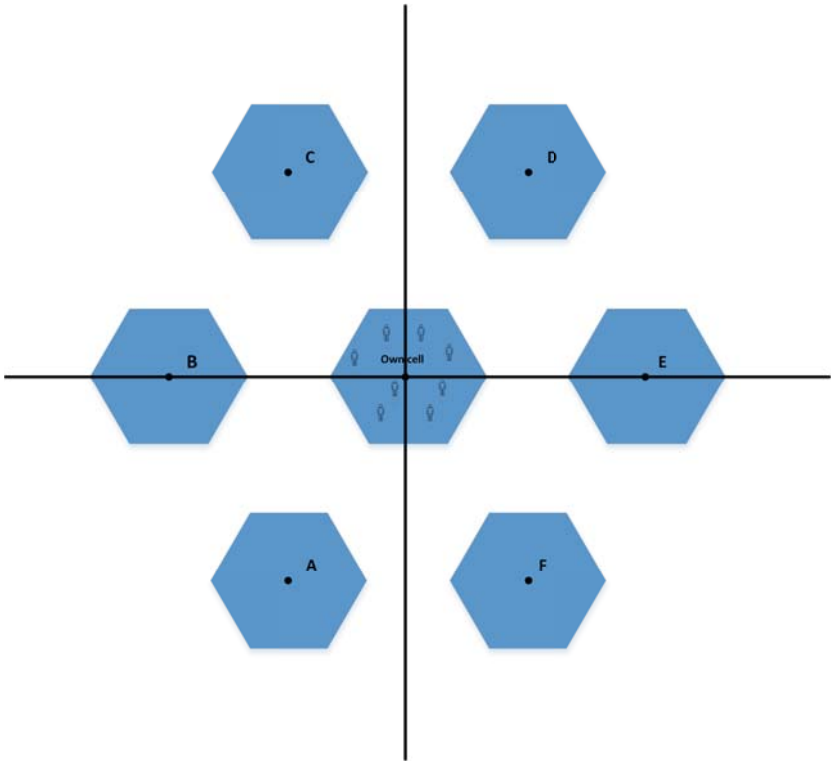

Figure 3.1: Small Cell cluster scenario

Goodput has been obtained via simulation for both bands. Figure 3.2 show the average cell goodput as a function of radius for the scenarios and made a comparison between the scenario with sharing, Northeast, and without sharing. Being the sharing represented in a traced line and without sharing in a line, respectively. Each scenario has been simulated 50 times and averaged, the confidence intervals have been also represented. PLR is the complementary of goodput, which all the results are presented in appendix E. All the figures represented in these section had a minimum distance of 0.015 km, because of the propagation model UMi LoS . As

expected, the goodput values for the scenario without sharing are higher than the ones for the sharing scenario, but considering that the threshold to a have a good video application working is 2% of PLR, only some values are acceptable. The respective PLR represented for both these scenarios for 2.6 GHz is represented in figure E.1. All the PLR values for the scenario with sharing are higher than the maximum acceptable values, so the UE will have video but without enough quality, or no video at all. Considering the scenario without sharing, only when the UE reaches $R = 0.175$ km, the PLR is appropriate, but only for all number of users expect 20, with the values of PLR decreasing as the UE reaches a fraction of the breakpoint distance.

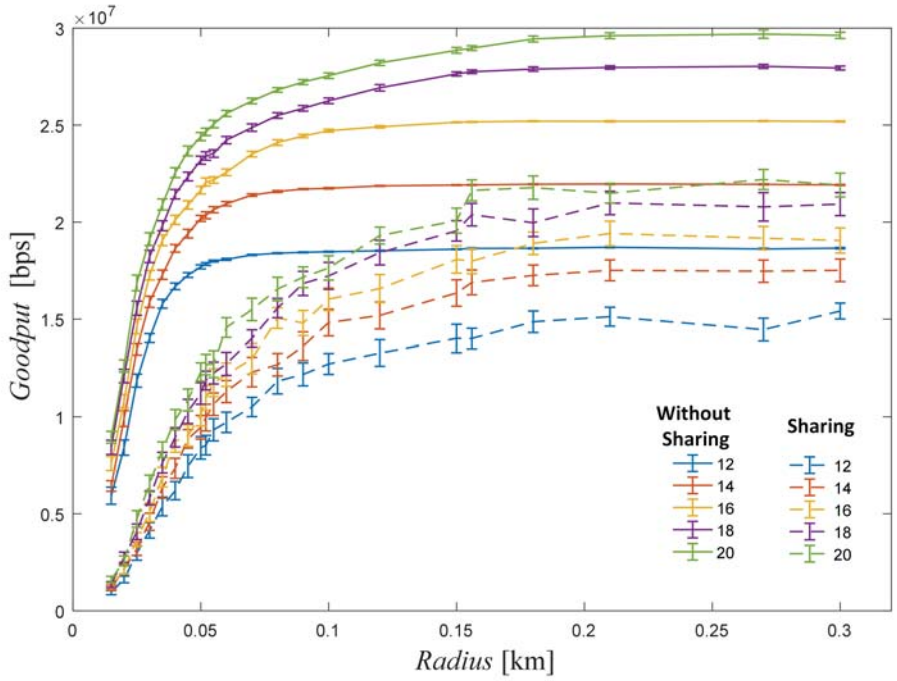

Figure 3.2: Goodput as a function of the cell radius with a transmitter power of 40 dBm, for the scenarios with/without sharing at 2.6 GHz

As for the scenarios with/without sharing for 3.5 GHz, the goodput values are represented in figure 3.3 and PLR in figure E.2, respectively. Considering the scenario with sharing, the behaviour is very similar to the ones at 2.6 GHz, with every PLR value higher than the threshold of 2%. So once again, even if the UE has higher values of goodput, the video will not have enough quality. For the scenario without sharing, only when the UE reaches a fraction of the breakpoint distance, the values are acceptable for a good video transmission.

As only the scenarios without sharing have acceptable values, a comparison between 2.6 GHz, represented in line, and 3.5 GHz, represented in traced line, was represented in figure 3.4. The goodput values are very similar with two differences in number of users. When the number of users are 12, 14 and 16, the values are almost the same for all the radius, but if we consider the remaining number of users, 18 and 20, the goodput values are the same, for both bands, until the breakpoint distance of 3.5 GHz is reached, i.e. 0.21 km. This behavior was expected for both bands, when the goodput is low, the PLR is high which create more physical layer errors. Also the transmitter power values for both bands are different, with the objective of having the same behavior due to the attenuation, which could generate similar goodput values for both bands.

In terms of delay both bands, 2.6 and 3.5 GHz, represented in figures 3.5a and 3.5b, the maximum

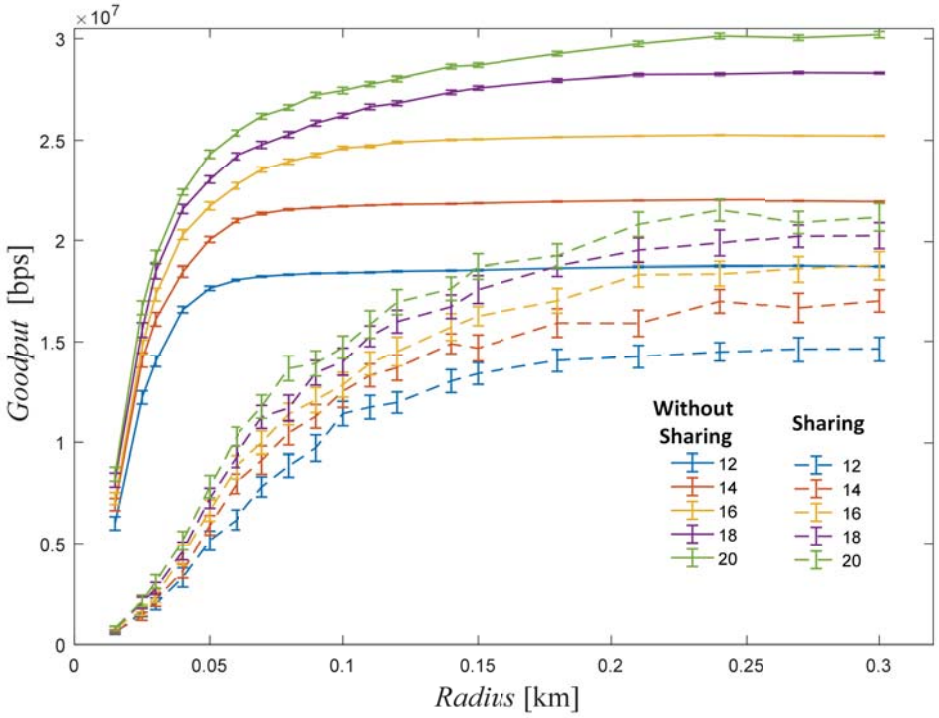

Figure 3.3: Goodput as a function of the cell radius with a transmitter power of 42.2778 dBm, for the scenarios with/without sharing at 3.5 GHz

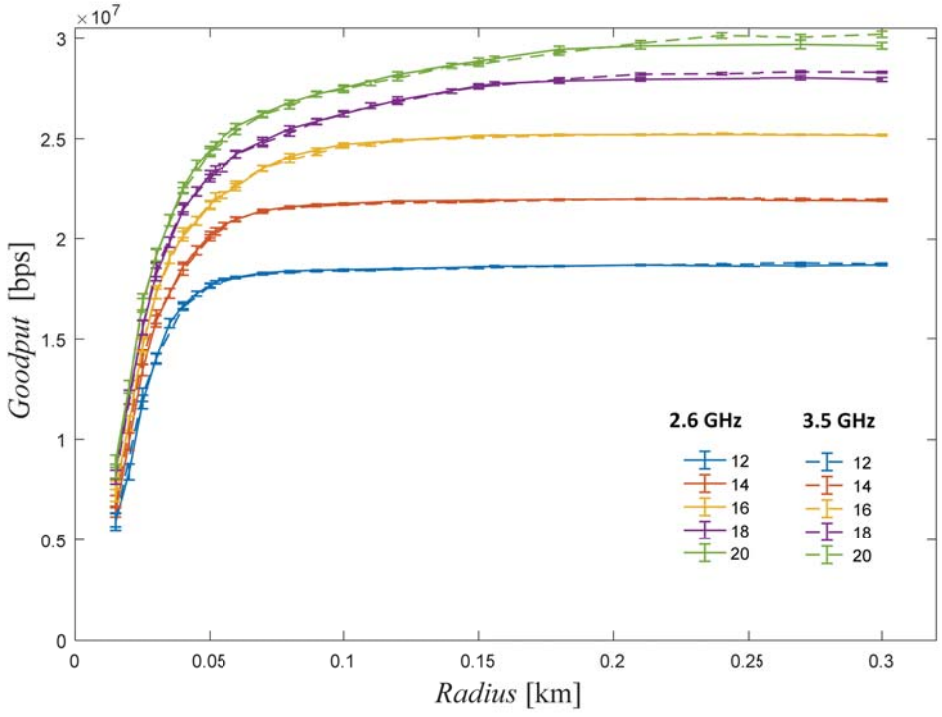

Figure 3.4: Comparison of foodput as a function of the cell radius between scenario without sharing for 2.6 and 3.5 GHz

value is 55 ms. With a maximum value of 55 ms even for a gaming application would work well, so the latency would be enoughly low. Even with the same maximum delay value, for a small

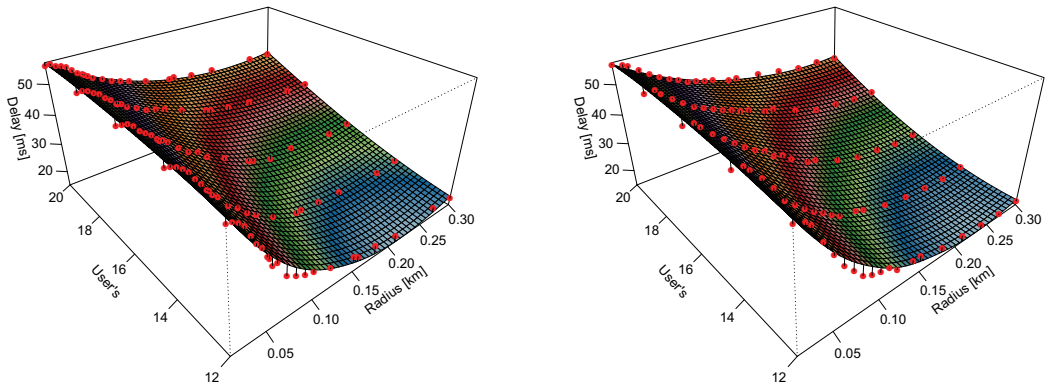

(a) Delay at 2.6 GHz

(b) Delay at 3.5 GHz

Figure 3.5: Delay values for both bands considering the scenario without sharing

number of users, 12 and 14, the 3.5 GHz band have a lower latency, because the area of the blue surface is higher than the one for the 2.6 GHz.

3.5 Comparison between analytical and simulation results

In the figure 3.6 are represented the simulation and analytical results for 2.6 GHz. When the analytical results were considered, the supported throughput values were obtained, but in the simulation the goodput was obtained. Throughput is the data rate for the packet with header, while the goodput is the data rate but only with the data, in this case the video. The values for analytical and simulation are different for shorter radius because of the packet loss ratio, as the analytical does not consider packet loss. The line type and behavior are similar for both cases.

3.6 Summary and Conclusions

For better understanding the performance of the pico-cells we considered a packet-level simulation using the open source framework called LTE-Sim. We have studied at 3.1 Mbps [34] , with a different number of users (running video applications) walking randomly in a central cell, with an uniform distribution. The confidence intervals were also represented [4]. For the video application to run properly the PLR values need to be less than 2%. We conclude that:

- When a scenario with sharing is considered the PLR values are always higher than the threshold, so there will be no quality in the video transmission for all cell radius;
- For scenarios with sharing, only when the users reach longer radius, i.e. 0.175 km, the PLR values are appropriate;

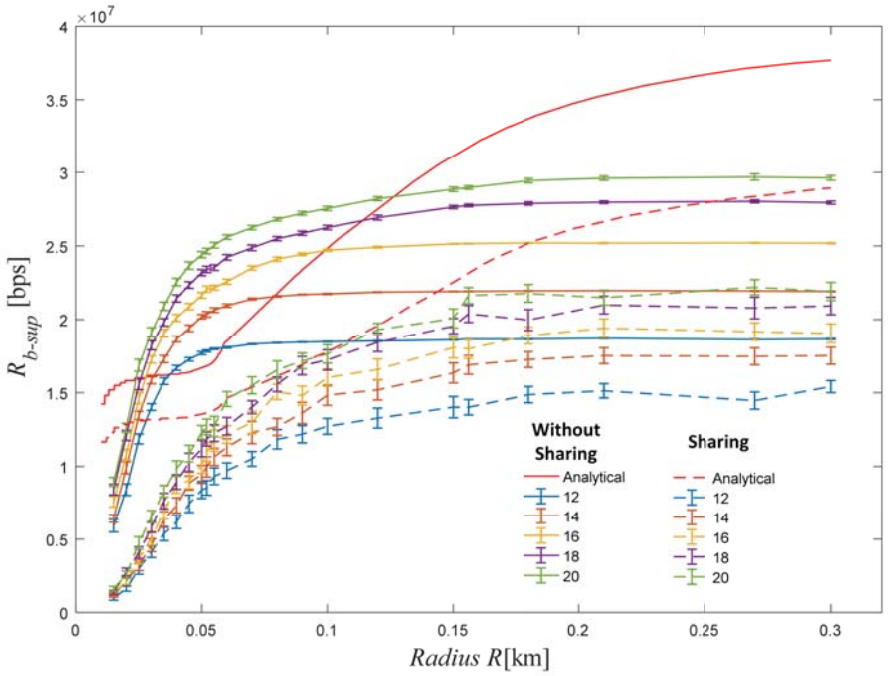

Figure 3.6: Comparison between analytical and simulation results for scenarios with/without sharing at 2.6 GHz

- By comparing the goodput values for 2.6 and 3.5 GHz for a small number of users, such as 12, 14 and 16, they are very similar. However for 18 and 20 users, the goodput values increase for longer radius.
- By comparing the analytical and simulation results for the supported throughout / goodput (without sharing) there are differences, as analytical results do not consider packet errors, and for a number of users higher than $16-18$, the PLR is too high even for distances longer than $100-150$ m, while for 16 or less users the PLR is only high for coverage distances up to circa 100 m. This differences between analytical and simulation results can be mainly explained by the fact that the number of users are not considered in the analytical formulation (saturation conditions are assumed instead), and also because of the high value for the PLR.
- In terms of delay in both bands, 2.6 and 3.5 GHz, the maximum value is 55 ms. For a delay of 55 ms a gaming application would work well, so the latency would be enoughly low.

Chapter 4

Conclusions and Future Research

4.1 Conclusions

This MSc dissertation explores the cellular and radio network optimization in Ultra High Frequency (UHF), Super High Frequency (SHF) and millimetre wavebands (mmWaves) in outdoor environments. In the mmWaves the linear cellular topology is considered while in the UHF/SHF bands cells with hexagonal shape are assumed. Performance evaluation includes the study of the behaviour of PHY, supported throughput, average CNIR and intermittent scenarios for 2.6, 3.5, 28, 38, 60 and 73 GHz. While the two-slope model is considered for the 2.6 and 3.5 GHz frequency bands, the modified Friis propagation model, with shadow fading, and different values for the standard deviation, is considered in the millimetre wavebands.We assume the computation of interference considers LoS propagation models. The computation of interference considers LoS propagation models. Different reuse patterns have been considered, i.e., $k = 3$ and $k = 4$ for 2.6 and 3.5 GHz frequency bands, while only $k = 3$ has been considered for the 28, 38, 60 and 73 GHz frequency bands. One of the main objectives has been to analyze the viability of spectrum sharing for UHF/SHF, as well as for the mmWaves. In chapter 2 we have learned that the 28 GHz frequency band has the highest supported throughput, reaching 45 Mbps. The supported throughput at the 38, 60 and 73 GHz is higher than the one for the UHF/SHF bands for the shortest Rs. For longer coverage distances, the supported throughput is clearly higher for the UHF/SHF frequency bands (compared to the 38, 60 and 73 GHz frequency bands) from the sharing scenario converges to the one from the scenario without sharing. The average CNIR has been analytically studied for different values of the transmitter power. We have been able to conclude that average CNIR does not depend of the transmitter power and that it has the same values at 2.6 GHz and 3.5 GHz frequency bands up to a cell radius of circa 50 m. Then, when the cell radius is longer than 50 m, the supported throughput at 2.6 GHz is higher than at 3.5 GHz. By comparing the curves for the supported throughput and the average CNIR, we can observe that the trend of the values, i.e., the line shapes, are very similar.

After the addressing analytical formulations and results in chapter 2, the next research aspect has been a packet-level simulation using the open source framework called LTE-Sim, a open source framework developed in the University of Bari [4], we have studied a SC cluster scenario, where there are different number of users walking randomly in a central cell, on a uniform distribution. When a scenario with sharing is considered the PLR values are always higher than the threshold, so there will be not enough quality in the video transmission for all cell radius. For the results, when scenarios with sharing are considered, the PLR values are appropriate for coverage distances longer than 175 m; Comparing the goodput values for 2.6 and 3.5 GHz for a small number of users, such as 12, 14 and 16, they are very similar. However for 18 and 20 users, the goodput values increase for longer radius. By comparing the analytical and simulation results for the supported throughout/goodput (without sharing) there are differences, as analytical results do not consider packet errors, and for a number of users higher than $16 - 18$, the PLR is too high even for distances longer than $100 - 150$ m, while for 16 or less users the PLR is only high for coverage distances up to circa 100 m. These differences between analytical and simulation

results can be mainly explained by the fact that the number of users are not considered in the analytical formulation (saturation conditions are assumed instead), and also because of the high value for the PLR. In both bands, a delay of 55 ms was achieved, even for a gaming application would work well, so the latency would be enoughly low.

4.2 Future Activities

This work considered the study of viability of spectrum sharing for Ultra High Frequencies and Super High frequencies. A suggestion for future work is the study of these scenarios, with $k = 3$ and $k = 4$, but for the 5 GHz frequency band because it is a widely used frequency band for LTE and usage certainly will increase with 5G New Radio.

References

[1] S. Parkvall, E. Dahlman, A. Furuskar, and M. Frenne, "Nr: The new 5g radio access technology," *IEEE Communications Standards Magazine*, vol. 1, no. 4, pp. 24–30, Dec 2017. vii, ix, 3

[2] S. Kavanagh. What is 5g new radio (5g nr). [Online]. Available: https://5g.co.uk/guides/what-is-5g-new-radio/ vii, ix, 3, 4

[3] (2017) Lte to 5g: Cellular and broadband innovation,. [Online]. Available: http://www.5gamericas.org/files/6415/0282/1551/2017_5G_Americas_Rysavy_LTE_5G_Innovation__Final_for_Upload.pdf vii, ix, 2, 3

[4] G. Piro, L. A. Grieco, G. Boggia, F. Capozzi, and P. Camarda, "Simulating lte cellular systems: An open-source framework," *IEEE Transactions on Vehicular Technology*, vol. 60, no. 2, pp. 498–513, Feb 2011. vii, ix, 54, 55, 59, 61

[5] Qualcomm. (2016) Making 5g nr a reality. [Online]. Available: https://www.qualcomm.com/invention/5g/5g-nr xiii, 2, 4, 5, 6

[6] Patrick Mannion´. (2017) Connect the dots: Massive, 5g readies to take low-latency iot mainstream. [Online]. Available: https://www.iotsolutionprovider.com/industrial/connect-the-dots-massive-5g-readies-to-take-low-latency-iot-mainstream xiii, 5

[7] Jeanette Wannstrom. (2013) Carrier aggregation explained. [Online]. Available: http://www.3gpp.org/technologies/keywords-acronyms/101-carrier-aggregation-explained xiii, 7, 8

[8] MetrocellMasterClass, "Heterogeneous networks," http://blog.3g4g.co.uk/2013/04/interference-management-in-hetnets.html, accessed: 2018-01-28. xiii, 9

[9] HetNet.com, "What are small cells? a basic guide to femtocells, picocells and microcells," http://hetnet.com/what-are-small-cells-a-basic-guide-to-femtocells-picocells-and-microcells/, accessed: 2018-01-28. xiii, 10

[10] (2018) Small cell networks market report- forecast to 2023. [Online]. Available: https://www.marketresearchfuture.com/reports/small-cell-networks-market-5360 xiii, 11

[11] H. Holma, A. Toskala, and J. Reunanen, *LTE Small Cell Optimization: 3GPP Evolution to Release 13*. Wiley, 2016. 1

[12] J. McMenamy, I. Macaluso, N. Marchetti, and L. Doyle, "A methodology to help operators share the spectrum through an enhanced form of carrier aggregation," in *2014 IEEE International Symposium on Dynamic Spectrum Access Networks (DYSPAN)*, April 2014, pp. 334–345. 1

[13] J. M. Peha, "Sharing spectrum through spectrum policy reform and cognitive radio," *Proceedings of the IEEE*, vol. 97, no. 4, pp. 708–719, April 2009. 1

[14] SCF, “Small cell vendors race to fulfill operator demand for lte,” press Released on 2012-02-07. 2

[15] A. Checko, H. L. Christiansen, Y. Yan, L. Scolari, G. Kardaras, M. S. Berger, and L. Dittmann, “Cloud ran for mobile networks 2014;a technology overview,” *IEEE Communications Surveys Tutorials*, vol. 17, no. 1, pp. 405–426, Firstquarter 2015. 2

[16] 3GPP, “3gpp,” http://www.3gpp.org/, accessed: 2018-01-28. 2

[17] National Instruments. (2017) 5 things to know about 5g new radio. [Online]. Available: http://www.ni.com/pt-pt/innovations/5g/new-radio.html 3

[18] C. Bockelmann, N. Pratas, H. Nikopour, K. Au, T. Svensson, C. Stefanovic, P. Popovski, and A. Dekorsy, “Massive machine-type communications in 5g: physical and mac-layer solutions,” *IEEE Communications Magazine*, vol. 54, no. 9, pp. 59–65, September 2016. 4

[19] Nokia. (2016) 5g for mission critical communication,achieve ultra-reliability and virtual zero latency. [Online]. Available: http://www.hit.bme.hu/~jakab/edu/litr/5G/Nokia_5G_for_Mission_Critical_Communication_White_Paper.pdf 4

[20] C.-P. Li, J. Jiang, W. Chen, T. Ji, and J. Smee, “5g ultra-reliable and low-latency systems design,” in *2017 European Conference on Networks and Communications (EuCNC)*, June 2017, pp. 1–5. 4

[21] Yitaek Hwang. (2017) What is cbrs? - lte in 3.5 ghz shared spectrum and what it means for iot. [Online]. Available: https://www.leverege.com/blogpost/what-is-cbrs-lte-3-5-ghz 6

[22] M. G. Kibria, G. P. Villardi, K. Nguyen, K. Ishizu, and F. Kojima, “Heterogeneous networks in shared spectrum access communications,” *IEEE Journal on Selected Areas in Communications*, vol. 35, no. 1, pp. 145–158, Jan 2017. 12

[23] R. R. Paulo, F. J. Velez, and G. Piro, “Design of coordinated henb deployments,” in *2018 IEEE 87th Vehicular Technology Conference (VTC Spring)*, June 2018, pp. 1–6. 13, 55

[24] Guidelines for evaluation of radio interface technologies for imt-advanced, report itu-r m.2135-1,. [Online]. Available: https://www.itu.int/dms_pub/itu-r/opb/rep/R-REP-M.2135-1-2009-PDF-E.pdf 15

[25] S. Sousa, F. J. Velez, and J. M. Peha, “Impact of propagation model on capacity in small-cell networks,” in *Performance Evaluation of Computer and Telecommunication Systems (SPECTS), 2017 International Symposium on*. IEEE, 2017, pp. 1–8. 30, 42, 45, 47

[26] F. J. Velez, D. Robalo, and J. A. Flores, “Lte radio and network planning: Basic coverage and interference constraints,” in *2015 7th IEEE Latin-American Conference on Communications (LATINCOM)*, Nov 2015, pp. 1–6. 30, 40, 45

[27] F. J. Velez, A. H. Aghvami, and O. Holland, “Basic limits for fixed worldwide interoperability for microwave access optimisation based in economic aspects,” *IET Communications*, vol. 4, no. 9, pp. 1116–1129, June 2010. 40

[28] E. Teixeira and F. J. Velez, “Cost/revenue trade-off of small cell networks in the millimetre waveband,” in *IEEE 87th Vehicular Technology Conference: VTC2018*. IEEE, 2018. 44, 45, 46, 47

[29] M. K. Samimi, T. S. Rappaport, and G. R. MacCartney, “Probabilistic omnidirectional path loss models for millimeter-wave outdoor communications,” *IEEE Wireless Communications Letters*, vol. 4, no. 4, pp. 357–360, Aug 2015. 44

[30] T. Rappaport, R. Heath, R. Daniels, and J. Murdock, *Millimeter wave wireless communications*. Prentice Hall, 2015, includes bibliographical references (pages 585-651) and index. 44

[31] A. I. Sulyman, A. T. Nassar, M. K. Samimi, G. R. Maccartney, T. S. Rappaport, and A. Alsanie, “Radio propagation path loss models for 5g cellular networks in the 28 ghz and 38 ghz millimeter-wave bands,” *IEEE Communications Magazine*, vol. 52, no. 9, pp. 78–86, September 2014. 44

[32] T. S. Rappaport, G. R. MacCartney, M. K. Samimi, and S. Sun, “Wideband millimeter-wave propagation measurements and channel models for future wireless communication system design,” *IEEE Transactions on Communications*, vol. 63, no. 9, pp. 3029–3056, Sept 2015. 44

[33] A. M. Law and D. M. Kelton, *Simulation Modeling and Analysis*, 3rd ed. McGraw-Hill Higher Education, 1999. 53

[34] D. Robalo and F. J. Velez, “Economic trade-off in the optimization of carrier aggregation with enhanced multi-band scheduling in lte-advanced scenarios,” *EURASIP Journal on Wireless Communications and Networking*, vol. 2015, no. 1, pp. 1–19, 2015. 55, 56, 59

[35] F. Capozzi, G. Piro, L. A. Grieco, G. Boggia, and P. Camarda, “Downlink packet scheduling in lte cellular networks: Key design issues and a survey,” *IEEE Communications Surveys Tutorials*, vol. 15, no. 2, pp. 678–700, Second 2013. 55

[36] Wigle.net, “Wigle,” https://wigle.net/, accessed: 2017-12-2. 67

[37] Google, “Maps javascript api,” https://developers.google.com/maps/documentation/javascript/examples/, accessed: 2017-12-2. 67

Appendix A

Mapping Tool

A.1 Introduction

Mapping Tool was a tool made in the programming language Matlab, this program as the objective of using the data collected by wigle.net to find the points with extra traffic, different places of study were discussed such as Parque das Nações, in Lisboa, or the Serra Shopping, in Covilhã. The tool will use the Wifi APs to identify that possible places in which exist an higher data traffic. In this chapter the tool will be defined, there will have instructions how to use and some examples. The proposal is to address frequency assignment locally, only considering interference from co-channel SCs in a given neighborhood while evaluating performance. As MCSs are present one will propose a dynamic procedure to define SINR threshold for the MCS that define the cell range. A given frequency will be assigned in each of the cells. If the SINR overcomes the established threshold then a new frequency will be assigned. Using the database from [36], it is possible to determine the position of the existing infrastructure and consideration of the choice of the placement/deployment of the Small Cell Layer eNBs. Frequency Assignment algorithms with and without spectrum sharing will then be proposed and applied to the new cellular topology, from a range of existing or new proposed algorithms with implications of RRH and Small Cells with Spectrum Sharing.
The purpose is to create a computational-geometry based tool to design wide and broadband cellular systems operating in different scenarios using spectrum sharing, on real environments, considering carrier aggregation. The maps and markers are based on [37].

A.2 Tool Functions

So to solve this problem it was created the Mapping Tool mentioned above made in Matlab that have been enhanced until now, and those enhancements and results will be explained using examples of the usage of the Tool as well as the implemented functions.
This tool perform the tasks above:

- Access to the Database (wigle.net);
- The User will need to insert the values on the boxes of latitude and longitude (Mapping by Coordinates);
- Operator Filtering;
- Mark the Filtered Hotspots on the map;
- Then it calculate the Distance between every Hotspot in the searched Area, filtering some of them (because on some cases there exist two channels on the same Hotspot, e.g. “FON-ZON Free Internet”).

A.3 Program Explained

This section is divided in three parts:

- Explanation Step-by-Step
  This part teaches how to use the tool, and the steps the user will need to follow;
- Explanation of the Code
  In this part all the code that have been implemented on the tool will be explained;
- Explanation with Examples
  In this part there will be explanations with examples.

A.3.1 Explanation Step-by-Step

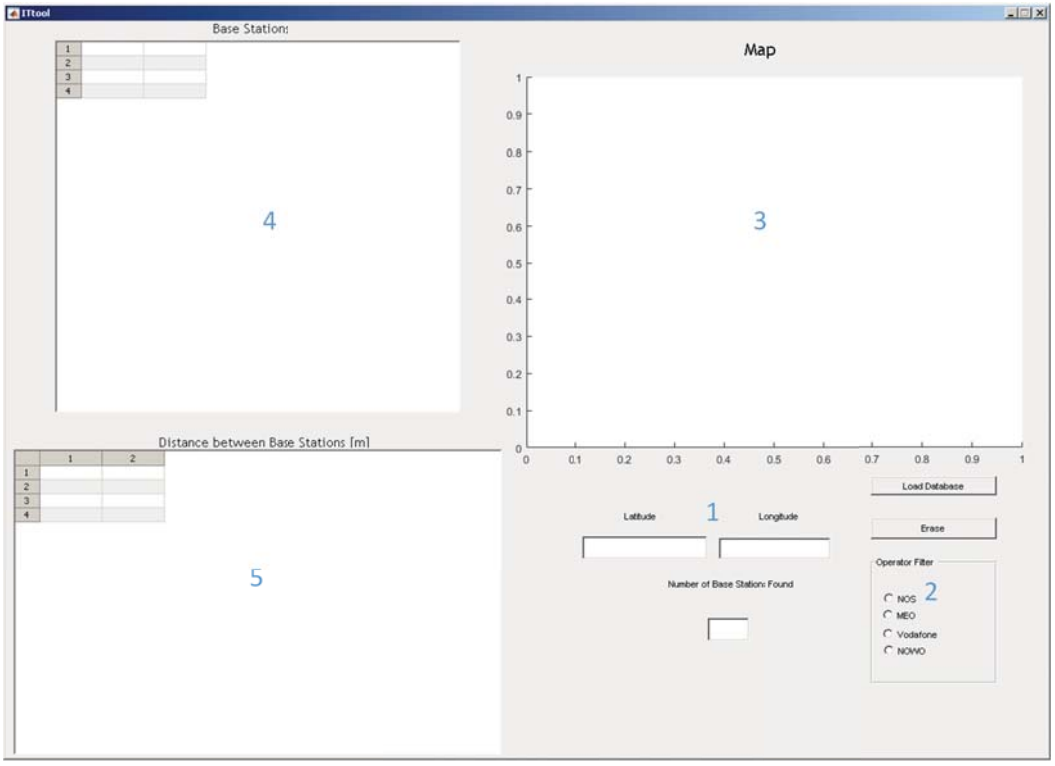

Figure A.1: ITtool

Above we have the ITtool layout. and we have the five numbers indicating the five steps.

- 1 - Insert Latitude and Longitude;
- 2 - Choose Operators (the user can click in more than one operator);
- 3 - After the user click on the Load Database button and choose the Database(explained above) the Map will appear with the Markers(which are the hotspot positions in the Map);
- 4 - All the base stations that have been found in the area shown in the map will be in the Base Stations table, and the total number will be found in the Number of Base stations found;
- 5 - The distances between every hotspot found will be in the Distance between Base Stations table.

A.3.2 Explanation of the Program Code

One of the most important Functions of the Tool is the function Get Map that works with the button “Load Database”, so when we press the button, the program get the latitude and longitude inserted previously by the user, then convert the type from String to Double, and insert the values on get google map function returning the map.
After showing the map, the program will save the corner points as a way to filter the figure because we only need the Hotspots from the map shown. This part of the code have been optimized, instead of using all the corners of the map, it only uses the $p1$ and $p3$ to get the interval of coordinates on the specific location and then filter the hotspots.
Then program will ask for the database file and will read the Document, all the Database have been previously downloaded from the wigle.net. After the database have been choosen, the tool will filter only what matters of all the information received from wigle.net that is MAC, SSID, Latitude, Longitude, Channel and QoS, which are respectively columns 2,3,9,10,11,13 as shown in the figure below, and will join every one of the columns on the final Table, to solve a speed performance trouble there was created a function called ”readdatabase”. The function ”readdatabase” let the user choose which database file wants to use A.2, these database files can be extrated from wigle.net in a csv or excel to be loaded in the tool.

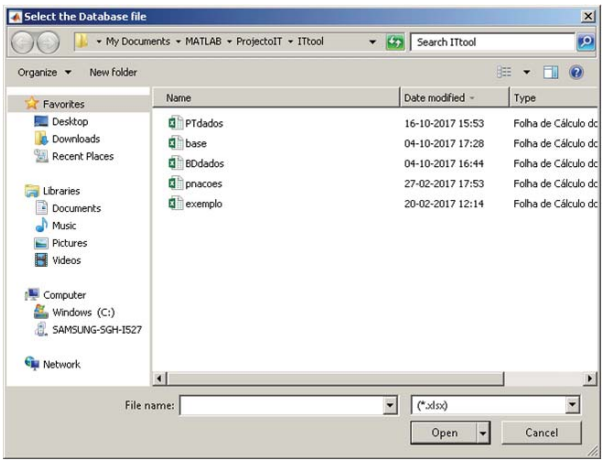

Figure A.2: Selection of the Database File

After the function readdatabase, the tool will save all the latitudes and the longitudes of the hotspots, and will start filtering all of them within the area of the map shown, saving all of the hotspots found in the finaltable. If no hotspots have been found then the program will print an error message on the screen show on A.3.

Figure A.3: Error Window

After all the area of map, coordinate filtering and the choice of database file, the program

will read the values of the Toggle buttons to choose operators. The Program will verify if any Operator has been Chosen, and if it is true, the program will try to extract the essids of the Filtered Networks and will apply an operator filter. If there is no Hotspot from operators, then the user will see an error Message on the screen, shown on A.3 else the program will send to the base Station Table's Handler.
Next the program will calculate the distance between every hotspot and will send the number of the total base stations found to the handler of the string with the same name. To calculate distances there was created a function called "distance". After all the distances have been calculated, the program will send the values to the Distances table Handler. On the table of distances we will have values such as "-1",that occurs because of ambiguity, the distance between Hotspot 1 and Hotspot 2 is the same as Hotspot 2 and Hotspot 1,so there won't be repetitions of the same Hotspots.
The function "distance" will compute the distance between two base stations/hotspots using the degrees computed by the function distance from Matlab, then will convert the result from degree to kilometers, and kilometers to meters.
The other function implemented in the ITtool is the "Clear Button". The function "Clear Button" reset everything and clear the console and the variables.
As new enhancement of the tool we have got markers on the map, these section of the program will take the latitude and longitude of the Hotspots Filtered by coordinates and operators, and mark them on the map. For this marker function to work, some code was modified and added on the get_google_map function.

A.3.3 Explanation with Examples

As the first example there will be used the Lisbon Coordinates and the Nos and Meo Operator Hotspots. So start to select the Operators chosen and insert the coordinates.

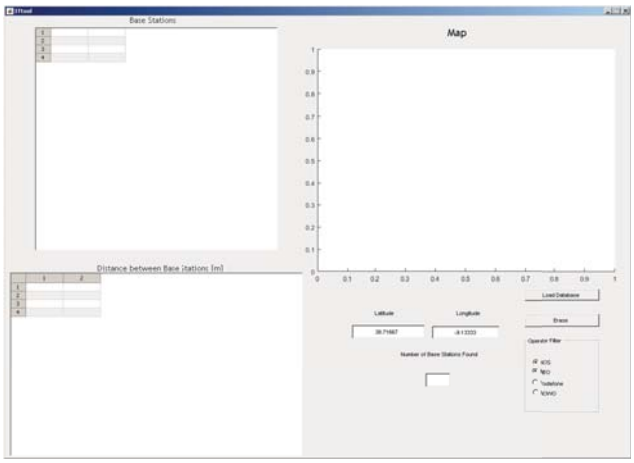

Figure A.4: Example with Lisbon

In this example we have used a database file called PTdados.xlsx with 8500 hotspots from different parts of Portugal but the user can choose which database wants to use. Above all of the Hotspots, the tool found only 318 hotspots.

A.3.4 Future Approach

On the next version of the Tool there will be implemented:

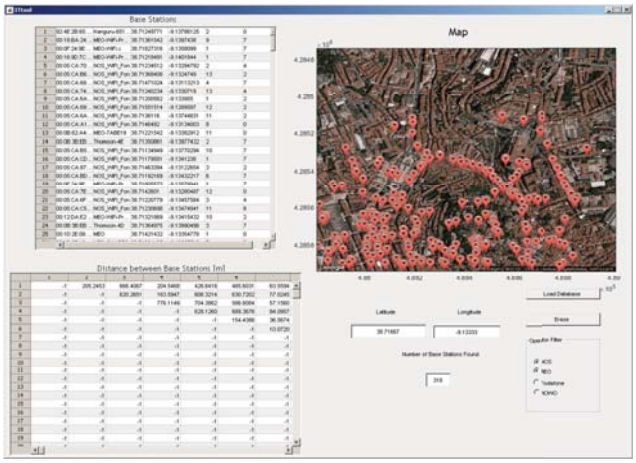

Figure A.5: Results with Meo and Nos operators found in Lisbon

- Image Processing (Because there are a lot of Hotspots in the same building)
- Propagation Models(e.g. WINNER II or Two Slope Propagation Model) and different Path Loss
- A Self Organizing Network
- Filter of the Hotspots that use two Channels(Because it's the same Hotspot with different SSIDs)
- Marker identified by color (one color for Operator for example)

A.4 Mapping Tool Program in Matlab

Listing A.1: Get Map Button Function

```
latitude = str2double(get(handles.latitude,'String'));
longitude = str2double(get(handles.longitude,'String'));
[xx yy M Mcolor zone] = get_google_map(latitude,longitude);
imagesc(xx,yy,M); shading flat; colormap(Mcolor);
```

Listing A.2: Coordinates of Corner Points of the Map

```
%% Save the coordinates of the Extreme Points of Map
format short
[Lat,Lon] = utm2deg(min(xx),min(yy),zone);
p1(1) = Lat;
p1(2) = Lon;
[Lat,Lon] = utm2deg(max(xx),max(yy),zone);
p3(1) = Lat;
p3(2) = Lon;
```

Listing A.3: readdatabase function - Reading and Filtering Interest Results from Wigle.net Database

```
%% This function is called by the main program,and it's called "
   readdatabase.m"
function [tabelatotal] = readdatabase
[FileName] = uigetfile('*.xlsx','Select␣the␣Database␣file'),
[num,txt,raw] = xlsread(FileName);
clear num;
clear txt;
interest = [2,3,9,10,11,13];

for m=1:6
v = genvarname('tabela', who);
eval([v '=␣raw(2:end,interest(m))']);
end
clc;

tabelatotal=[tabela,tabela1,tabela2,tabela3,tabela4,tabela5];
end
```

Listing A.4: Filter Hotspots by Coordinates

```
%% Function readdatabase will choose the Database File and filter the
   interest Data (MAC,SSID,LAT,LON,Channel e QoS)
table = readdatabase;

%% Filter the Hotspots by Coordinates
latitudes = str2double(table(1:end,3));
longitudes = str2double(table(1:end,4));
contador = 1;
for i = 1:length(table)
        if latitudes(i)>=p1(1) && latitudes(i)<=p3(1) && longitudes(i)
           >= p1(2) && longitudes(i)<= p3(2)
            for m=1:6
            finaltable(contador,m) = table(i,m);
            end
            contador = contador + 1;
            end
end
aux = exist('finaltable','var');
if aux == 0
 Error;
return;
end
```

Listing A.5: Read the values of the Toggle Buttons to choose the Operators

```
%% Load the Operator Filter Values
NOS = getappdata(0,'NOS');
MEO = getappdata(0,'MEO');
Vodafone = getappdata(0,'Vodafone');
NOWO = getappdata(0,'NOWO');
auxtable = finaltable;
```

Listing A.6: Filtering Hotspots by Operator

```
%% Filter the chosen Hotspots(if some of them have been selected)
if NOS == 1 || MEO == 1 || Vodafone == 1 || NOWO == 1
    clear finaltable;
    ssid = auxtable(1:end,2);
    contador = 1;
    name = [];
if NOS == 1
    name = [string('NOS'),string('Optimus'),string('Kanguru')];
end
if MEO == 1
      name = [name,string('MEO'),string('Thomson')];
end
if Vodafone == 1
     name = [name,string('Vodafone')];
end
if NOWO == 1
     name = [name,string('NOWO'), string('Cabovisao')];
end

for i=1:length(ssid)
    essid = ssid(i,1);
    essid = char(essid);
  for n=1:length(name)
     k = strfind(essid,name(n));
    if k == 1
        for m=1:6
             finaltable(contador,m) = auxtable(i,m);
        end
    contador = contador + 1;
    end
   end
end

end

exist finaltable;
if ans == 0
 Error;
else
  set(handles.tabelaDB,'Data',finaltable);
```

Listing A.7: Total Hotspots found and Distance

```
%% Total Value of BS found and Calculate the Distance between them
finaltablesize = size(finaltable);
number_bs = finaltablesize(1);
set(handles.number_bs,'String',number_bs);
for  i=1:number_bs
 for n=1:number_bs
     distances(i,n) = -1;
 end
end

data = finaltable;
data1 = data(1:end,3);
data1 = str2double(data1);
data2= data(1:end,4);
data2 = str2double(data2);
data = [data1,data2];

for  i=1:number_bs
 for n=i+1:number_bs
     latA = data(i,1);
     lonA = data(i,2);
     latB = data(n,1);
     lonB = data(n,2);
     [distanciabs] = distance(latA,lonA,latB,lonB);
     distances(i,n) = distanciabs;
 end
end
 set(handles.TabelaDis,'Data',distances);
end
```

Listing A.8: Total Hotspots found and Distance

```
%% This function compute the distance in m between two
%% base stations/hotspots
function [distancebs] = distance(latA,lonA,latB,lonB)

[arclen,az] = distance(latA,lonA,latB,lonB);
c = deg2km(arclen);

%% distance converted from km to m
distancebs =  c*1000;
end
```

Listing A.9: Clear Results

```
%% Clear all the Results
clc; %Clear console
cla; %Clear figure
set(handles.tabelaDB,'data',cell(size(get(handles.tabelaDB,'data')))) %
    Clear tables
set(handles.TabelaDis,'Data', cell(size(get(handles.TabelaDis,'Data')))
    );
set(handles.number_bs,'String',''); %Clear string
```

Listing A.10: Hotspot Markers

```
%% Create the markers for the Hotspots

markerlist = {'color:red','style:tiny'};
finaltablesize = size(finaltable);
if finaltablesize(1) > 270
    finaltablesize(1) = 270;
end

for i=1:finaltablesize(1) % the limit of markers is 288
    location = [finaltable(i,3),',',finaltable(i,4)];
    location = strjoin(location);
    markerlist = [markerlist,location];
end

finaltablesize(1),
markeruse = 1;
setappdata(0,'markeruse',markeruse);
setappdata(0,'markerlist',markerlist);

[xx yy M Mcolor zone] = get_google_map(latitude,longitude);
imagesc(xx,yy,M); shading flat; colormap(Mcolor);
```

Appendix B

Simulation Programs in Matlab

B.1 Introduction

In this section is presented the programs that were created and used to create the graphics in chapter 2. As way to create a faster and easier process to get the different performance parameters, different functions/programs were created or optimized, for example oBStoSS, this one that is the most important function of all, therefore without it it would not be possible to obtain the rest of the graphics.

B.2 How it works

There are various programs, but one is the most important of all, that program/application is called Rb_raio, with the objective of manage all the other functions in order to obtain certain results or parameters.In this program the user can choose what frequencies he wants to use, the distances or coverage radius, bandwidth, graphic colors, scales and cenarios, obtaining results such as:

- Supported Throughput;
- 3D MCS view;
- Intermittent scenarios;
- And much more.

In the Rb_raio are included diverse functions, each one to obtain a different parameter. Rb_raio is divided into various parts, being some of these:

- The Choice and Computation part-Responsible for choice of the function, the computing and organize the values;
- the Representation part-Responsible for represent the graphics with the right colors, fonts, sizes and names;
- The final part which is the file saving-Responsible for saving the graphics and the obtained results.

Inside of this program there is different functions such as $gerargrafico\_commcs$, intermittent and the differents oBStoSS functions depending on the scenario chosen by the user. All of these functions will be shown in the subsection B.3 and properly explained. In subsection are the source codes for the programs used being Rb_raio divided in B.2, B.3, B.5, B.6 and B.7.

B.3 Simulation Programs in Matlab

Listing B.1: Variable Initialization and precaching for better performance Part I

```
% Variaveis de Controlo
choice='2D'; %escolher entre graficos 2D e 3D
holdvar = 1; %escolher se deseja juntar gráficos
save = 0; %escolher se deseja gravar o gráfico (1-yes,0-no)
freqt = [2.6 3.5]; %escolher frequencia(s) desejadas de 2-6GHz
freqm = [28 38 60 73]; %escolher frequencia(s) se mmWave ativado
posinterf = [0 1 2 4]; %escolher localizaçao de interferente(1-4)
%ou sem interferer(0)
Rmax= 300; % inserir Raio máximo
band = 20; % inserir largura de banda 5, 10 ou 20 MHz
build = 0; % escolher graficos com tipologia para edificios
cenario = 5; %escolher 25 HeNB ou 4 HeNB (Building)
PHY = 0; %escolher entre Throughput/SNIR ou não
ci = 0; %escolher entre C/I ou não
own = 1; %escolher gráficos com tipologia hexagonal
mmWave = 1; %escolher gráficos de mmWave(1,0)
intermittentvar = 0; %escolher se deseja ou não o cenário intermitente
alfa = (0:0.01:1); % Alfa varies between 5% and 100%, with a step of 5%
%(used for the sharing)
MCsvar = 0; %Plot 3D MCS Graphs (1-true and 0-false)
add_legend = 1; %escolher entre adicionar mais legendas(1,0)
Font_Type='Times New Roman'; % inserir tipo de letra a utilizar
Font_Size_Legend= 16; % inserir tamanho da letra da legenda
Font_Size= 16; % inserir tamanho de letra do gráfico

%% Inicialização de variaveis para calculo e representacao de graficos

%traio deve começar 10 para Umi LOS
if build == 0
    traio =(5:5:Rmax);
else
traio=(10:0.01:Rmax);
end

d1 = traio;
t1=length(traio);
if build == 1
    Rbsup=zeros(1,t1);
else
Rbsup=zeros(length(freqt),length(posinterf),t1);
end
antenas=cell(1,length(posinterf));
cints=cell(length(freqt),length(posinterf));
str=cell(length(freqt),length(posinterf));
Rbsupfinal=zeros(length(freqt),length(alfa),length(Rbsup));
Rbsupfinal1=zeros(length(freqm),length(alfa),length(Rbsup));
aux_legend = 'DisplayName';
```

Listing B.2: Variable Initialization and precaching for better performance partII

```
for i=1:length(posinterf)
if posinterf(i)~=0
    antenas(i)={'omni1'};
else
    antenas(i)={'omni'};
end
end
```

Listing B.3: Compute and organize values

```
%% Compute 2D

%For Continuos Scenario
if strcmp(choice,'2D') == 1 && intermittentvar == 0

if build == 1
    if PHY == 0 || ci == 0
for t=1:t1
 t,
[d,fin2,fin,throughputaux,csobreidB, SINR, vectorRB]= oBStoSS3build
(ci,PHY,cenario,0.01,traio(t),20,5,0,0,10,7,2.6,'omni','DL','Build',
'NLoS');
 Rbsup(1,t)=throughputaux;
 d1(t)=traio(t);
end
figure,
% p = polyfit(d1,Rbsup(1,:),4); % Fits a
%fifth degree polynomial to exp(a) in the Least squares sense
% v = polyval(p,d1);
plot(d1,v,d1,Rbsup(1,:),'.'); % You will see the difference.
% ylim([0 64]);
xlabel({'\it␣Size␣\rm[m]'},'FontName',Font_Type,
'FontSize',Font_Size); % y-axis label
ylabel({'\it␣Rb_{sup}␣\rm[Mbps]'},'FontName',Font_Type,
'FontSize',Font_Size); % y-axis label
    else
[d,fin2,fin,throughputaux,csobreidB, SINR, vectorRB]= oBStoSS3build
(ci,PHY,cenario,0.0001,traio(t1),20,5,0,0,10,7,2.6,'omni','DL','Build',
'NLoS');
    end
end

if own == 1
for n=1:length(freqt)
for m=1:length(posinterf)
for t=1:t1
    t,
antena = num2str(cell2mat(antenas(1,m)));
[cint,~,~,~,~,throughputaux]= oBStoSS(3,0.01,traio(t),-7,17,0,
posinterf(m),band,5,freqt(n),antena,'DL','Umi','LoS'); %% modificar freqt
Rbsup(n,m,t)=throughputaux;
cints(n,m)={cint};
end
end
end
end
```



```
if mmWave ==1
load('ThpX100.mat');
load('Thp0100.mat');
```

Listing B.4: Plot 2D graphics in the respective legends Part I

```
%% Plot 2D Graphs with respective legends

if own == 1
[~,sizevar,~] = size(Rbsup);
color = 'color';
if mmWave == 1
%rgb=[1,0,0;1,0,1];
rgb=[0 0 1;0 1 0;1 0 0;0 0 0];
else
rgb=[0 0 1;0 1 0;1 0 0;0 0 0;1 1 0];
end

for n=1:length(freqt)
    for i=1:sizevar

     if mmWave==1
    aux = strcat(num2str(freqt(n)),' ','GHz');
     else
    aux = strcat(num2str(freqt(n)),' ','GHz',' ',cints{n,i});
     end

     aux1 = rgb(i,:);

   v = matlab.lang.makeValidName('p');
    Rbsupvar = reshape(Rbsup(n,i,:),[1,t1]);
    eval([v ' = plot(d1,Rbsupvar,aux_legend,aux,color,aux1)']);
    legend('show');
    legend('-DynamicLegend');
    lgd1.FontName = Font_Type;
    lgd1.FontSize = Font_Size_Legend;
              hold on;
        if sizevar > 1
            hold on;
        end
    end
end

%title1=strcat({'Supported Throughput for'},
{' '},{num2str(freqt(n))},{' '},{'GHz'});
%title(title1);
legend('boxoff');

grid on;
xlabel({'\it Cov. distance R\rm[m]'},'FontName',Font_Type,'FontSize',Font_Size); % x-axi
ylabel({'\it R_{b-sup} \rm[Mbps]'},'FontName',Font_Type,'FontSize',Font_Size); % y-axis
clc
end

%% Plot 2D Graphs with respective legends
```

Listing B.5: Plot 2D graphics in the respective legends Part II

```
if mmWave == 1
%     if own == 1
%         cont = n*i; %junçao de gráficos
%         set(gca);
%     end
color = 'color';
rgb=[0,0,0;0,0,1;1,0.6,0;0,1,0];

    for n=1:length(freqm)
    for i=1:2

    aux = strcat(num2str(freqm(n)),' ','GHz with Sharing');
    aux1 = rgb(n,:);

    v = matlab.lang.makeValidName('p');
    if i == 1
    aux = strcat(num2str(freqm(n)),' ','GHz');
    eval([v ' = plot(d1,SX100(n,:),aux_legend,aux,color,aux1)']);
    else
         eval([v ' = plot(d1,S0100(n,:),aux_legend,aux,color,aux1)']);
    end
    legend('show');
    legend('-DynamicLegend');
    lgd1.FontName = Font_Type;
    lgd1.FontSize = Font_Size_Legend;
            hold on;
    end
    end
grid on;
xlabel({'\it Cov. distance R\rm[m]'},'FontName',Font_Type,
'FontSize',Font_Size); % x-axis label
ylabel({'\it R_{b-sup} \rm[Mbps]'},'FontName',Font_Type,
'FontSize',Font_Size); % y-axis label
end

%For intermittent Scenario
elseif strcmp(choice,'2D') == 1 && intermittentvar == 1

for n=1:length(freqt)
    for m=1:length(posinterf)
        for t=1:t1
        antena = num2str(cell2mat(antenas(1,m)));
        %First Rbsup needs to be with sharing
        [cint,fin2,fin,d,SINR,throughputaux] = oBStoSS(3,0.01,traio(t),-7,17,0,posi
        Rbsup(m,t)=throughputaux;
        end
    end
end

for t=1:length(alfa)
```

Listing B.6: Choose programs to 3D graphics

```
%% Compute 3D Graphs and Represent
elseif strcmp(choice,'3D') == 1
    if intermittentvar == 1
        intermittent(holdvar,freqm,mmWave,own,alfa,traio,freqt,band,
antenas,posinterf,Font_Type,Font_Size);
    end
    if MCsvar == 1 && own == 1
        if length(freqt)>1
            for i=1:length(freqt)
                for n=1:length(posinterf)
                    antena = num2str(cell2mat(antenas(1,n)));
                    gerargrafico_commcs(antena,posinterf(n),freqt(i),traio,Font_Size,
Font_Size_Legend,Font_Type,band);
                end
            end
        else
            for n=1:length(posinterf)
                antena = num2str(cell2mat(antenas(1,1)));
                gerargrafico_commcs(antena,posinterf(n),freqt,traio,Font_Size,
                                                                Font_Size_Legend,Font_Ty
            end
        end
    end
    if build == 1 && MCsvar == 1
        gerargrafico_commcsbuild(ci,PHY,cenario,traio,Font_Size,
                                 Font_Type);
    end
    if build == 1 && intermittentvar == 1
        Rbsupportedbuild(ci,PHY,cenario,traio,band,Font_Type,Font_Size);
    end
end
%% Guarda Gráficos(3D)
if save == 1
    graphsave(choice,traio,freqt,band);
end
clear,
clc,
```

Listing B.7: Save 2D graphics in a file

```
%% Save 2D Graphics
if save == 1
graphsave(choice,traio,freqt,band);
end
```

Appendix C

3D view of the PHY throughput mapped into MCSs

C.1 Introduction

In this appendix there are the 3D view charts for frequency band of 3.5 GHz. it was represented the 3D graphics for the best case scenarios with and without sharing, these 3D graphs were obtained with normalized distance, coverage radius and MCS.That way it is possible to understand the relation between the coverage radius and the distance walked by the UE, for the MCS. The results obtained were for the best cases, no interferer scenario and the northeast sharing scenario, considering the reuse patterns $k = 3$ and $k = 4$. We can conclude that for the no interferer scenario, represented in figure C.1 and figure C.3, the highest values of PHY throughput are achieved when the normalized distance is up to 40%, however as the cell radius increases, the PHY throughput values for the cell keep in the highest values for longer normalized distances. For the northeast scenario, represented in figures C.2 and figure C.4, the higher the cell radius is, and the shorter normalized distances is, the higher the PHY throughput values is.

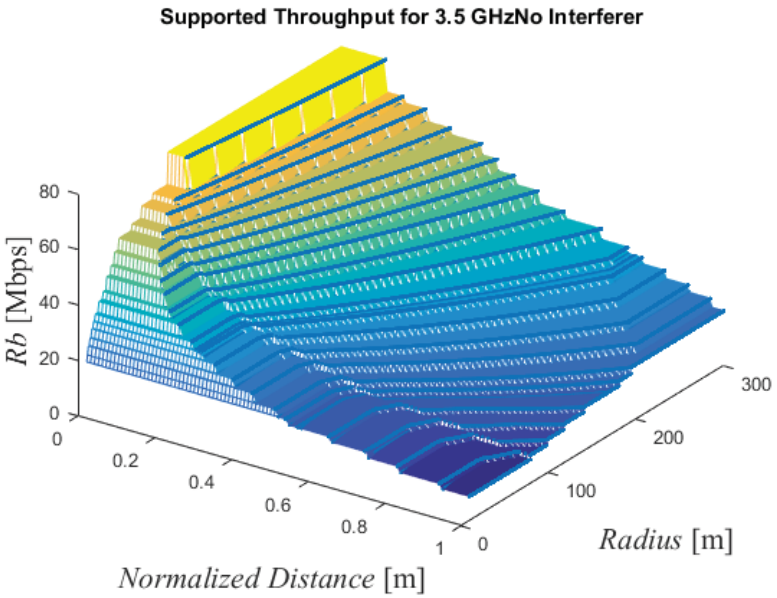

Figure C.1: 3D View of the PHY throughput mapped into MCSs with No Interferer for 3.5 GHz with $k = 3$

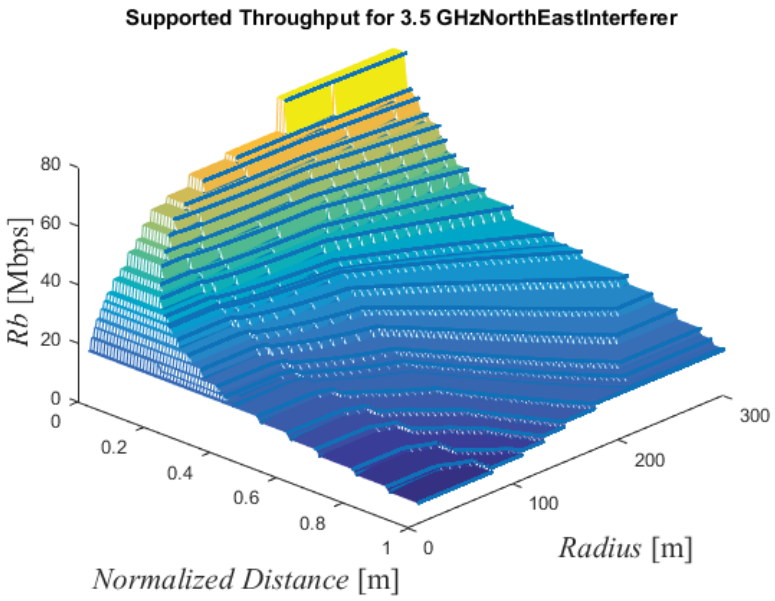

Figure C.2: 3D view of the PHY throughput mapped into MCSs with Northeast Interferer for 3.5 GHz with $k = 3$

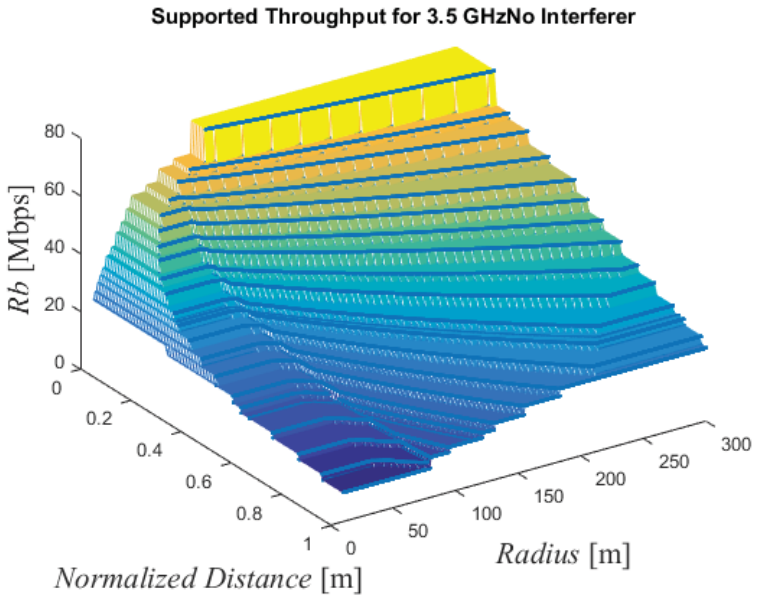

Figure C.3: 3D view of the PHY throughput mapped into MCSs with No Interferer for 3.5 GHz with $k = 4$

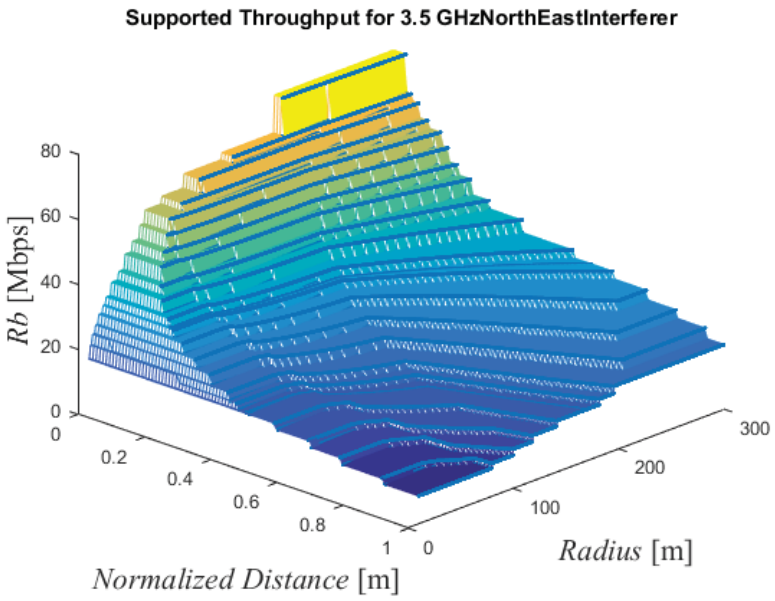

Figure C.4: 3D view of the PHY throughput mapped into MCSs with Northeast Interferer for 3.5 GHz with $k = 4$

Appendix D

AverageCNIR in Matlab

D.1 Introduction

This program was made in Matlab2016 with the objective of generate the Average CNIR. The program contains the mathematical models for the interferers, as well as the central cell, it computes the own power and the interferers powers and use the CNIR formula that was defined in the 2.5. The program will be divided below to be easy to understand how it works.

D.2 AverageCNIR Program in Matlab

Listing D.1: Variable Initialization

```
%% Variable Initialization
syms x y;
pe = 10^(PE/10);
ge = 10^(GE/10);
gr = 10^(GR/10);
% inicio = 0.05;
inicio = 1;
%r = inicio*(sqrt(3)/2);
A_ow = (3*(sqrt(3)/2))*(final^2 -inicio^2);
A_cell = 3*(sqrt(3)/2)*(final^2);
LB =largurabanda*10^6;
N=-204+10*log10(LB)+NF ;%noise en db
n=10^(N/10);%noise en lineal;
F=f*10^9;
dBPmilinha=4*hBS*hUE*F/(3*10^8);
cte = 7.8 - 18*log10(hBS)-18*log10(hUE);
```

Listing D.2: Compute Own Power Part I

```
%% Cálculo dos Integrais para obter a potência da própria
%% First Choice
if final <= dBPmilinha
Pathloss = @(x,y) 1./(sqrt(x.^(2)+y.^(2))).^2.2;
ymax1 = @(x) (sqrt(3)./3)*x;
ymax2 = @(x) (sqrt(3)*(final-x));

int1_value = integral2(Pathloss,inicio,(3/4) * final,0,ymax1);
int2_value = integral2(Pathloss,(3/4)*final,final,0,ymax2);

Powtotal = 12*pe*ge*gr*10^(-2.8)*(int1_value + int2_value)/(f^(2)*A_ow);

%% Second Choice
elseif final> dBPmilinha && final<= dBPmilinha/(sqrt(3)/2)
%% first branch
Pathloss = @(x,y) 1./(sqrt(x.^2+y.^2)).^2.2;

ymax1 = @(x) (sqrt(3)/3)*x;
ymax2 = @(x) (sqrt(3)*(final-x));
ymax3 = @(x) (sqrt(dBPmilinha^2 - x.^2));

int1_value = integral2(Pathloss,inicio,(3/4) * final,0,ymax1);
int2_value = integral2(Pathloss,(3/4) * final,
(6*final+sqrt(16*(156^2)-12*(final^2)))/8,0,ymax2);
int3_value = integral2(Pathloss,
(6*final+sqrt(16*(156^2)-12*(final^2)))/8,dBPmilinha,0,ymax3);

Powa = 12*pe*ge*gr*10.^(-2.8)*(int1_value + int2_value + int3_value)/
(f^(2)*A_ow);

%% second branch

Pathloss = @(x,y) 1./(sqrt(x.^2+y.^2)).^4;

int1_value = integral2(Pathloss,(6*final+
sqrt(16*(156^2)-12*(final^2)))/8,dBPmilinha,ymax3,ymax2);
int2_value = integral2(Pathloss,dBPmilinha,final,0,ymax2);

Powb = 12*pe*ge*gr*10.^(-cte/10)*(int1_value + int2_value)/
(f.^(0.2)*A_ow);

Powtotal = Powa + Powb;
```

Listing D.3: Compute Own Power Part II

```
%% Last Choice
elseif final > dBPmilinha/(sqrt(3)/2)

%% first branch
ymax1 = @(x) (sqrt(3)/3)*x;
ymax2 = @(x) (sqrt(3)*(final-x));
ymax3 = @(x) sqrt(dBPmilinha^(2) - x.^2);
Pathloss = @(x,y) 1./(sqrt(x.^2+y.^2)).^2.2;

int1 = integral2(Pathloss,inicio,(sqrt(3)/2)*dBPmilinha,0,ymax1);
int2 = integral2(Pathloss,(sqrt(3)/2)*dBPmilinha,dBPmilinha,0,ymax3);
Powa = 12*pe*ge*gr*10.^(-2.8)*(int1 + int2)/(f^(2)*A_ow);

%% second branch
Pathloss = @(x,y) 1./(sqrt(x.^2+y.^2)).^4;

int1_value = integral2(Pathloss,(sqrt(3)/2) *
dBPmilinha,dBPmilinha,ymax3,ymax1);
int2_value = integral2(Pathloss,dBPmilinha,(3/4)*final,0,ymax1);
int3_value = integral2(Pathloss,(3/4)*final,final,0,ymax2);

Powb =12*pe*ge*gr*10.^(-cte/10)*(int1_value + int2_value + int3_value)/
(f.^(0.2)*A_ow);

Powtotal = Powa + Powb;

end
```

Listing D.4: Compute Interferers Power Part I

```
%% Cálculo dos integrais para obter a Potência dos interferentes

%% Scenario 1 (folhas)
if final >= dBPmilinha/2
Pathloss = @(x,y) 1./(sqrt((3*final - x).^2+y.^2)).^4;
ymax1 = @(x) (sqrt(3)*(-x+final));
ymax2 = @(x) (sqrt(3)*(x+final));

limite_y=(sqrt(3)/2) * final;

int5_value = integral2(Pathloss,final/2,final,0,ymax1);
int6_value = integral2(Pathloss,-final/2,final/2,0,limite_y);
int7_value = integral2(Pathloss,-final,-final/2,0,ymax2);

Pinttotal = 12*pe*ge*gr*10.^(-cte/10)*(int5_value+int6_value
+int7_value)/(f.^(0.2)*A_cell);

%% Scenario 2 (folhas)
elseif final >= dBPmilinha/(156/59) && final < dBPmilinha/2

ymax3 = @(x) sqrt(dBPmilinha^(2) - (3*final-x).^2);
ymax2 = @(x) (sqrt(3)*(x+final));
x_int = (12*final - sqrt(16*(dBPmilinha^2) - 48*(final^2)))/(8);
ymax1 = @(x) (sqrt(3)*(-x+final));

Pathloss = @(x,y) 1./(sqrt((3*final - x).^2+y.^2)).^2.2;

int5_value = integral2(Pathloss,3*final-dBPmilinha,x_int,0,ymax3);
int6_value = integral2(Pathloss,x_int,final,0,ymax1);
Pint1 = 12*pe*ge*gr*10.^(-2.8)*(int5_value+int6_value)/(f^(2)*A_cell);

Pathloss = @(x,y) 1./(sqrt((3*final - x).^2+y.^2)).^4;

int5_value = integral2(Pathloss,-final,-final/2,0,ymax2);
 %triangulo
int6_value = integral2(Pathloss,-final/2,final/2,0,(sqrt(3)/2) * final);
%quadrado
int7_value = integral2(Pathloss,final/2,3*final-dBPmilinha,0,ymax1);
% poligono
int8_value = integral2(Pathloss,3*final-dBPmilinha,x_int,ymax3,ymax1);
%triangulopequeno-intersecçao circuferencia

Pint2 = 12*pe*ge*gr*10.^(-cte/10)*(int5_value+int6_value+int7_value
+int8_value)/(f.^(0.2)*A_cell);

Pinttotal = (Pint1+Pint2);
```

Listing D.5: Compute Interferers Power Part II

```
%% Scenario 3 (tanto o 3',3''e 3 das folhas são iguais)
elseif final >= dBPmilinha/(156/43) && final < dBPmilinha/(156/59)
limite_y = (sqrt(3)/2) * final;
ymax1 = @(x) (sqrt(3)*(-x+final));
ymax2 = @(x) (sqrt(3)*(x+final));
y_int = @(x) sqrt(dBPmilinha.^(2) - (3*final-x).^2);

Pathloss = @(x,y) 1./(sqrt((3*final - x).^2+y.^2)).^2.2;

int5_value = integral2(Pathloss,final/2,final,0,ymax1);
int6_value = integral2(Pathloss,3*final-(sqrt(4*dBPmilinha^2 -
3*final^2)/2),final/2,0,limite_y);
int7_value = integral2(Pathloss,3*final-dBPmilinha,3*final-
(sqrt(4*dBPmilinha^2 - 3*final^2)/2),0,y_int);

Pint1 = 12*pe*ge*gr*10^(-2.8)*(int5_value+int6_value+int7_value)
/(f^(2)*A_cell);

Pathloss = @(x,y) 1./(sqrt((3*final - x).^2+y.^2)).^4;

int5_value = integral2(Pathloss,-final,-final/2,0,ymax2);
int6_value = integral2(Pathloss,-final/2,3*final - dBPmilinha,
0,limite_y);
int7_value = integral2(Pathloss,3*final-dBPmilinha,3*final-
(sqrt(4*dBPmilinha^2 - 3*final^2)/2),y_int,limite_y);

Pint2 = 12*pe*ge*gr*10.^(-cte/10)*(int5_value+int6_value+int7_value)/
(f^(0.2)*A_cell);

Pinttotal = (Pint1+Pint2);

%% Scenario 4 (folhas)
elseif final > dBPmilinha/4 && final < dBPmilinha/(156/43)
ymax1 = @(x) (sqrt(3)*(-x+final));
ymax2 = @(x) (sqrt(3)*(x+final));
y_int = @(x) sqrt(dBPmilinha.^(2) - (3*final-x).^2);
Pathloss = @(x,y) 1./(sqrt((3*final - x).^2+y.^2)).^2.2;
x_int = - sqrt((dBPmilinha^2 - 12*final^2))/2;

int5_value = integral2(Pathloss,final/2,final,0,ymax1);
int6_value = integral2(Pathloss,-final/2,final/2,0,(sqrt(3)/2) * final);
int7_value = integral2(Pathloss,x_int,-final/2,0,ymax2);
int8_value = integral2(Pathloss,3*final-dBPmilinha,x_int,0,y_int);

Pint1 = 12*pe*ge*gr*10^(-2.8)*(int5_value+int6_value+int7_value+
int8_value)/(f^(2)*A_cell);

Pathloss = @(x,y) 1./(sqrt((3*final - x).^2+y.^2)).^4;
```

Listing D.6: Compute Interferers Power Part III

```
int5_value = integral2(Pathloss,3*final-dBPmilinha,x_int,y_int,ymax2);
int6_value = integral2(Pathloss,-final,3*final-dBPmilinha,0,ymax2);

Pint2 = 12*pe*ge*gr*10.^(-cte/10)*(int5_value+int6_value)/
(f^(0.2)*A_cell);

Pinttotal = (Pint1+Pint2);

%% Scenario 5(folhas)
elseif final <= dBPmilinha/4
Pathloss = @(x,y) 1./(sqrt((3*final - x).^2+y.^2)).^2.2;
ymax1 = @(x) (sqrt(3)*(-x+final));
ymax2 = @(x) (sqrt(3)*(x+final));

int5_value = integral2(Pathloss,final/2,final,0,ymax1);
int6_value = integral2(Pathloss,-final/2,final/2,0,(sqrt(3)/2) * final);
int7_value = integral2(Pathloss,-final,-final/2,0,ymax2);

Pinttotal = 12*pe*ge*gr*10.^(-2.8)*(int5_value+int6_value+int7_value)/
(f^(2)*A_cell);
end

%Compute Average SINR
CNIR_avg = Powtotal/(Pinttotal + n);
```

Appendix E

Packet Loss Ratio

In the Small Cell scenario , the PLR was obtained for both bands with two graphics both, one which shows the average cell PLR per radius coverage and the other which shows the average cell PLR per number of users, for 2.6 GHz bands represented in the figures **??** and **??**, with different transmitter powers such as 40 dBm and 42.2478 dBm. In this context, the 2% PLR threshold is exceeded for the most of the coverage radius, being only in accord between 12 and 20 users, for the higher coverage radius values, being these ones 156 m, 210 m, 270 m and 300 m.

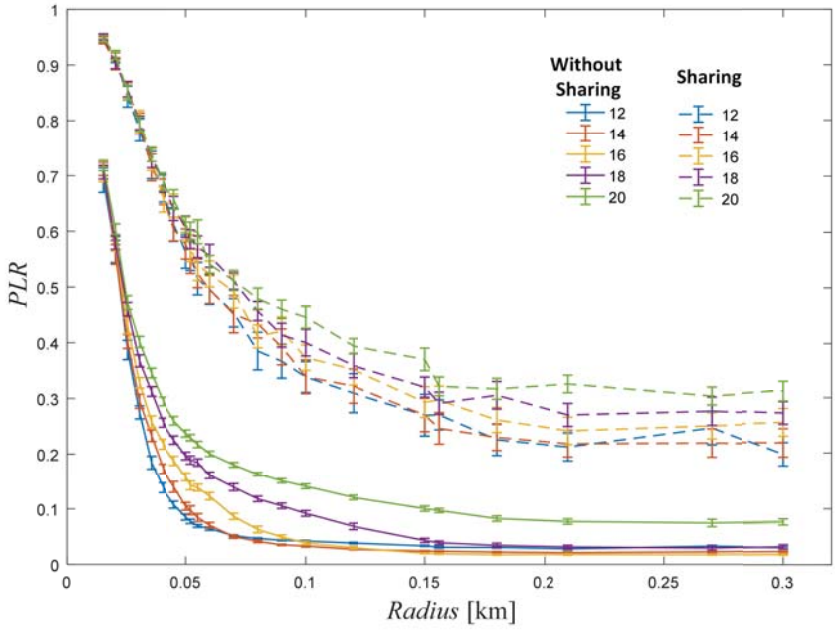

Figure E.1: Packet Loss Ratio per radius with a transmitter power of 40 dBm, for the scenarios with/without sharing at 2.6 GHz

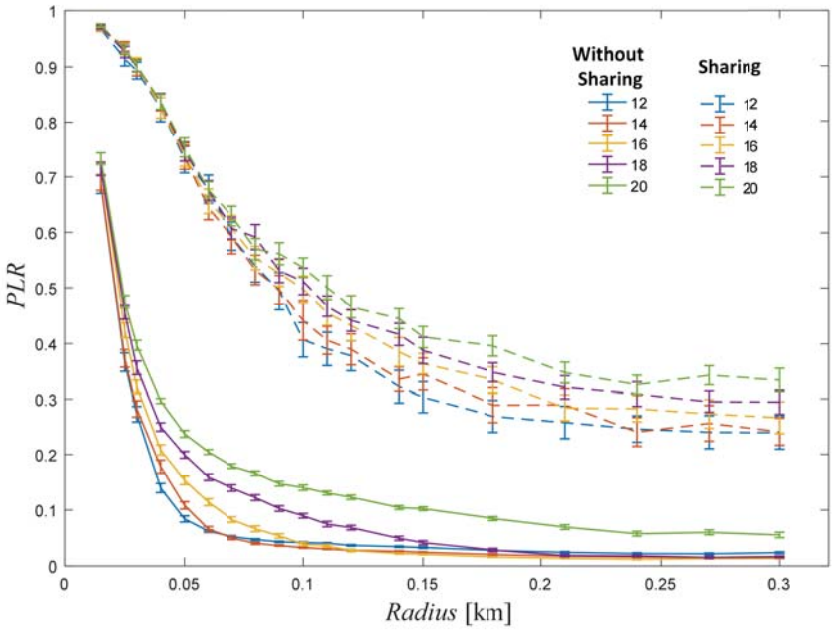

Figure E.2: Packet Loss Ratio per radius with a transmitter power of 42.2778 dBm, for the scenarios with/without sharing at 3.5 GHz

Appendix F

LTE-Sim

F.1 LTE-Sim Program

Listing F.1: LTE-SIM Propagation Model with PathLoss Part I

```
/* -*- Mode:C++; c-file-style:"gnu"; indent-tabs-mode:nil; -*- */
/*
 * Copyright (c) 2010,2011,2012,2013 TELEMATICS LAB, Politecnico di
    Bari
 *
 * This file is part of LTE-Sim
 *
 * LTE-Sim is free software; you can redistribute it and/or modify
 * it under the terms of the GNU General Public License version 3 as
 * published by the Free Software Foundation;
 *
 * LTE-Sim is distributed in the hope that it will be useful,
 * but WITHOUT ANY WARRANTY; without even the implied warranty of
 * MERCHANTABILITY or FITNESS FOR A PARTICULAR PURPOSE.  See the
 * GNU General Public License for more details.
 *
 * You should have received a copy of the GNU General Public License
 * along with LTE-Sim; if not, see <http://www.gnu.org/licenses/>.
 *
 * Author: Giuseppe Piro <g.piro@poliba.it>
 */

#include "UMI-LoS-dual-slope.h"
#include "../../device/UserEquipment.h"
#include "../../device/ENodeB.h"
#include "../../device/HeNodeB.h"
#include "../../utility/RandomVariable.h"
#include "shadowing-trace.h"
#include "../../core/spectrum/bandwidth-manager.h"
#include "../../phy/lte-phy.h"
#include "../../core/eventScheduler/simulator.h"
#include "../../load-parameters.h"

UMILoSdualslope::UMILoSdualslope(NetworkNode* src, NetworkNode* dst,
    double Fc)
{
  SetSamplingPeriod (0.5);

  m_penetrationLoss = 10;
  m_shadowing = 0;
  m_pathLoss = 0;
  SetFastFading (new FastFading ());
```

Listing F.2: LTE-SIM Propagation Model with PathLoss Part II

```
  SetSourceNode (src);
  SetDestinationNode (dst);

#ifdef TEST_PROPAGATION_LOSS_MODEL
  std::cout << "Created Channe Realization between "
                  << src->GetIDNetworkNode () << " and " << dst->
                      GetIDNetworkNode () << std::endl;
#endif


  if (_simple_jakes_model_)
          SetChannelType (ChannelRealization::CHANNEL_TYPE_JAKES);
  if (_PED_A_)
          SetChannelType (ChannelRealization::CHANNEL_TYPE_PED_A);
  if (_PED_B_)
          SetChannelType (ChannelRealization::CHANNEL_TYPE_PED_B);
  if (_VEH_A_)
          SetChannelType (ChannelRealization::CHANNEL_TYPE_VEH_A);
  if (_VEH_B_)
          SetChannelType (ChannelRealization::CHANNEL_TYPE_VEH_B);

  UpdateModels ();

}

UMILoSdualslope::~UMILoSdualslope()
{
}

void
UMILoSdualslope::SetPenetrationLoss (double pnl)
{
  m_penetrationLoss = pnl;
}

double
UMILoSdualslope::GetPenetrationLoss (void)
{
  return m_penetrationLoss;
}
```

Listing F.3: LTE-SIM Propagation Model with PathLoss Part III

```
double
UMILoSdualslope::GetPathLoss (void)
{
  /*
   * According to  ---  insert standard Bruno ---
   * the Path Loss Model For Dual slope
   * for distance =< dBP
   * L = 22 * log10 (r) + 28 + 20 * log10 (fc)
   * for for distance > dBP
   * L = 40 * log10 (r) + 7.8 - 18 * log10 (hBS) - 18 * log10 (hUE) + 2
       * log10 (fc),
   * r in meters, is the distance between two nodes
   *  fc in GHz
   *  hBS in m
   *  hUE in m
   ****************************************
   * dBP- Brak point distance, assording to
   *  dBP = (4 * hUE * hBS * fc) / ( 3 * 10 ^ 8 )
   * fc in Hz
   */
  double distance;

  if (GetSourceNode ()->GetNodeType () == NetworkNode::TYPE_UE
                && GetDestinationNode ()->GetNodeType () ==
                    NetworkNode::TYPE_ENODEB)
    {
          UserEquipment* ue = (UserEquipment*) GetSourceNode ();
          ENodeB* enb = (ENodeB*) GetDestinationNode ();

          distance =  ue->GetMobilityModel ()->GetAbsolutePosition ()->
              GetDistance (enb->GetMobilityModel ()->
              GetAbsolutePosition ());
    }

  else if (GetDestinationNode ()->GetNodeType () == NetworkNode::
     TYPE_UE
                && GetSourceNode ()->GetNodeType () == NetworkNode::
                    TYPE_ENODEB)
    {
          UserEquipment* ue = (UserEquipment*) GetDestinationNode ();
          ENodeB* enb = (ENodeB*) GetSourceNode ();
          distance =  ue->GetMobilityModel ()->GetAbsolutePosition ()->
              GetDistance (enb->GetMobilityModel ()->
              GetAbsolutePosition ());
    }
```

Listing F.4: LTE-SIM Propagation Model with PathLoss Part IV

```
  double dBP;
  double Fc;
  dBP = (4. * 0.5 * 9. * 2.6 *pow (10.0, 9.0)) / ( 3 * pow (10.0, 8.0)
      );


  if ( distance <= dBP)
  {

          m_pathLoss = 22 *  log10 ( distance ) + 28 + 20 * log10 (Fc);
  }

  else
  {

          m_pathLoss = 40 *  log10 ( distance ) + 7.8 - 18 * log10 (9.)
              - 18 * log10 (0.5) + 2 * log10 (Fc);
  }

  return m_pathLoss;
}


void
UMiLoSdualslope::SetShadowing (double sh)
{
  m_shadowing = sh;
}

double
UMiLoSdualslope::GetShadowing (void)
{
  return m_shadowing;
}

void
UMiLoSdualslope::UpdateModels ()
{

#ifdef TEST_PROPAGATION_LOSS_MODEL
  std::cout << "\t --> UpdateModels" << std::endl;
#endif
```

Listing F.5: LTE-SIM Propagation Model with PathLoss Part V

```
  //update shadowing
  m_shadowing = 0;
  double probability = GetRandomVariable (101) / 100.0;
  for (int i = 0; i < 201; i++)
    {
          if (probability <= shadowing_probability[i])
            {
                  m_shadowing = shadowing_value[i];
          break;
            }
    }
  UpdateFastFading ();
  SetLastUpdate ();
}
std::vector<double>
UMILoSdualslope::GetLoss ()
{
#ifdef TEST_PROPAGATION_LOSS_MODEL
  std::cout << "\t  --> compute loss between "
                  << GetSourceNode ()->GetIDNetworkNode () << " and "
                  << GetDestinationNode ()->GetIDNetworkNode () << std
                     ::endl;
#endif
  if (NeedForUpdate ())
    {
           UpdateModels ();
    }

  std::vector<double> loss;
  int now_ms = Simulator::Init()->Now () * 1000;
  int lastUpdate_ms = GetLastUpdate () * 1000;
  int index = now_ms - lastUpdate_ms;

  int nbOfSubChannels = GetSourceNode ()->GetPhy ()->
     GetBandwidthManager ()->GetDlSubChannels ().size ();

  for (int i = 0; i < nbOfSubChannels; i++)
    {
          double l = GetFastFading ()->at (i).at (index) - GetPathLoss
             () - GetPenetrationLoss () - GetShadowing ();
          loss.push_back (l);
```

Listing F.6: LTE-SIM Propagation Model with PathLoss Part VI

```
#ifdef TEST_PROPAGATION_LOSS_MODEL
       std::cout << "\t\t mlp = " << GetFastFading ()->at (i).at (index
           )
                 << " pl = " << GetPathLoss ()
          << " pnl = " << GetPenetrationLoss()
          << " sh = " << GetShadowing()
          << " LOSS = " << l
                 << std::endl;
#endif
    }

  return loss;
}
```